THE EFFECT OF INSULIN ON STRESS-RESPONSE PATHWAYS IN A CELLULAR MODEL OF RAT CARDIOMYOCYTES

by

Quinton RD Jones

Submitted in partial fulfilment of the requirements
for the degree of Master of Science

at

Dalhousie University
Halifax, Nova Scotia
August 2011

DALHOUSIE UNIVERSITY

DEPARTMENT OF ANATOMY AND NEUROBIOLOGY

The undersigned hereby certify that they have read and recommend to the Faculty of Graduate Studies for acceptance a thesis entitled "THE EFFECT OF INSULIN ON STRESS-RESPONSE PATHWAYS IN A CELLULAR MODEL OF RAT CARDIOMYOCYTES" by Quinton RD Jones in partial fulfilment of the requirements for the degree of Master of Science.

Dated: August 5, 2001

Supervisor: _____

Readers: _____

_____

_____

DALHOUSIE UNIVERSITY

DATE: August 5, 2011

AUTHOR: Quinton RD Jones

TITLE: THE EFFECT OF INSULIN ON STRESS-RESPONSE PATHWAYS IN A CELLULAR MODEL OF RAT CARDIOMYOCYTES

DEPARTMENT OR SCHOOL: Department of Anatomy and Neurobiology

DEGREE: MSc CONVOCATION: October YEAR: 2011

_____

Signature of Author

Table of Contents

List of Figures

Abstract

Insulin and cellular stressors both activate p38 MAPK. Insulin protects cardiac tissue in a p38 MAPK-dependent manner. Paradoxically, inhibiting p38 MAPK is also protective. Hsp27 phosphorylation is regulated by p38 MAPK. Insulin was tested in H9c2 cardiomyocytes subjected to media exchange, 6 hours of oxygen-glucose deprivation, and reoxygenation. Insulin suppressed stress-induced phosphorylation of Hsp27 due to media-exchange or oxygen-glucose deprivation. Surprisingly, insulin increased Hsp27 phosphorylation during reoxygenation. Insulin also reduced total p38 MAPK levels. Insulin before oxygen-glucose deprivation prevented both localization of Hsp27 to the nucleus and localization of phospho-p38 MAPK to the cytoplasm. Insulin during oxygen-glucose deprivation caused the localization of phospho-p38 MAPK in the cytoplasm, but did not increase Hsp27 phosphorylation until reoxygenation. In conclusion, insulin may protect before oxygen-glucose deprivation by redirecting phospho-p38 MAPK to the nucleus away from damaging pathways in the cytoplasm and protects during oxygen-glucose deprivation by priming phospho-p38 MAPK to phosphorylate Hsp27.

List of Abbreviations and Symbols Used

AKT	aka. PKB (Protein Kinase B)
AMI	Acute myocardial infarction
AS160	Akt substrate of 160 kDa
ASK1	Apoptosis signal-regulating kinase 1
ATF-2	Activating Transcription Factor
CON	Control treatment, media not replaced
DM	Differentiating Media (1% FBS)
DMEM	Dulbecco's Modified Eagle Media
ERK	Extracellular-signal-regulated kinase
FBS	Fetal Bovine Serum
GDP	Guanosine diphosphate
GIK	A cocktail of glucose, insulin, and potassium
GLUT4	Glucose transporter type 4
Grb2	Growth factor receptor-bound protein 2
GTP	Guanosine-5'-triphosphate
HSF	Heat Shock (transcription) Factor
HSP	Heat Shock Protein
HspB1	a 'small' HSP family that includes Hsp27 and mouse Hsp25
Ins	Insulin supplementation. Media was replaced with supplemented media
IR	Insulin Receptor
IRS	Insulin Receptor Substrate
JNK	c-Jun N-terminal kinase
kDa	kiloDalton
MAP3K	MAPK Kinase Kinase
MAPK	Mitogen-Activated Protein Kinase
MEF-2	Myocyte Enhancer Factor-2
MK2	MAPK Activated Protein Kinase-2
MK5	MAPK Activating Protein Kinase-5 (aka. PRAK)
MKK	MAPK Kinase (e.g., MKK3 or MKK6)
mt	Mitochondria
mTORC2	mammalian target of rapamycin complex 2
No Ins	No insulin during treatment. Media was replaced with fresh media
OGD	oxygen-glucose deprivation
p38 MAPK	p38 Mitogen-Activated Protein Kinase
PBS	phosphate-buffered saline
PBS-T	phosphate-buffered saline (with 0.1% Triton X-100)
PH domain	Pleckstrin Homology domain

PI3K	Phosphatidylinositol 3-kinase
PIP2	Phosphatidylinositol 4,5-bisphosphate
PIP3	Phosphatidylinositol (3,4,5)-trisphosphate
PKB	Protein Kinase B (a.k.a., AKT)
PKC	Protein Kinase C
PKD	Protein Kinase D
PM	Proliferative media (10% FBS)
PRAK	p38-regulated/activated protein kinase (MK5)
PVDF	polyvinylidene fluoride
ROS	Reactive Oxygen Species
SEM	Standard Error of the Mean
Sos	Son-of-Sevenless
TBS-T	Tris-Buffered Saline with 0.1% Tween-20
TNF-α	Tumor Necrosis Factor-alpha
VDAC1	Voltage Dependant Anion Channel 1

Acknowledgements

"There is no alternative but to building, society by society, a critical mass of informed citizenry."
Paul Collier, to the Royal Society, 2010

My first thanks are to Dr. Currie. I will always appreciate his enthusiasm and endless patience for my efforts. I also appreciate his guidance and his interest in teaching me. More importantly, he always showed a curiosity for everything that crossed his desk. This delight with new data, or new perspectives, is very inspiring. His interest in teaching, and his interest in learning, is contagious.

I also thank my supervisory committee members. Each member, Dr. Eileen Denovan-Wright, Dr. Gary Allen, and Dr. Kazue Semba, allowed me to squeeze them for all of their advice whenever I requested. They all met with me privately, and showed enthusiasm for helping me. I greatly enjoyed their critical questions and their desire to see me succeed. Their mentorship was valuable, and I appreciate it.

Both the 15E lab and the Anatomy & Neurobiology department were excellent companions and comrades. Coffee, pranks, advice, joking, sympathy, trouble-shooting, spitballing, beer, socializing, easy conversations, and rapid, frantic assistance. A group of friends where they wanted to be. Thanks!

Kay Murphy is a godsend. Endless optimism bundled with tireless energy. Wisdom coupled with glee. A great combination. Her heart was with us, and we could tell. Yes, 'godsend' is accurate.

My final thanks to my wife, Patricia Jones. Patricia provided the level of moral support and absolute love and affection that made this journey possible. She enjoyed the process of my Masters education, and backed me all the way. My son Connor and my daughter Madi were very fond of the idea of my Masters education as well, and showed curiosity that we love in children and a patience that we don't expect. Finally, my extended family, all of them.

Quinton Jones

"We need to find important things interesting"

CHAPTER 1: INTRODUCTION

Cardiovascular Disease in Canada

Life-expectancy in Canada has been rising for decades. Between 1979-2005, life-expectancy at birth has been rising at approximately 0.20 years/year (r-squared = 0.9915; Statistics Canada, CANSIM Tables 102-0025 and 102-0511). Concomitantly, there has been a decrease in the death-rate associated with cardiovascular disease and cancer. For example, the mortality rate due to heart attack, stroke, breast cancer, and prostate cancer all decreased between 2000 and 2004 (Statistics Canada, CANSIM Table 102-0126). In 2007, there was an increase in the total number of Canadians who died due to major cardiovascular disease; however the age-standardized mortality rate continues to decrease (Statistics Canada, CANSIM Table 102-0552).

The Canadian rate of death for acute myocardial infarction (AMI) decreased ~38% between 1994 and 2004, but hospitalizations for AMI decreased ~9% in the same time period (after standardizing for age and sex). While a decrease in the rate of death is encouraging, the ability to thrive after an AMI continues to be important, and is arguably becoming even more important as the relative ratio of AMI survival increases. For example, remembering that the Canadian population is aging, the total number of people over 75 years admitted for AMI has risen, even though the number of deaths due to AMI in that cohort has decreased (Tu *et al.*, 2009).

Insulin as a Protective Agent

Following treatment for AMI, reperfusion injury can be a source of further injury, and so interventions and therapies that can reduce reperfusion injury should be considered.

Beginning in the 1960's, a cocktail of glucose, insulin, and potassium (GIK) was used as a therapy to stabilize heart function after AMI (Sodi-Pallares *et al.*, 1962). These therapies sought to reduce injury associated with AMI by using the theory that glucose would allow anaerobic metabolism to continue (and allow higher insulin levels), insulin would suppress free fatty acid production, and that potassium would stabilize electrochemical gradients (and prevent osmolarity issues during infusion). Meta-analysis by Fath-Ordoubadi *et al.* (1997) indicated that using GIK therapy reduced mortality after AMI, however there had been no large-scale studies.

The large-scale CREATE-ECLA study (Mehta *et al.*, 2005) was performed specifically to test the utility of GIK therapy. This study was a cross-institution study with 20,201 patients split between the GIK therapy group and the usual-care group. Unfortunately, there was no difference in 30-day mortality between the groups. The CREATE-ECLA results have suggested further areas of investigation, such as controlling blood glucose within tighter margins, but studies based on this theme are merely suggestive (reviewed in Cheung *et al.*, 2006).

Regardless of the apparent failure of GIK therapy, additional research has shown that insulin itself might be a protective intervention for AMI. For example, in a rat model of AMI which requires excision of the heart, beginning insulin perfusion during reperfusion can reduce relative infarct size to 55% of that caused by untreated reperfusion. However, delaying inclusion of insulin in the reperfusion buffer until 15 minutes of reperfusion does not reduce relative infarct size (Jonassen *et al.*, 2001). Alternatively, giving higher doses of insulin (over 150 X greater concentration than Jonassen *et al.*, 2001) entirely before the onset of ischemia (and reperfusion) resulted in a

relative infarct size that was only 41% the size of that compared to untreated rats subjected to ischemia/reperfusion (Fuglesteg *et al.*, 2009).

Experiments using insulin infusion in live animals have also been performed. For example, Chai *et al.* (2008) used insulin perfusion in the "high-physiological range" in rats subjected to ligation of the left anterior descending coronary artery as a model of heart injury. The protective effect of insulin was greater if included before ischemia than if included before reperfusion. Interestingly, while insulin perfusion started 30 minutes after reperfusion failed to provide a protective effect, inhibiting the stress activated protein kinase p38 Mitogen-Activated Protein Kinase (p38 MAPK) before reperfusion increased the protective potential of insulin given *after* 30 minutes of reperfusion (Chai *et al.*, 2008).

In addition to insulin perfusion, a one-time insulin injection appears to have a protective effect in models of ischemia and reperfusion. A physiologic dose of insulin injected six hours before heart isolation for Langendorff perfusion protected left-ventricular function during ischemia/reperfusion (Li *et al.*, 2006). Correspondingly, a physiologic dose of insulin one hour before ischemia also protected left-ventricular function (Li *et al.*, 2008). Interestingly, inhibiting p38 MAPK before insulin injection reduced the protective effect associated with insulin.

Ischemic Pre-conditioning as a Protective Mechanism

Ischemic pre-conditioning is an alternative method of reducing damage associated with AMI. Original studies of ischemic preconditioning involved surgically restricting blood flow to an organ for short periods of time (e.g., 5 minutes) with similar periods of reperfusion between ischemic events. This pretreatment was first used in dogs to show a

reduction in infarct size following forty minutes of ischemia (Murry *et al.*, 1986), and has since been used in multiple animal models and in different organs. Remote ischemic preconditioning can also provide protection by using transient ischemia/reperfusion in one organ to protect a different organ from damage due to extended ischemia. For example, a mesenteric artery occlusion followed by reperfusion can protect the heart during a subsequent occlusion of a coronary artery (Verdouw *et al.*, 1996).

Remote ischemic preconditioning protocols have been expanded to non-invasive techniques, such as using a blood-pressure cuff on a limb in order to temporarily restrict bloodflow. This technique has been used to improve indicators of damage in children undergoing surgery for congenital heart defects (Cheung *et al.*, 2006). Further, remote ischemic post-conditioning performed by ambulance staff before patients underwent primary percutaneous coronary intervention was shown to significantly increase myocardial salvage (Bøtker *et al.*, 2010).

As with insulin, ischemic pre-conditioning has an interesting relationship with p38 MAPK. Pre-conditioning before ischemia increases the amount of p38 MAPK that is phosphorylated and activated (as measured by activity of enzymes downstream of the p38 MAPK cascade) during the early stages of ischemia. Consistent with the effect of pre-conditioning to cause activation of p38 MAPK, inhibiting p38 MAPK before pre-conditioning will prevent pre-conditioning from causing a protective effect (Nakano *et al.*, 2000b, Sato *et al.*, 2000). One mechanism of action might be through the adenosine receptor, because antagonizing the adenosine receptor will prevent the ischemia-induced activation of p38 MAPK and the subsequent protection (Nakano *et al.*, 2000a). As well,

using an agonist to activate the adenosine receptor will induce a protective effect that can be prevented if p38 MAPK is inhibited (Ballard-Croft *et al.*, 2005).

p38 MAPK Inhibition as a Protective Mechanism

Insulin pretreatment and ischemic pre-conditioning both appear to require p38 MAPK function to generate the protective effect in ischemia-reperfusion injury. Such a requirement might appear to be paradoxical, because inhibition of p38 MAPK can reduce injury associated with ischemia-reperfusion. In Langendorff-perfused rabbit hearts, inhibition of p38 MAPK (via infusion with inhibitor) increased functional recovery of hearts during reperfusion and also decreased necrosis observed after reperfusion (Ma *et al.*, 1999). Rats subjected to ischemia-reperfusion using occlusion of the left anterior descending coronary artery had increased indicators of apoptosis in their hearts four hours after reperfusion; an injection of inhibitor before onset of reperfusion reduced apoptosis induced by reperfusion (Gao *et al.*, 2004). One key to the paradox might be an effect during reperfusion, both ischemic pre-conditioning and p38 MAPK inhibition prevent reperfusion-induced p38 MAPK phosphorylation (Moolman *et al.*, 2006).

p38 MAPK and Ischemia-Reperfusion Injury

As mentioned, the inhibition of p38 MAPK during ischemia-reperfusion is associated with reduced injury due to reperfusion. There are multiple putative routes by which activated p38 MAPK can be associated with increased injury during ischemia-reperfusion.

Ischemia is associated with the activation of p38 MAPK, specifically through the phosphorylation of a dual Thr-Gly-Tyr motif (Raingeaud *et al.*, 1995). In cardiac

ischemia, p38 MAPK is activated by MAPK Kinase 3 and MAPK Kinase 6 (MKK3 and MKK6). Of these, MKK6 is preferentially activated by apoptosis signal-regulating kinase (ASK)1. As well, c-Jun N-terminal kinase (JNK; the other Stress-Activated Protein Kinase) is not activated as rapidly during cardiac ischemia (Harding *et al.*, 2010). Both JNK and p38 MAPK activation is transient, with p38 MAPK activation peaking more quickly and decaying more quickly (Shimizu *et al.*, 1998). During chemical hypoxia in cardiomyoctyes, p38 MAPK is also activated by Protein Kinase C ε (PKCε), and inhibition of either kinase reduces cell death (Jung *et al.*, 2004).

During ischemia, some p38 MAPK activity becomes associated with the mitochondria. Activated p38 MAPK translocates to the mitochondria and increases phosphorylation of αB-crystallin (a small heat shock protein, detailed below) via an intermediary protein, MAPK Activated Protein Kinase 2 (MK2). The phosphorylation of αB-crystallin inhibits mitochondrial membrane disruption (Whittaker *et al.*, 2009). On the other hand, p38 MAPK activation of MK2 during ischemia might activate Bax, an apoptosis-inducing protein (Capano and Crompton, 2006).

p38 MAPK is involved in three aspects of reperfusion-associated injury: reactive-oxygen species (ROS) production, gene activation, and cytoskeletal reorganization (Figure 1.1). p38 MAPK is rapidly activated during reperfusion, however activation will decay with continued reperfusion. Experiments in both cardiomyocytes (Kim *et al.*, 2006) and heart tissue (Yue *et al.*, 2002) suggest that ROS production activates p38 the mitochondrial pore protein Voltage Dependant Anion Channel 1 (VDAC-1; phosphorylation of VDAC-1 increases mitochondrial membrane permeability and increases cytoplasmic ROS as a consequence). Inhibition of p38 MAPK inhibited

phosphorylation of VDAC-1 induced by selenium (Tomasello *et al.*, 2009) and inhibited phosphorylation of VDAC-1 observed after ischemia-reperfusion (Schwertz *et al.*, 2007).

Phosphorylated p38 MAPK activates transcription factors (reviewed in Rose *et al.*, 2010). Many of these activated transcription factors are important during development or during cellular division. That said, many stresses, including ischemic-preconditioning (Maulik *et al.*, 2008), also increase phosphorylated levels of p38 MAPK that acts as a kinase in the nucleus to then activate transcription factors. The activated transcription factors regulate heart remodeling after injury. For example, in pig myocardium, ischemia causes Activating Transcription Factor-2 (ATF-2) to become phosphorylated, and inhibiting p38 MAPK will reduce this phosphorylation (Barancik *et al.*, 2000). Cultured rat neonatal cardiomyocytes have increased levels of phosphorylated Myocyte Enhancer Factor-2 (MEF-2) during hypoxia, and inhibiting p38 MAPK reduces this increase (Zhang *et al.*, 2010). Overexpression of MKK6, a p38 MAPK activator, in neonatal ventricular myocytes, increases activation of p38 MAPK and thus the phosphorylation of the Serum Response Factor (SRF) co-activator Activating Transcription Factor-6 (ATF-6), and pharmacological inhibition of p38 MAPK prevented this effect (Thuerauf *et al.*, 1998). Phosphorylated p38 MAPK can be in both the cytoplasm and the nuclei of cardiomyocytes, and the mechanism causing phosphorylated p38 MAPK to migrate between the nuclei and cytoplasm are not well understood (Gorog *et al.*, 2009). The p38 MAPK kinases, MKK3 and MKK6 are found in both the cytoplasm and nuclei of cells (Ben-Levy *et al.*, 1998).

One mechanism by which we can measure p38 MAPK activation within the nucleus is with MK2. p38 MAPK does not have a known nuclear export signal and is

believed to bind to MK2 within the nucleus in order to leave the nucleus. MK2 contains a nuclear localization signal that is masked by binding to p38 MAPK, and the nuclear export signal of MK2 is exposed when MK2 is phosphorylated (Meng *et al.*, 2002). MK2 is phosphorylated by p38 MAPK at four sites, but the phosphorylation of MK2 Thr 334 is necessary for the function of the nuclear export signal (Ben-Levy *et al.*, 1998; Engel *et al.*, 1998). The MK2/p38 MAPK heterodimer is believed to be kinase-inactive while they are dephosphorylated (Haar *et al.*, 2007), and the phosphorylated forms have a lower affinity for each other (~10 X) than the dephosphorylated heterodimer (Lukas *et al.*, 2004). In other words, activated p38 MAPK within the nucleus will phosphorylate MK2. The activated heterodimer will leave the nucleus and potentially dissociate into individual enzymes. Because activated p38 MAPK heterodimerized with MK2 can leave the nucleus, one indicator of nuclear export of activated p38 MAPK can be through the action of MK2. Activated MK2 will phosphorylate the 27 kilo-Dalton (kDa) Heat Shock Protein, Hsp27 (Stokoe *et al.*, 1992).

Heat Shock Proteins and Hsp27

The intra-cellular milieu is dense, crowded, and energetic. These close quarters often result in unfavorable interactions that cause misfolding of proteins. In order to compensate, cells produce chaperone proteins that interact with misfolded proteins. Up to 5% of the cell mass can consist of chaperone proteins (Linquist, 2010). These proteins correct the folding of other proteins or target misfolded proteins for degradation. Heat Shock Proteins (HSP) are a major class of chaperone proteins and are commonly activated and/or synthesized when the cell is under stress. HSPs are so named because their presence in cells was first observed after cells had been exposed to non-lethal

hyperthermia (Ritossa, 1962; Moran *et al.*, 1978).

There are eight families of HSP in mammals (Noble *et al.*, 2008), and the names are derived from the kDa mass of the proteins. These families are: large Hsp (> 110 kDa), Hsp90 (~ 90 kDa), Hsp70 (~ 70 kDa), Hsp60 (~ 60 kDa), Hsp40 (~ 40 kDa), Hsp32 (~ 32 kDa), "small Hsps" (< 30 kDa), and Hsp10 (~10 kDa). Hsp32 and Hsp10 are not always classified as an HSP in humans (Kampinga *et al.*, 2009). HSPs are induced by hyperthermia and other stressors (e.g., alcohol, anoxia, heavy metals, oxidative stress, hormones, and high pH; Whitesell *et al.*, 2003; Zhang *et al.*, 2002). HSP production is associated with increased resistance to further metabolic insults.

HSP genes can be activated by cell stress, and HSP genes are regulated by the Heat Shock (transcription) Factor (HSF) protein, HSF1. Briefly, HSF1 is inhibited by the constitutively expressed Hsp90. Many of the Hsp90 client proteins require an intracellular signal to complete folding (e.g., the triggering of a signal cascade), and so Hsp90 is highly expressed although functionally sequestered due to its affinity for these "incompletely" folded proteins (Lindquist, 2010). In the event of a cellular stress, Hsp90 is more attracted to denatured proteins than to HSF1, liberating HSF1. HSF1 is maintained in a monomeric state by Hsp90 (Zou *et al.*, 1998) and release of HSF1 exposes phosphorylated serine 121. Dephosphorylation of HSF1 at serine 121 causes a conformational shift that decreases its affinity for Hsp90, induces trimerization, and causes nuclear localization. HSP gene promoters contain the Heat Shock Element. Trimerized HSF1 associates with the Heat Shock Element and initiates the transcription of HSP genes (Morimoto, 1993). Cellular stress also activates pathways that appear to inhibit HSP production. An example repressor of HSF1 is that stress-activated

Extracellular-Signal-Regulated Kinase 1/2 (EKR1/2) leads to phosphorylation of HSF1 on serines 303 and 307 and reduces the binding to the Heat Shock Element (Wang *et al.*, 2003). As well, stress-activated MK2 phosphorylates serine 121 of HSF1 and increases the affinity of HSF1 for Hsp90 (Wang *et al.*, 2006). The paradoxical effect of stress-related pathways on HSF1 warrant further investigation.

One family of the HSPs is "small HSPs" (sHSPs). sHsps are characterized by an α-crystallin domain flanked by C- and N- terminal sequences. The α-crystallin domain is highly conserved and is found in archaea, bacteria, and eukarya. α-Crystallin is named because of its discovery in the lens of the vertebrate eye, where it is in high abundance. This domain is (on average) 94 amino-acids long and only the fungi commonly contain insertions within this domain. The C- and N-terminals are highly variable and determine the function of the sHsp. The number of sHsp genes correlates with genome size and gene duplication events were common in multicellular eukaryote history. There are nine human sHsps, however they are not completely conserved amongst the primates (Kriehuber *et al.*, 2010).

HspB1, a member of the sHsp family, is an ATP-independent chaperone and is found in mammals, birds, fish, reptiles, and amphibians (Franck, 2004). In addition to the α-crystallin domain, HspB1 contains a weakly conserved WDPF (Trp, Asp, Pro, Phe) domain in the N-terminal. In rats and humans, HspB1 is commonly called Hsp27. The N-terminal region is essential for oligomerisation while the C-terminal region is required for protein interactions and protein solubility. The N-terminal contains phosphorylatable serines that are important for protein function. Human Hsp27 has three phosphorylatable serines, while rats and mice have two. Human Hsp27 serine 78 can be phosphorylated,

but is not found in rodents. The other two of the phosphorylatable serines (Hsp27 serine 15 and Hsp27 serine 82) are conserved between humans and rats (Kostenko and Moens, 2009). Mouse HspB1 also contains serine 15, and mouse serine 86 is homologous to serine 82 (of rat or human HspB1) and so can be phosphorylated (Stokoe, 1992). These phosphorylation sites are important for protein function. For example, experiments comparing non-phosphorylatable mutants (substituting serine for nonphosphorylatable amino acids or for phospho-mimic amino acids) show that serine phosphorylation is a component of protecting the cell against heat stress and cytochalasin D-induced disruption (Lavoie *et al.*, 1995), that it affects the ability to confer resistance to oxidative stress (Huot *et al.*, 1995), and that it controls whether Hsp27 disrupts cell proliferation (Salinthone, 2007). The oligomerization state of Hsp27 is also associated with function. For example, while phosphorylation of Hsp27 affects oligomerization state, it is the oligomerization state that affects the ability of Hsp27 to confer resistance to Tumor Necrosis Factor-α (TNF-α; Mehlen *et al.*, 1997). Oligomerization can be independent of phosphorylation state. For example, Mehlen *et al.* (1997) substituted serines for non-phosphorylatable hydrophobic amino acids (Ala or Gly) that resulted in different oligomer sizes, and the size of the oligomer affected TNF-α resistance. In general, however, smaller oligomers (< 150 kDa) are associated with protecting a cell during filamentous actin disruption. Larger oligomers (> 450 kDa) are associated with inhibiting apoptotic signals (Paul *et al.*, 2010).

Hsp27 serine 82 is phosphorylated *in vivo* by MK2, MK5, AKT/Protein Kinase B (AKT/PKB), and Protein Kinase D (PKD). MK2 also phosphorylates Hsp27 serine 15. These kinases each have upstream regulators. MK2 is activated by p38 MAPK and

activation is associated with cell exposure to cytokines and cellular stress (Clifton *et al.*, 1996). MK5 (also known as p38-regulated/activated protein kinase (PRAK)) is activated via p38 MAPK by cellular stressors such as anisomycin, TNF-α, or oxidative stress. By mass, activated MK2 and MK5 phosphorylate Hsp27 to a similar intensity (though this might be a ceiling effect; New *et al.*, 1998), but mouse embryonic fibroblasts that were null for either MK2 or MK5 give clearly different results. MK2-/- fibroblasts do not phosphorylate HspB1 after stimulation of the p38 MAPK pathway (using arsenite or ultraviolet treatments), but MK5-/- fibroblasts phosphorylate HspB1 after arsenite treatment (Shi *et al.*, 2003). MK5 appears to have less relative effect upon Hsp27 compared to MK2 *in vivo*. Alternatively to p38 MAPK, ERK3 and ERK4 activate MK5 (Aberg *et al.*, 2009), but the physiological role of these atypical mitogens is associated with developmental effects (Rousseau *et al.*, 2010) and their activation is not enhanced through mitogenic or stressful stimuli (Déléris *et al.*, 2008). Insulin-induced activation of AKT/PKB will be discussed, however phosphatidylinositol 3-kinase (PI3K) is also activated by the transmembrane Trysosine Receptor Kinase class of proteins (see Schlessinger, 2000 for review) and so AKT/PKB (a.k.a. AKT) is activated by stimuli other than insulin. AKT can reduce p38 MAPK activity (Manning and Cantley, 2007) by inhibiting multiple kinases upstream of p38 MAPK, but also phosphorylates Hsp27 serine 82 *in vitro* and might contribute some of the phosphorylation *in vivo* (Rane *et al.,* 2003). Finally, activated PKD can phosphorylate Hsp27 serine 82 *in vitro* (Döppler et al., 2005) and *in vivo* (e.g., in order to repress androgen receptors in prostate cancer cells (Hassan *et al.*, 2009) or through activation by vascular endothelial growth factor (Evans *et al.*, 2008)), but PKD phosphorylation of Hsp27 serine 82 is not broadly observed in

multiple cell types. Interestingly, Hsp27 serine 82 phosphorylation can result in the activation of PKD, as seen in diabetic cardiomyocytes. Briefly, MK2-induces phosphorylation of Hsp27 serine 86 in murine HspB1 (Hsp25) and this disinhibits it from Protein Kinase C (PKC) δ. Activated PKCδ then phosphorylates PKD, and is an important step of increasing lipid metabolism in diabetic cardiomyocytes (Kim *et al.*, 2008). Thus, it appears that Hsp27 serine 82 phosphorylation releases suppression of PKC and vis versa (Tanabe *et al.*, 2008).

The Insulin Polypeptide

The insulin polypeptide contains an A-chain and a B-chain connected via two disulfide bridges. The insulin gene is transcribed and translated into preproinsulin and is directed to the endoplasmic reticulum where an N-terminal sequence is cleaved to form proinsulin (reviewed by Bell, 1980). En route to the Golgi network, the middle portion, the 'C-peptide', promotes the binding of the intra-A-chain disulfide bond as well as the A-chain to the B-chain via disulfide bridges (reviewed by Steiner *et al.*, 1980). Proinsulin forms hexamers in the trans-Golgi network, and while in secretory granules the C-peptide is cleaved away and leaves insulin hexamers. The hexamers dissociate to the active monomer form once insulin is secreted from pancreatic beta cells (Osterbye *et al.*, 2001).

The human preproinsulin gene is located on the distal end of the short arm of chromosome 11 (Harper *et al.*, 1981) and contains an untranslated intron within the 'C' portion of the gene. In comparison, laboratory rats and mice contain two variants of the preproinsulin gene. Preproinsulin-2 is homologous to the human preproinsulin gene, and resides on chromosome 1 for the rat and chromosome 7 for the mouse. The

preproinsulin-1 genes do not contain an intron within the 'C' portion of the gene and is considered a retroposon. This gene is also on chromosome 1 in the rat and is on chromosome 6 in the mouse (Soares *et al.*, 1985).

Causes of Insulin Release

The normal biology of insulin has been explored for some time. John Macleod and Frederick Banting received the 1923 Nobel Prize in Physiology or Medicine for the discovery of insulin as the blood-glucose-lowering hormone produced in the pancreas. Insulin is the main blood-glucose-lowering hormone. The pancreatic islets release insulin in response to a rise in blood glucose levels. Insulin triggers the uptake and storage of blood glucose in the liver. Conversely, a decrease in blood glucose signals the pancreatic islets to release glucagon. Glucagon stimulates hepatocytes to produce and release glucose into the blood via transporter facilitated diffusion (Thorens, 1996). Insulin secretion occurs in an oscillatory manner every 5 – 10 minutes. Oscillatory cycling is considered to protect the presentation of the insulin receptor on the surface membrane. In support of this belief, pulsatile insulin secretion is more effective in lowering blood glucose than continuous infusion (Matthews *et al.*, 1983). In comparison, insulin being released according to an extended cycle (such as, experimental interventions that control and slow insulin blood cycles (by suppressing the pancreas and artificially introducing insulin), the slowing of the cycle associated with aging, and cycle disruption associated with noninsulin-dependent diabetes) is less effective in lowering blood glucose compared to healthy subjects (reviewed in Paolisso *et al.*, 1991). Within islets, beta cell synchronization is coordinated through gap junctions (Benninger *et al.*, 2008). Between islets, insulin-release cycles are due to oscillations in blood glucose. In other words,

insulin release is followed by a decrease in blood glucose, and this drop in blood sugar stops beta cells from releasing insulin.

Insulin release is under multiple forms of control. A rise in blood glucose causes increased transport of glucose into the pancreatic beta cell through facilitated diffusion transport. Glucose undergoes glycolysis and the rise in ATP/ADP causes ATP-sensitive potassium channels to close (Henquin 2000). The resulting depolarization of membrane potential results in an influx of calcium cations through voltage-gated calcium channels and the cations induce insulin release (Nunemaker *et al.*, 2009). Insulin release can also be affected by changes in relative plasma amino acid concentrations (Martin and Soria, 1995), by free fatty acids that increase secretion (Haber *et al.*, 2006), and through neuroendocrine actions of somatostatin, adrenaline and noradrenaline that suppress insulin release (Hauge-Evans *et al.*, 2009; Miller, 1981) or through acetylcholine that induces insulin release (Lechin and van der Dijs, 2006).

Insulin Signal Transduction

Monomeric insulin will affect a cell through two routes. Insulin binds to transmembrane insulin receptors that activate tyrosine kinases known as Insulin Receptor Substrate (IRS) proteins. Insulin can also bind to Insulin-like Growth Factor Receptors and activate other kinase effects. Both routes can activate two main intracellular cascades: the PI3K–AKT/ PKB pathway, and the Ras–MAPK pathway. Due to isoforms, there are a multitude of potential routes an insulin signal may take once it activates a receptor (Taniguchi *et al.*, 2006).

Each pathway begins at a receptor. There are three receptors for insulin: the two Insulin Receptors (IR) and one of the Insulin-like Growth Factor (IGF) Receptors, IGF

Receptor-1 (note that IGF Receptor -2, the other IGF Receptor, cannot bind insulin). The heterotetramer IGF Receptors are not important in adipose and hepatic glucose regulation, but do affect muscle glucose uptake in normal conditions (Binoux, 1995). The two IGF Receptor genes are more similar to the IR-A isoform than the IR-B isoform (see below). The IRs are produced by one gene in mammals: the IR-A is expressed mainly in development or in mitogenic cells; unlike IGF Receptor and IR-A, IR-B is transcribed with an additional exon and is the dominant metabolic receptor. IR-B is the most important receptor for insulin function in both the liver and pancreas and the most numerous insulin receptor in adipose and skeletal muscle tissue. Like IGF Receptor -1, IR-A and IR-B are heterotetramers and contain two extracellular domains and two intracellular domains. The intracellular domains each contain phosphotyrosine binding sites, a protein kinase domain for auto- and substrate-phosphorylation, and a docking site for IRS proteins (Belfiore *et al.*, 2009). Despite the strong homologies between IGF Receptor and IR proteins, IGF-1 shows 100 X more affinity for IGF Receptor -1 than insulin does. Binding of insulin causes a conformational shift that increases autophosphorylation of the receptor as well as phosphorylation of IRS (Vardatsikos *et al.*, 2009).

There are six mammalian IRS proteins (Taniguchi, 2006). IRS-1 and IRS-2 are in many tissues. IRS-3 functions in liver, adipocyte, brain, and fibroblast cells. IRS-4 is expressed in muscle tissues. IRS-5 and -6 do not contribute to insulin metabolic signaling. In most cases, IRS-1 is considered to be the key mediator of the insulin-induced metabolic pathway (Flati *et al.*, 2009). IRS proteins contain an exposed pleckstrin homology (PH) domain, and proteins containing this domain are attracted to

the cell membrane. As well, IRS proteins contain phosphotyrosine-binding domains and tyrosines available for phosphorylation via IRs and downstream negative-feedback mechanisms (Dupont *et al.*, 2009).

Insulin Signaling Pathways

The mitogenic Ras (Figure 1.2) pathway begins with IRS-1 causing a complexing of Grb2 with Sos, this activates Sos that then exchanges GTP for GDP on Ras. Ras is a kinase for c-Raf , and c-Raf is activated to phosphorylate MAPK Kinases (MKK). There are at least four families of downstream MAPKs (JNK, ERK1/2, ERK5, and p38 MAPK). Activated JNK will inhibit IRS-1 via phosphorylation of serine 307. This is a negative-feedback loop for the Ras pathway (Zick, 2001) but not a major one (Rui *et al.*, 2001). Activated ERK will phosphorylate Sos and sequester Sos (or the Sos/Grb2 complex) from the cell membrane (Buday *et al.*, 1995; Chen *et al.*, 1996). The Ras pathway is considered mitogenic because dominant negative mutations of Ras, Sos, or Grb2 do not change glucose metabolism, but do reduce the effect of insulin on DNA synthesis (Ogawa *et al.*, 1998). This pathway is similarly described for IGF Receptor activation, though the IGF Receptor -1 canonical pathway is described to preferentially activate ERK1/2 over p38 MAPK; p38 MAPK is considered a stress-response protein in the IGF Receptor pathway (Vardatsikos *et al.*, 2009). Of the MKKs, MKK 6 is the main kinase for the p38 MAPK family (Yong, 2009) and is activated by insulin (Fujishiro, 2001).

The metabolic PI3K-AKT/PKB pathway (Figure 1.2) begins with the IRS activating a two-protein lipid kinase (class I PI3K) that acts to phosphorylate membrane-bound phosphatidylinositol 4,5-bisphosphate (PIP2) to create the intramembrane

secondary messenger phosphatidylinositol (3,4,5)-trisphosphate (PIP3). AKT/PKB also contains a PH domain, and the domain attracts AKT/PKB to the cell membrane, especially when PIP3 concentrations increase. Once near the membrane, AKT/PKB is activated by phosphorylation of serine 473 by mTORC2 and threonine 308 by phosphoinositide-dependant kinase-1 or DNA-dependent protein kinase (Bozulic and Hemmings, 2009). AKT/PKB activation contributes to a feedback cycle for insulin: AKT/PKB might also phosphorylate IRS-1 at serine 307 to reduce its responsiveness to the insulin receptor (Lawlor and Alessi, 2001). Again, this canonical pathway is similar for IGF1R activation, the only different constituents are the receptor and agonist (Vardatsikos *et al.*, 2009).

AKT can go on to phosphorylate Akt substrate of 160 kDa (AS160). Phosphorylation of AS160 is associated with a shift of the cellular equilibrium of the main glucose transporter (GLUT4) for muscle and adipose cells, between an intracellular pool and the cell membrane. Before insulin pathway activation, 90% of the GLUT4 proteins are separated from the cell membrane in intracellular membrane pools, although there is flux between the surface and non-surface pools. With insulin signaling, the flux shifts so that 50% of GLUT4 is retained within the cell membrane (Leney and Tavaré, 2009). AS160 controls GLUT4 flux, though the relationship is not simple. Knockdown of AS160 with siRNA increases GLUT4 flux to the cell membrane (Eguez *et al.*, 2005) but inhibiting AS160 action with a dominant-negative mutant decreases GLUT4 flux to the cell membrane (Zeigerer *et al.*, 2004).

Hypothesis Introduction

As discussed, cellular stress can cause the activation of p38 MAPK. The activation of p38 MAPK is associated with increased cellular damage, such as ROS created during reperfusion. Inhibiting p38 MAPK can reduce the damage caused by ischemia/reperfusion. In comparison, insulin is known to reduce damage associated with reperfusion injury in cardiac tissue. Historically these doses have been sufficient to risk hypoglycemia in people (see Cheung *et al.*, 2006, for review). A dose that does not change blood sugar levels (Li *et al.*, 2004) can protect contractile function after ischemia/reperfusion (Li *et al.*, 2008). This protection of contractile function was dependent upon p38 MAPK function.

Normally p38 MAPK is activated through dual phosphorylation while in the cytoplasm and that the resulting conformational change unmasks a (putative) phosphorylation-dependent nuclear localization signal (Gong *et al.*, 2010). Also, p38 MAPK can be activated while in the nucleus. Once in the nucleus, p38 MAPK binds with MK2 and phosphorylates it. The resulting complex conceals a nuclear localization signal on MK2, and the phosphorylation of MK2 reveals a nuclear export signal allowing the two activated proteins to leave the nucleus (Zheng *et al.*, 2006). Activated MK2 in the cytoplasm will phosphorylate Hsp27. Dephosphorylation of p38 MAPK also increases the likelihood that it will exit from the nucleus (Gong *et al.*, 2010).

Hsp27 is also involved with p38 MAPK. Hsp27 constitutively binds p38 MAPK while both are non-phosphorylated. p38 MAPK phosphorylation decreases the affinity for Hsp27. Similarly, phosphorylation of Hsp27 also decreases its affinity for p38 MAPK. Because activated p38 MAPK migrates to the nucleus, p38 MAPK can be

dissociated from Hsp27 within the nucleus, due to activated MK2 phosphorylating Hsp27 (Zheng *et al.*, 2006).

Metabolic stress signaling causes the phosphorylation of p38 MAPK and its migration to the nucleus. Insulin signaling activates proteins upstream of both Hsp27 and p38 MAPK. If both stress and insulin are occurring at the same time, the two signaling systems might compete for access to the p38 MAPK (and its function) despite both signaling pathways being involved in the phosphorylation of p38 MAPK.

Hypothesis

Using cell culture and oxygen-glucose deprivation (OGD) followed by reoxygenation, as well as insulin, I predict that stressing H9c2 cardiomyocytes will increase Hsp27 phosphorylation. However, treating H9c2 cells with insulin will cause phosphorylation of p38 MAPK but prevent the stress-induced increase of phosphorylated p38 MAPK in the nucleus. The functional sequestration of p38 MAPK from the stress-induced cascade will prevent phospho-p38 MAPK from activating MK2 and causing stress-induced increase in Hsp27 serine 82 phosphorylation.

Figure 1.1. Mechanisms by which p38 MAPK activates indicators of cellular distress. Cellular stress activates the canonical and alternate MAPK pathways. MAPK Kinase Kinases activate (MAP3K) to phosphorylate MAPK Kinases. The MAPK Kinases phosphorylate p38 MAPK. Phospho-p38 MAPK can migrate to the mitochondria where it induces the phosphorylation of a mitochondrial outer membrane pore-forming protein VDAC-1. Phosphorylation of VDAC-1 increases ROS in the perimitochondrial area. The presence of ROS also causes activation of p38 MAPK, and is a potential positive feedback mechanism. Alternatively, phospho-p38 MAPK can translocate to the nucleus where it is an important activator of transcription factors associated with cellular distress such at ATF-2, SRF, and MEF2. mt = mitochondria; MAP3K = MAPK Kinase Kinase

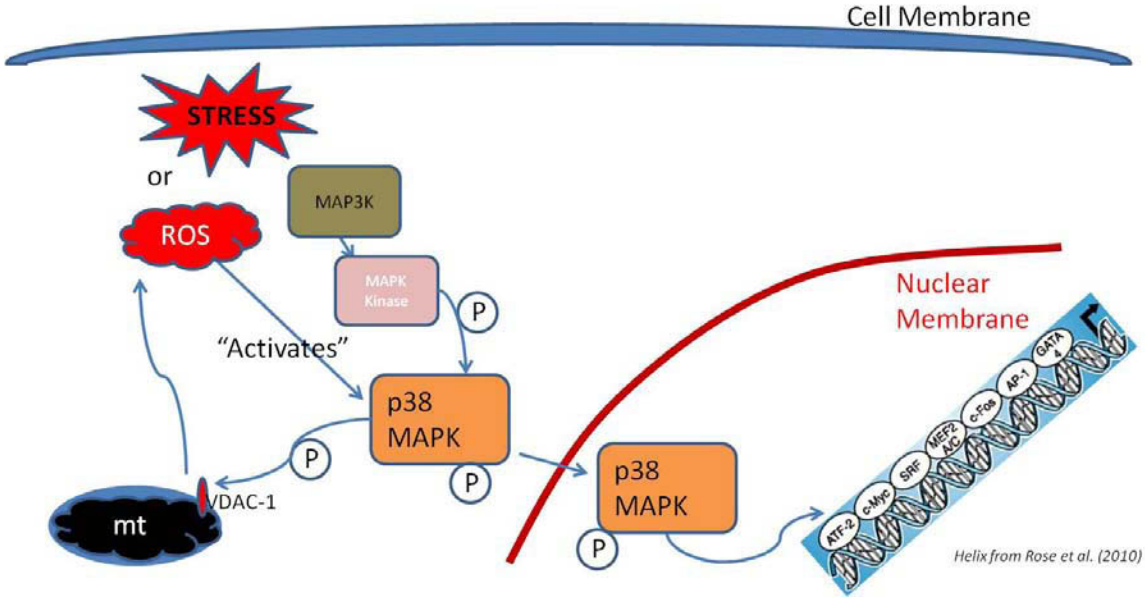
Cell Membrane
STRESS
or
ROS
MAP3K
MAPK Kinase
P
"Activates"
p38 MAPK
P
P
VDAC-1
mt
Nuclear Membrane
p38 MAPK
P
ATF-2
c-Myc
SRF
MEF2 A/C
c-Fos
AP-1
GATA 4
Helix from Rose et al. (2010)

Figure 1.1.

Figure 1.2. The canonical insulin pathways to kinases of HSP27.

In the Ras-Raf-MAPK pathway, the activated Insulin Receptor Substrate (IRS) acts as a scaffold to induce complexing of Grb2 with Sos; it must be near the cell surface to be available to IRS-1. Complexed Sos is a GTP exchanger replacing a GDP for a GTP on Ras. Ras becomes a kinase for c-Raf, which then phosphorylates MAPK Kinase. MAPK Kinase phosphorylates p38 MAPK. p38 MAPK also phosphorylates Sos to inactivate it as part of a negative feedback loop. p38 MAPK phosphorylates MK2, which is a kinase for Hsp27 serine 82

The PI3K-AKT/PKB pathway activates the two-protein complex PI3K that converts PIP_2 to the intramembrane messenger PIP_3. The accumulation of PIP_3 promotes the migration of AKT/PKB to the membrane where it is phosphorylated by mTORC2 and phosphoinositide-dependant kinase-1. Activated AKT can phosphorylate AS160. This enzyme induces the mobilization of the glucose transporter GLUT4 from cytosolic stores to the surface membrane. Additionally, activated AKT/PKB will phosphorylate Hsp27 at serine 82.

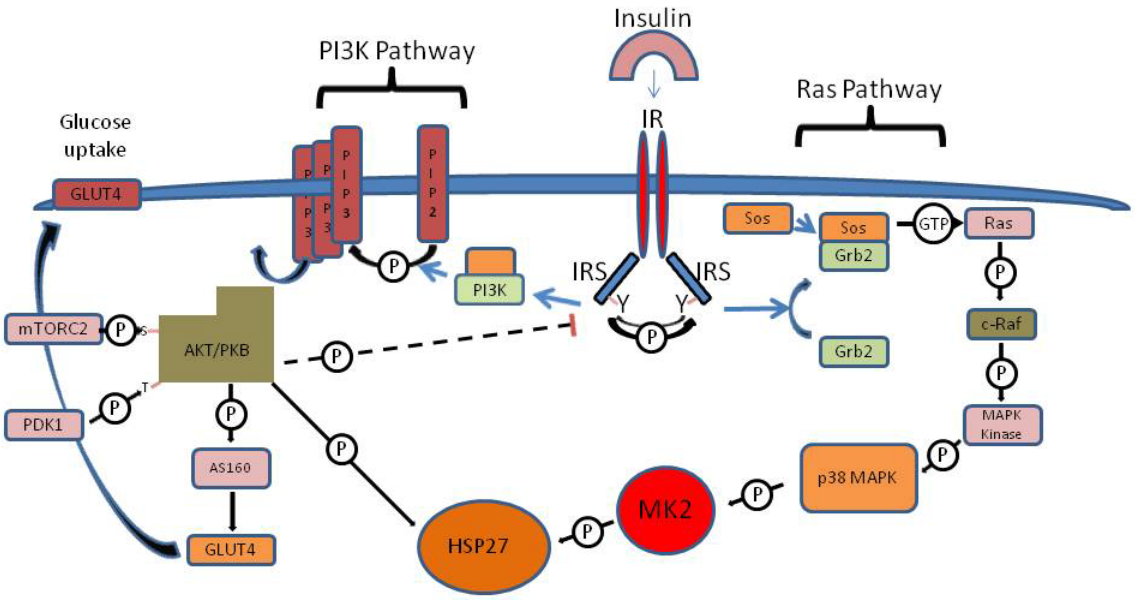
Insulin
PI3K Pathway
Ras Pathway
IR
Glucose uptake
GLUT4
PIP3
PIP2
Sos
Grb2
GTP
Ras
PI3K
IRS
IRS
Y
Y
mTORC2
AKT/PKB
c-Raf
PDK1
MAPK Kinase
AS160
p38 MAPK
MK2
HSP27
GLUT4
P

Figure 1.2.

CHAPTER 2: MATERIALS AND METHODS

Cell Culture

H9c2 rat neonate cardiomyocyte cells (ATTC; Cat. # CRL-1446; lot # 58279608, passage #13) were incubated and maintained at 37 °C in air supplemented with 5% CO_2. Proliferative media (PM) was Dulbecco's Modified Eagle Media (DMEM; from ATTC # 30-2002) supplemented with 1% Penicillin-Streptomycin (Gibco 15140) and 10% Fetal Bovine Serum (FBS; Gibco 12483). Media was refreshed every two days. All experiments were performed using cells between passages 19 and 24 to limit differentiation into fibroblasts.

Passaging

H9c2 cardiomyocytes were passaged upon reaching 80% confluence as follows. PM was aspirated and 1 ml of TrypLE Express (Gibco 12604) was added to dilute any remaining media. After a second aspiration, 2 ml of TrypLE was added and the cells were allowed to lift into suspension, taking care to not bump samples and so to avoid clumping. The TrypLE was inactivated with additional PM and the cells pelleted via centrifugation. After decanting, the cells were resuspended and counted. 1.2×10^5 cells were added to 20 ml of CO_2-conditioned media and incubated in 75 cm^2 flasks .

Preparation of sample trays consisted of the same protocol as passaging, however 4×10^4 cells were added to each well of a six-well tray containing 2 ml of CO_2-conditioned media and incubated. Cells were grown to 40% confluence with PM being refreshed every two days until beginning differentiation. 40% confluence was reached in 2-3 days.

Differentiation

Upon reaching 40% confluence, PM from sample trays was removed and cells were refreshed with Differentiating Media (DM; DMEM supplemented with 1% pen/strep and 1% FBS). Cells were allowed to differentiate for 6 days. DM was refreshed every two days.

Treatment

Cells were subjected to the following conditions, after six days of differentiation. Control (CON): cells were kept in the original DM, but were removed from the incubator for the same length of time other cells were. No Insulin (No Ins): cells had DM aspirated and replaced with fresh DM. Insulin-treated (INS): cells had DM aspirated and replaced with 2 ml of DM supplemented with 200 μU/ml insulin. Insulin supplementation of 20 and 2,000 μU/ml was also tested. Oxygen-glucose deprivation (OGD) conditions were generated thusly: the day before experiment, no-glucose, no-pyruvate DMEM (Gibco #11966) was placed into a sealed Modular Incubator Chamber (bullups-rothenberg) that was fully flushed with anoxic gas (5% CO_2, 5% H_2, 90% N_2; Praxair). The chamber was placed into a 37 °C incubator for at least four hours. The chamber was reflushed with anoxic gas, and the chamber incubated at 37 °C overnight. For OGD treatment, cells had DM aspirated and OGD media added. The cells were placed into the chamber and fully flushed with anoxic gas and placed into a 37 °C incubator. OGD was also supplemented with insulin. Before placing OGD media onto cells, insulin was added (200 μU/ml) to the media. The cells were then placed into the chamber and treated identically to OGD-treated cells. Reoxygenation: cells were removed from anoxic conditions and media aspirated. Fresh DM was added to the cells and the cells were incubated at 37 °C for one

or two hours. After treatment, cells were collected. Note 200 μU/ml insulin = 1.2 nmol/L insulin = 7.7 ng/ml (Volund, 1993).

Collection

After treatment, wells were washed twice with ice-cold 0.1 M sodium phosphate buffer (pH 7.4) and then treated with 80 μl of Sample Buffer (95% Laemmli Sample Buffer (Biorad) + 5.0% β-mercaptoethanol)) mixed with 100 μl of Homogenising Buffer (0.32 M sucrose in 0.1 M sodium phosphate buffer (ph 7.4), and including one Roche Complete Mini protease inhibitor tablet per 10 ml). The trays were immediately frozen to -80 °C until thawed and samples placed into microtubes and refrozen.

Western Analysis

Samples were thawed and heated to 95 °C for 20 minutes. Samples were then cooled to room temperature before loading onto gels. Samples were not cooled on ice, because the samples would thicken too much to allow accurate loading. For Hsp27 quantification, 15 well, 10%, 1 mm thick gels were loaded with 3 μl of sample. Samples were run through the 2.5% loading gel at 75 V for 20 minutes and then run at 125 V for 75 minutes through the lower gel. For p38 MAPK quantification, 12% gels were used and the run was for 155 minutes. Protein was then transferred onto polyvinylidene fluoride (PVDF) membrane (Millipore Immobilon-P) at 100 V for one hour. All PVDF membranes were allowed to dry for at least one hour, and at least 20 minutes after marking with a solvent-resistant pen, before beginning immunochemistry.

All membranes were wet in methanol and blocked for at least one hour in 5% skim milk power (Hsp27 analysis) or 5% bovine serum albumin (p38 MAPK analysis) dissolved in Tris-Buffered Saline with 0.1% Tween-20 (Sigma)(TBS-T). Primary antibodies were suspended in the same buffer as was used to block the membrane. The membrane and antibodies were sealed in a plastic bag overnight at 4 °C, with light agitation. Membranes were rinsed the next day in TBS-T (2 quick rinses, 1 X 30 minutes, 3 X 5 minutes) before immersion in secondary antibody (1:10,000 goat anti-rabbit HRP, Santa Cruz, sc-2301) for 1 hr. After a second round of rinsing, the horseradish peroxidase was exposed using an ECL-plus kit from GE Healthcare. Digital images of the membranes were captured on a Storm 840 (Amersham Biosciences). Densitometric analysis was performed using ImageQuant TL (version 2005; Amersham Biosciences).

Mouse anti-IRβ (1:10,000; Assay Designs #905-683-100) and goat anti-mouse (1:7,000; Santa Cruz Biotechnology, inc. # sc-2302) antibodies were used to confirm the presence of Insulin Receptor β in 6-day differentiated cells. The following primary antibodies were also used, and all were raised in rabbit. Hsp27 (StressGen SPA-801E) at 1:20,000 dilution. Hsp27 phosphorylation at serine 82 (StressGen SPA-524PU) at 1:20,000 dilution. Actin (Sigma A2066) at 1:20,000 dilution. p38 MAPK (StressGen KAS-MA009) at 1:10,000 dilution. Phosphorylated Thr180/Tyr182 of p38 MAPK (PhosphoSpecific Solutions Inc.; p190-1803) at 1:1000 dilution. All antibodies were suspended in the same solution as was used for blocking.

Calf Intestinal Alkaline Phosphatase (New England Biolabs, M0290S) was used to confirm the antibody specificity for phosphorylated p38 MAPK and Hsp27. Cells

were removed from the incubator, washed twice with phosphate buffer, and dissociated using 100 µl of homogenizing buffer. 20 units of phosphatase (prepared according to manufacturer instruction) was added and the solution was transferred to a microtube and allowed to incubate at room temperature for 30 minutes. 70 µl of sample buffer was added, and samples frozen until Western analysis. Additionally, after PVDF transfer during Western analysis, 100 units of phosphatase was placed on the membrane for one hour. This additional step allowed the dephosphorylation of any phospho-proteins exposed on the surface of the membrane. After one hour, the membrane was washed twice with the blocking solution and then placed into the primary antibodies and normal immunochemistry continued.

Some membranes were exposed by first horizontally cutting the PVDF membrane (after blotting) such that < 40 kDa was separated from > 40 kDa protein samples. This separated Hsp27 and p38 MAPK proteins from actin proteins, and allowed each protein to be assessed in its own batch of primary antibodies.

Immunocytochemistry

Six-well trays were prepared with 3 coverslips per well (12 mm x 1 mm; Fisher Scientific). Coverslips were incubated with 2 ml of 0.01% poly-L-lysine (Sigma) for one hour (37 °C) and then washed twice with distilled water and allowed to dry. Similar to protein analysis, 4×10^4 cells were added to each well and allowed to replicate in GM and differentiate for 6 days in DM. OGD treatments were the same as previously mentioned.

After treatment, media was aspirated and the cells washed twice with ice-cold 0.1 M sodium phosphate buffer solution. Cells on coverslips were then removed and placed

into 4% paraformaldehyde solution for 10 minutes. After fixation, coverslips were washed (3 X 5 min) in phosphate-buffered saline (PBS).

Antibodies were suspended in 10% donkey serum (Jackson Immunoresearch Laboratories, Inc) in phosphate-buffered saline with 0.1% Triton X-100 (Sigma)(PBS-T). Antibody for phospho-p38 MAPK (Stressgen, KAP-MA022) was used at 1:500 dilution. Antibody for Hsp27 (Stressgen, SPA-801E) was used at 1:5000 dilution. Cells on coverslips were placed in 1 ml of antibody solution and left overnight at 4 °C. The next day, cells were washed in PBS-T (3 X 5 min). The PBS-T was replaced with secondary antibody (donkey anti-rabbit; 1:500; Jackson Immunoresearch Laboratories, Inc; 711 165 152) diluted in 10% donkey serum made in PBS-T. Because fluorescence was being used, all immunocytochemistry protocols took place in dark conditions and the secondary antibody was protected from light as much as possible. The coverslips were exposed to secondary antibody for one hour and then washed again for with PBS (no Triton X-100; 3 X 5 min). 200 units of fluorescent-conjugated phalloidin (Invitrogen Alexa Fluor® 488 phalloidin, A12379) was added for 20 minutes and then washed with PBS (3 X 5 min). Finally, 2 µl of Hoescht stain (Sigma, H6024) was added to 1 ml of PBS for each coverslip, for ten minutes, and then washed with PBS (3 X 5 min).

Controls for the preparation of immunocytofluoresence consisted of the following. Cells were exposed only to the anti-rabbit secondary. Cells were exposed to only primary antibodies for either Hsp27 or phospho-p38. Cells were only exposed to the phalloidin stain. Cells were only exposed to the Hoescht stain. Cells on coverslips incubated with only the anti-rabbit secondary did not fluoresce. Cells exposed only to primary antibodies did not fluoresce.

Cells on coverslips were placed on microscope slides with aqueous mounting media (Sigma) and sealed with clear nail polish. Images were captured using a Zeiss Axioplan II MOT microscope and an AxioCam HRC colour camera.

Statistical Analysis

Data are expressed as mean ± standard error of the mean (SEM). Statistical analysis was performed using Graphpad Prism 4 for Windows, Version 4.03 (GraphPad Software Inc.). Analysis of variance was used to determine significance, and Tukey's honestly significant difference post-hoc comparison was used to determine significant differences. $P < 0.05$ was used to determine statistical significance.

CHAPTER 3: RESULTS

Control Experiments for Western Analysis and Immunohistochemistry.

The presence of Insulin Receptor β in 6-day differentiated cells was confirmed using Western blotting. The phospho-specificity of the antibodies for phosphorylated Hsp27 serine 82 was confirmed by reduced binding of anti-phospho antibodies on PVDF membranes for samples treated with Calf Alkaline Intestinal Phosphatase *before* loading samples in the gel, as well as by reduced binding of anti-phospho antibodies on PVDF membranes treated with Calf Alkaline Intestinal Phosphatase *after* transferring protein to PVDF membrane. The phospho-specificity of the antibodies for phosphorylated p38 MAPK was confirmed by reduced binding of anti-phospho antibodies on PVDF membranes on PVDF membranes treated with Calf Alkaline Intestinal Phosphatase *after* transferring protein to PVDF membrane.

Immunocytochemical controls confirmed that cells treated only with primary antibodies for Hsp27 (control for no secondary antibody), phospho-p38 MAPK (control for no secondary antibody), and anti-rabbit secondary antibodies (control for no primary antibody) did not fluoresce. Phalloidin and Hoescht stains did not fluoresce differently in cells treated with these two stains individually compared to these stains included with the tested antibodies.

The Effect of Insulin Supplementation in H9c2 Cells.

Media exchange increased relative levels of phosphorylated Hsp27 serine 82 in differentiated H9c2 cells.

Differentiated H9c2 cells were removed from incubation and the media was exchanged for fresh media. After one hour of further normal incubation, relative levels

of phosphorylated Hsp27 serine 82 were significantly higher ($p < 0.05$) in cells with media exchange (No Ins) compared to cells without media exchange (Con; Figure 3.1 A).

After one hour relative levels of phospho-p38 MAPK were not significantly different in cells with media exchange (No Ins) compared to cells without media exchange (Con; Figure 3.1 B).

The increase in phosphorylated Hsp27 serine 82 was interpreted to be a response to the stress of media exchange, and thus 'media exchange' as a stressor was examined further.

Insulin supplementation reduced short-term relative levels of phosphorylated Hsp27 serine 82 and reduced levels of p38 MAPK in differentiated cells.

Differentiated H9c2 cells were removed from incubation and the media was exchanged for fresh media (No Ins) or with fresh media supplemented with 200 μU/ml insulin (Ins). Cells were harvested for Western analysis after 15, 30, 45, and 60 minutes. The treatments resulted in no difference in the total Hsp27 levels (Figure 3.2 A). However, 15 minutes after media exchange, Ins-treated cells had significantly lower ($p < 0.05$) relative levels of phosphorylated Hsp27 serine 82 than cells without insulin. The difference was no longer present after 30, 45, and 60 minutes (Figure 3.2 B).

At each time point, insulin-supplemented cells had less p38 MAPK. This reduction was significant at 15 ($p < 0.05$), 30 ($p < 0.001$), and 60 ($p < 0.001$) minutes (Figure 3.3 A, B, C, D). However, the treatments resulted in no difference in relative phospho-p38 MAPK levels (Figure 3.3).

The stress of media exchange was associated with an increase in phosphorylated Hsp27 serine 82 that was evident by fifteen minutes. However, insulin supplementation during media exchange appeared to suppress the increase (in phosphorylated Hsp27 serine 82) induced by media exchange. Because levels of phosphorylated Hsp27 serine 82 were not different at one hour, it was interpreted that insulin was then causing an increase of phosphorylated Hsp27 serine 82 via insulin-induced signaling. A one hr insulin treatment was later used as a '*pretreatment*' for further stressors, and a one hr normal pretreatment (without insulin supplementation) was used as a control for insulin pretreatment.

Various insulin doses had similar effect on relative levels of phosphorylated Hsp27 serine 82 and on relative levels of phospho-p38 MAPK in differentiated cells after one hour.

Differentiated H9c2 cells were removed from incubation and the media was exchanged for fresh media (No Ins) or with media supplemented with 20, 200, or 2000 μU/ml of insulin. After one hour, cells with media exchange and either 0, 20, 200, or 2000 μU/ml of insulin supplementation had similar relative levels of phosphorylated Hsp27 serine 82 (Figure 3.4 A). Additionally, the various tested levels of insulin supplementation did not change total Hsp27 levels (Figure 3.4 B).

After one hour, the various tested levels of insulin supplementation did not change relative levels of phospho-p38 MAPK (Figure 3.5 A). All insulin-supplemented groups had lower averages of total p38 MAPK than cells without supplementation; however the reduction was not significant (n=4, Figure 3.5 B).

Because different insulin doses produced similar effects over two orders of magnitude, it was determined that there was potentially a ceiling effect from insulin treatment, and so the original dose (200 μU/ml) continued to be acceptable as a *pretreatment*.

Media exchange increased relative levels of phosphorylated Hsp27 serine 82 in proliferative H9c2 cells.

Differentiated H9c2 cells require more maintenance in order to conduct experiments and so proliferative cells H9c2 cells were tested for differences in the insulin response. Proliferative H9c2 cells were removed from incubation and the media was exchanged for fresh media. After one hour of further normal incubation, relative levels of phosphorylated Hsp27 serine 82 were significantly higher ($p < 0.001$) in cells with media exchange (No Ins) compared to cells without media exchange (Con; Figure 3.6 A). Like differentiated cells, H9c2 cells were interpreted to experience a stress-response to media exchange.

Insulin supplementation decreased relative levels of phosphorylated Hsp27 serine 82 and did not change total p38 MAPK levels in proliferative cells.

Proliferative H9c2 cells were removed from incubation and the media was exchanged for fresh media (No Ins) or with media supplemented with 20, 200, or 2000 μU/ml of insulin. After one hour, cells with 200 μU/ml of insulin supplementation had lower ($p < 0.05$) relative levels of phosphorylated Hsp27 serine 82 (Figure 3.7 A). The various tested levels of insulin supplementation did not change total Hsp27 levels (Figure 3.7 B).

After one hour, the various tested levels of insulin supplementation did not change total levels of p38 MAPK compared to cells without supplementation (Figure 3.8 A).

Proliferative cells had different responses to one hr insulin supplementation than differentiated cells in that insulin supplementation of 200 μU/ml was associated with lower levels of phosphorylated Hsp27 serine 82 at one hr in proliferative cells. As well, the tested doses did not consistently produce lower total levels of p38 MAPK in proliferative cells. These differences, as well as reports that Insulin Receptor Substrate 1/2 is different in amount and phosphorylation states between the proliferative and differentiated H9c2 cells (Lim *et al.*, 2007), indicated that further experiments should be performed using differentiated H9c2 cells.

The Effect of Insulin Supplementation and Oxygen-Glucose Deprivation in Differentiated H9c2 Cells (Hsp27).

Insulin pretreatment (media exchange for 1 hr, with or without insulin) was used in further experiments to activate insulin pathways. Oxygen-glucose deprivation (6 hrs) and reoxygenation (1 or 2 hrs) was used as stronger stressors for the cells.

Insulin supplementation altered the relative levels of phosphorylated Hsp27 serine 82.

Differentiated H9c2 cells were removed from incubation and the media was exchanged with fresh media with either 0 or 200 μU/ml of insulin. After one hour, media was replaced with fresh media or with insulin-supplemented media for six additional hours of incubation. After six hours, insulin-pretreated cells had significantly more ($p <$

0.01) total Hsp27 than cells pretreated in normal media. As well, after six hours of incubation with insulin, insulin-pretreated cells had significantly more ($p < 0.05$) total Hsp27 than cells with normal pretreatment and a further six hours of normal incubation (Figure 3.9 A). The various treatments resulted in similar total levels of phosphorylated Hsp27 serine 82 (Figure 3.9 B). After six hours, insulin-pretreated cells had significantly lower ($p < 0.01$) relative levels of phosphorylated Hsp27 serine 82 than cells pretreated in normal media. Further, after six hours of incubation with insulin, insulin-pretreated cells had significantly lower ($p < 0.05$) relative levels of phosphorylated Hsp27 serine 82 than cells with normal pretreatment and a further six hours of normal incubation (Figure 3.9 C).

The insulin-associated decrease in relative levels of phosphorylated Hsp27 serine 82 was best explained as being due to the insulin-associated relative decrease in total Hsp27.

Oxygen-glucose deprivation followed by reoxygenation increased the relative levels of phosphorylated Hsp27 serine 82.

Differentiated H9c2 cells were removed from incubation and the media was exchanged with fresh media. After one hour, media was replaced with either fresh media for six additional hours of incubation or with glucose-free media for six hours of oxygen-glucose deprivation (OGD). After six hours, cells were either harvested for Western analysis or refreshed with new media for reoxygenation. The various treatments resulted in similar total levels of Hsp27 (Figure 3.10 A). As well, the various treatments caused similar total levels of phosphorylated Hsp27 serine 82 (Figure 3.10 B). However, after one hour of reoxygenation, cells had significantly higher relative levels of phosphorylated

Hsp27 serine 82 than cells with OGD alone ($p < 0.01$) or cells with six hours of normal incubation ($p < 0.01$; Figure 3.10 C).

Reoxygenation appeared to trigger a stress-response in differentiated cells, indicating that OGD and reoxygenation were different stressors for the cells. OGD was not associated with an increase in Hsp27 phosphorylation, however reoxygenation was.

Two hours of reoxygenation returned relative levels of phosphorylated Hsp27 serine 82 to oxygen-glucose deprivation levels.

Differentiated H9c2 cells were removed from incubation and the media was exchanged with fresh media. After one hour, media was replaced with glucose-free media for six hours of OGD. After six hours of OGD, cells were either harvested for Western analysis or refreshed with new media for one or two hours of reoxygenation. The various treatments caused similar total levels of Hsp27 (Figure 3.11 A). However, after one hour of reoxygenation, cells had higher ($p < 0.01$) total levels of phosphorylated Hsp27 serine 82 than OGD alone. After two hours of reoxygenation, total levels of phosphorylated Hsp27 serine 82 were less ($p < 0.05$) than after one hour of reoxygenation (Figure 3.11 B). Further, after one hour of reoxygenation, cells had significantly higher ($p < 0.01$) relative levels of phosphorylated Hsp27 serine 82 than cells with OGD alone. After two hours of reoxygenation, relative levels of phosphorylated Hsp27 serine 82 were similar to OGD alone (Figure 3.11 C).

Reoxygenation of one hr was considered to be sufficient to generate the reoxygenation stress response, and that two hrs of reoxygenation were sufficient to begin the return of cells to a pre-stress condition.

Insulin pretreatment and oxygen-glucose deprivation followed by reoxygenation increased the relative levels of phosphorylated Hsp27 serine 82.

Differentiated H9c2 cells were removed from incubation and the media was exchanged with insulin-supplemented media. After one hour, media was replaced with either fresh media for six additional hours of incubation or with glucose-free media for six hours of OGD. After six hours, cells were either harvested for Western analysis or refreshed with new media for one hour of reoxygenation. The various treatments caused similar total levels of Hsp27 (Figure 3.12 A). However, after one hour of reoxygenation, cells had significantly higher ($p < 0.05$) total levels of phosphorylated Hsp27 serine 82 than cells with OGD alone (Figure 3.12 B). As well, after one hour of reoxygenation, cells had significantly higher ($p < 0.01$) relative levels of phosphorylated Hsp27 serine 82 than cells with OGD alone (Figure 3.12 C).

Reoxygenation after insulin treatments appeared to trigger a stress-response in differentiated cells, indicating that OGD and reoxygenation were stressors even with the presence of insulin.

Insulin pretreatment and oxygen-glucose deprivation did not change levels of phosphorylated Hsp27 serine 82.

Differentiated H9c2 cells were removed from incubation and the media was exchanged with fresh media with either 0 or 200 μU/ml of insulin. After one hour, media was replaced with either fresh media for six additional hours of incubation or with glucose-free media for six hours of OGD. The various treatments resulted in similar total levels of Hsp27 (Figure 3.13 A). As well, the various treatments caused similar total

levels of phosphorylated Hsp27 serine 82 (Figure 3.13 B), and comparable relative levels of phosphorylated Hsp27 serine 82 (Figure 3.13 C).

Insulin pretreatment or supplementation did not change the effect of oxygen-glucose deprivation on relative levels of phosphorylated Hsp27 serine 82.

Differentiated H9c2 cells were removed from incubation and the media was exchanged with fresh media with either 0 or 200 μU/ml of insulin. After one hour, media was replaced with either glucose-free media or glucose-free media supplemented with insulin for six hours of OGD. The various treatments resulted in similar total levels of Hsp27 (Figure 3.14 A). As well, the various treatments caused similar total levels of phosphorylated Hsp27 serine 82 (Figure 3.14 B) and equivalent relative levels of phosphorylated Hsp27 serine 82 (Figure 3.14 C).

Neither insulin pretreatment nor insulin supplementation were associated with changes in Hsp27 serine 82 phosphorylation during OGD. Additionally, OGD prevented the increase in Hsp27 expression associated with insulin pretreatment followed by 6 hrs of normal incubation.

Insulin supplementation increased total levels of phosphorylated Hsp27 serine 82 during reoxygenation.

Differentiated H9c2 cells were removed from incubation and the media was exchanged with fresh media with either 0 or 200 μU/ml of insulin. After one hour, media was replaced with glucose-free media or glucose-free media supplemented with insulin for six hours of OGD. After OGD, cells were refreshed with new media for one hour of reoxygenation. The various treatments caused similar total levels of Hsp27 (Figure 3.15

A). However, 1 hr of reoxygenation after insulin supplementation during OGD resulted in higher ($p < 0.05$) total levels of phosphorylated Hsp27 serine 82 than 1 hr reoxygenation after unsupplemented OGD with insulin-pretreatment (Figure 3.15 B). Regardless, the various treatments caused similar relative levels of phosphorylated Hsp27 serine 82 (Figure 3.15 C).

Insulin during OGD was associated with higher total levels of phosphorylated Hsp27 serine 82 during reoxygenation. This indicated that insulin treatments before and during OGD did not suppress Hsp27 serine 82 phosphorylation during reoxygenation.

Insulin pretreatment and supplementation did not change the effect of longer reoxygenation on relative levels of phosphorylated Hsp27 serine 82.

Differentiated H9c2 cells were removed from incubation and the media was exchanged with fresh media with either 0 or 200 μU/ml of insulin. After one hour, media was replaced with glucose-free media or glucose-free media supplemented with insulin for six hours of OGD. After OGD, cells were refreshed with new media for two hours of reoxygenation. However, the various treatments resulted in similar total levels of Hsp27 (Figure 3.16 A), corresponding total levels of phosphorylated Hsp27 serine 82 (Figure 3.16 B), and similar relative levels of phosphorylated Hsp27 serine 82 (Figure 3.16 C).

Combining Hsp27 data between Western membranes

Previous results were analyzed using an $n = 4$ due to space limitations on Western membranes. Some of the experiments were performed with an $n = 8$, but results were analyzed across different membranes. In replication of experiments, inter-treatment variance was found to be similar. This allowed combinations of data between replicates,

however because samples were on different membranes, variance due to membranes disallowed certain combinations. Specifically, 2-way ANOVA was performed when membranes contained samples from two experimental protocols (e.g, each membrane contained four samples from a 'normal incubation' group and four samples from an 'OGD' group; the two membranes had samples from another set of experiments to create an n = 8 for each group). When the 2-way ANOVA showed no statistical effect from the membranes, data were combined for further analysis by ANOVA. Each membrane contained a total of three experimental conditions, therefore combining data between membranes with two conditions in common allowed for additional total comparisons. Because the limiting factor of this analysis is variance caused by membranes, not all interesting combinations were available.

Membranes for Hsp27 were compared between five conditions (Figure 3.17 A). There were no additional significant changes observed between total Hsp27 levels when comparing between a single condition change. Cells pretreated with insulin before OGD had higher ($p < 0.05$) total levels of Hsp27 than normally pretreated cells after one or two hours of reoxygenation.

Relative levels of phosphorylated Hsp27 serine 82 were compared between five conditions (Figure 3.17 B). Cells subjected to reoxygenation for one or two hours after OGD significantly increased ($p < 0.05$) relative levels of phosphorylated Hsp27 serine 82 compared to cells with OGD alone. Cells with insulin pretreatment and OGD had lower (but not significantly, $p < 0.07$) relative levels of phosphorylated Hsp27 serine 82 than cells with normal pretreatment and OGD. Interestingly, the significant reduction of

relative levels of phosphorylated Hsp27 serine 82 observed between one and two hours of reoxygenation is no longer present.

The Effect of Insulin Supplementation and Oxygen-Glucose Deprivation on Hsp27 Immunocytochemistry

Immunocytochemistry was performed for Hsp27. Filamentous actin was stained with phalloidin, and nuclei were stained with Hoescht. The localization was performed after cells were pretreated (with or without insulin) followed by six hrs of incubation (both with and without OGD and with and without insulin). Cells with OGD (with or without insulin) were examined after 0, 1, or 2 hrs of reoxygenation.

Insulin treatments were associated with localized rearrangement of Hsp27 in differentiated H9c2 cells in normal incubation conditions.

Differentiated H9c2 cells were removed from incubation and the media was replaced with fresh media supplemented with 0 or 200 μU/ml of insulin. After one hour, media was again replaced with fresh media, with or without insulin, for six additional hours. Cells were then removed from incubation and fixed for analysis using immunocytochemistry. Three treatment groups were compared: normal pretreatment followed by six hours of normal incubation (Figure 3.18 Aa, Ba, Ca), insulin pretreatment followed by six hours of normal incubation (Figure 3.18 Ab, Bb, Cb), and insulin pretreatment followed by six hours of insulin-supplemented incubation (Figure 3.18 Ac, Bc, Cc).

Cells given no insulin (Figure 3.18 Aa, Ba, Ca) showed Hsp27-immunoreactivity throughout the cytoplasm and in the perinuclear area. The Hsp27-immunoreactivity in

the nuclear area was less than in the perinuclear area. Cells with insulin pretreatment (Figure 3.18 Ab, Bb, Cb) showed Hsp27-immunoreactivity throughout the cytoplasm and in the nuclear area. Compared to normal pretreatment, there was less Hsp27-immunoreactivity in the perinuclear area. In cells with insulin pretreatment and six additional hours of insulin-supplemented incubation (Figure 3.18 Ac, Bc, Cc), Hsp27-immunoreactivity was throughout the cytoplasm, in the perinuclear area, and in the nuclear area. Compared to cells only given insulin during pretreatment, there was a greater contrast between the perinuclear area and the nuclear area suggesting either an increased concentration of Hsp27-immunoreactivity in the perinuclear area or exclusion from the nucleus.

The distribution of actin was similar whether the cells were given no insulin or six hours of insulin-supplemented incubation. In all cases, actin was regular and organized in peripheral regions, and was disorganized in perinuclear regions (Figure 3.18 Ba, Bb, Bc).

Oxygen-glucose deprivation was associated with localized rearrangement of Hsp27 in differentiated H9c2 cells in an insulin-dependent manner.

Differentiated H9c2 cells were removed from incubation and the media was replaced with fresh media supplemented with 0 or 200 μU/ml of insulin. After one hour, media was replaced with glucose-free media, with or without insulin, and cells were placed into hypoxic incubation for six hours. Cells were then removed from incubation and fixed for analysis using immunocytochemistry. Three treatment groups were compared: normal pretreatment followed by six hours of OGD (Figure 3.19 Aa, Ba, Ca), insulin-supplemented pretreatment followed by six hours of OGD (Figure 3.19 Ab, Bb,

Cb), and insulin-supplemented pretreatment followed by six hours of insulin-supplemented OGD (Figure 3.19 Ac, Bc, Cc).

Cells given no insulin (Figure 3.19 Aa, Ba, Ca) showed Hsp27-immunoreactivity throughout the cytoplasm, in the perinuclear area, and in the nucleus. Hsp27-immunoreactivity was more in the nuclei during OGD compared to normal incubation (Figure 3.18 Aa). In comparison to normal pretreatment, pretreating with insulin before OGD (Figure 3.19 Ab, Bb, Cb) resulted in Hsp27-immunoreactivity being concentrated in the perinuclear area compared with Hsp27-immunoreactivity in peripheral cytoplasm and within the nuclei. Insulin during both pretreatment and during OGD (Figure 3.19 Ac, Bc, Cc) increased Hsp27-immunoreactivity concentration in the perinuclear area compared to peripheral cytoplasm and the nuclei.

In all three treatment sets, after OGD actin (Figure 3.19 Ba, Bb, Bc) was less regular and organized (both peripherally and in the perinuclear area) compared to cells given normal incubation conditions (Figure 3.18 Ba, Bb, Bc). As well, actin formed condensates that were most notable in the cells pretreated with insulin before regular OGD. These condensates appeared to be in proximity to concentrations of Hsp27-immunoreactivity (Figure 3.19 Ca, Cb, Cc).

One hour of reoxygenation caused a similar rearrangement of Hsp27 regardless of insulin supplementation

Differentiated H9c2 cells were removed from incubation and the media was replaced with fresh media supplemented with 0 or 200 μU/ml of insulin. After one hour, media was replaced with glucose-free media, with or without insulin, and cells were placed into hypoxic incubation for six hours. After OGD, the media was refreshed for

one hour of reoxygenation. Three treatment groups were compared: normal pretreatment followed by six hours of OGD and 1 hour of reoxygenation (Figure 3.20 Aa, Ba, Ca), insulin-supplemented pretreatment followed by six hours of OGD and 1 hour of reoxygenation (Figure 3.20 Ab, Bb, Cb), and insulin-supplemented pretreatment followed by six hours of insulin-supplemented OGD and 1 hour of reoxygenation (Figure 3.20 Ac, Bc, Cc).

In all three treatments, following one hour of reoxygenation, Hsp27-immunoreactivity (Figure 3.20 Aa, Ab, Ac) was cytoplasmic, perinuclear, and nuclear. The perinuclear area appeared to have greater Hsp27-immunoreactivity compared to the nuclei and cytoplasm, suggesting that Hsp27 was excluded from the nuclei or that there was accumulation in the perinuclear area. In normally pretreated cells (Figure 3.20 Aa, Ba, Ca), Hsp27-immunoreactivity was different after reoxygenation compared to OGD alone. After reoxygenation, Hsp27-immunoreactivity was lower in the nuclei compared to OGD, and Hsp27-immunoreactivity was higher in the perinuclear area compared to OGD. In addition, there was less Hsp27-immunoreactivity associated with actin condensates compared to OGD (Figure 3.19 Aa). In insulin-pretreated cells after reoxygenation (Figure 3.20 Ab, Bc, Cb), there was less Hsp27-immunoreactivity associated with actin condensates compared to OGD (Figure 3.19 Ab). Reoxygenated cells with insulin during both pretreatment and during OGD (Figure 3.20 Ac, Bc, Cc), had lower Hsp27-immunoreactivity observed in the perinuclear area than similarly treated cells during OGD alone (Figure 3.19 Ac); thus, the contrast of Hsp27-immunoreactivity between the nuclei and the perinuclear area was less obvious after reoxygenation than after OGD alone.

In all three treatment sets, after reoxygenation actin (Figure 3.20 Ba, Bb, Bc) was organized and regular in peripheral regions and was disorganized in perinuclear regions. Regions of actin condensates were less common than during OGD, however they were not completely removed after one hour of reoxygenation.

Two hours of reoxygenation caused a similar rearrangement of Hsp27 regardless of insulin supplementation.

Differentiated H9c2 cells were removed from incubation and the media was replaced with fresh media supplemented with 0 or 200 μU/ml of insulin. After one hour, media was replaced with glucose-free media, with or without insulin, and cells were placed into hypoxic incubation for six hours. After OGD, the media was refreshed for two hours of reoxygenation. Three treatment groups were compared: normal pretreatment followed by six hours of OGD and 2 hours of reoxygenation (Figure 3.21 Aa, Ba, Ca), insulin-supplemented pretreatment followed by six hours of OGD and 2 hours of reoxygenation (Figure 3.21 Ab, Bb, Cb), and insulin-supplemented pretreatment followed by six hours of insulin-supplemented OGD and 2 hours of reoxygenation (Figure 3.21 Ac, Bc, Cc).

In all three treatments following two hours of reoxygenation, Hsp27-immunoreactivity (Figure 3.21 Aa, Ab, Ac) was cytoplasmic, perinuclear, and nuclear. The Hsp27-immunoreactivity in the nuclear area was less than in the perinuclear area, and the Hsp27-immunoreactivity was very similar to cells given normal incubation for six hours (Figure 3.18 Aa). As well, actin (Figure 3.21 Ba, Bb, Bc) was regular and organized except in the perinuclear areas. After two hours of reoxygenation actin appeared similar to normal incubation conditions (Figure 3.18 Ba).

The Effect of Insulin Supplementation and Oxygen-Glucose Deprivation in Differentiated H9c2 Cells (p38 MAPK).

The effect of insulin, OGD, and reoxygenation were determined on phosphorylation of Hsp27 serine 82. p38 MAPK is an upstream regulator of Hsp27 serine 82 phosphorylation and activated p38 MAPK must complex with the nuclear protein MK2 before the activated complex can phosphorylate Hsp27. Western analysis was performed for p38 MAPK in order to understand the relationship between p38 MAPK , Hsp27 and insulin supplementation in the context of the stressors.

Insulin supplementation reduced p38 MAPK levels in normal incubation.

Differentiated H9c2 cells were removed from incubation and the media was exchanged with fresh media with either 0 or 200 μU/ml of insulin. After one hour, media was replaced with fresh media or with insulin-supplemented media for six additional hours of incubation. The seven-hour insulin supplemented group had lower ($p < 0.05$) total levels of p38 MAPK compared to unsupplemented cells. The one-hour insulin supplemented group had an intermediate average of total p38 MAPK (Figure 3.22 A). However, the various treatments caused similar total levels of phospho-p38 MAPK (Figure 3.22 B), and comparable relative levels of phospho-p38 MAPK (Figure 3.22 C).

Oxygen-glucose deprivation reduced total levels of p38 MAPK.

Differentiated H9c2 cells were removed from incubation and the media was exchanged with fresh media. After one hour, media was replaced with either fresh media for six additional hours of incubation or with glucose-free media for six hours of OGD. After six hours, cells were either harvested for Western analysis or refreshed with new

media for reoxygenation. Cells with OGD or with OGD followed by reoxygenation had significantly lower ($p < 0.01$) levels of total p38 MAPK (Figure 3.23 A). However, the various treatments caused similar total levels of phospho-p38 MAPK (Figure 3.23 B), and similar relative levels of phospho-p38 MAPK (Figure 3.23 C).

Oxygen-glucose deprivation following insulin supplementation reduced total levels of p38 MAPK.

Differentiated H9c2 cells were removed from incubation and the media was exchanged with insulin-supplemented media. After one hour, media was replaced with either fresh media for six additional hours of incubation or with glucose-free media for six hours of OGD. After six hours, cells were either harvested for Western analysis or refreshed with new media for one hour of reoxygenation. Cells with OGD or with OGD followed by reoxygenation had significantly lower ($p < 0.01$) levels of total p38 MAPK (Figure 3.24 A). However, the various treatments caused similar total levels of phospho-p38 MAPK (Figure 3.24 B), and similar relative levels of phospho-p38 MAPK (Figure 3.24 C).

Insulin supplementation during oxygen-glucose deprivation increased levels of total p38 MAPK following one hour of reoxygenation.

Differentiated H9c2 cells were removed from incubation and the media was exchanged with fresh media with either 0 or 200 μU/ml of insulin. After one hour, media was replaced with glucose-free media or glucose-free media supplemented with insulin for six hours of OGD. After OGD, cells were refreshed with new media for one hour of reoxygenation. Insulin pretreatment and insulin supplementation during OGD resulted in higher ($p < 0.05$) levels of total p38 MAPK than in cells with no insulin supplementation

(Figure 3.25 A). However, the various treatments caused correspondingly similar total levels of phospho-p38 MAPK (Figure 3.25 B), and interestingly, similar but corresponding relative levels of phospho-p38 MAPK (Figure 3.25 C).

Insulin supplementation during oxygen-glucose deprivation did not change levels of total p38 MAPK following two hours of reoxygenation.

Differentiated H9c2 cells were removed from incubation and the media was exchanged with fresh media with either 0 or 200 μU/ml of insulin. After one hour, media was replaced with glucose-free media or glucose-free media supplemented with insulin for six hours of OGD. After OGD, cells were refreshed with new media for two hours of reoxygenation. However, the various treatments resulted in similar total levels of p38 MAPK (Figure 3.26 A), similar total levels of phospho-p38 MAPK (Figure 3.26 B), and similar relative levels of phospho-p38 MAPK (Figure 3.26 C).

Combining p38 MAPK data between Western membranes.

Membranes for p38 MAPK were compared between six conditions (Figure 3.27 A). Insulin pretreatment followed by incubation with insulin for six hours decreased ($p < 0.05$) total levels of p38 MAPK compared to normally pretreated or insulin-pretreated cells with six additional hours of normal incubation. Insulin pretreatment followed by incubation with insulin for six hours also resulted in lower ($p < 0.05$) levels of p38 MAPK than cells with insulin pretreatment and six hours of OGD. Additionally, insulin-pretreatment followed by OGD and 1 hr of reoxygenation resulted in total levels of p38 MAPK being lower ($p < 0.05$) than in cells with normal pretreatment and normal six hrs of incubation. Further, average total levels of p38 MAPK for OGD alone (with or

without insulin pretreatment) were intermediate between the normally incubated cells and those with reoxygenation.

Relative levels of phospho-p38 MAPK were compared between six conditions (Figure 3.27 B). Insulin pretreatment followed by incubation with insulin for six hours increased ($p < 0.05$) relative levels of phospho-p38 MAPK compared to normally pretreated cells with six additional hours of normal incubation. Cells incubated with insulin pretreatment and with insulin-supplemented normal media also had higher ($p < 0.05$) relative levels of phospho-p38 MAPK than cells with normal pretreatment and 6 hrs of OGD.

The Effect of Insulin Supplementation and Oxygen-Glucose Deprivation on Phospho-p38 MAPK Immunocytochemistry

Immunocytochemistry was performed for phospho-p38 MAPK. Filamentous actin was stained with phalloidin and nuclei were stained with Hoescht. The localization was performed after cells were pretreated (with or without insulin) followed by six hrs of incubation (both with and without OGD and with and without insulin). Cells with OGD (with or without insulin) were examined after 0, 1, or 2 hrs of reoxygenation.

Insulin caused no change in distribution of phospho-p38 MAPK in differentiated H9c2 cells in normal incubation conditions.

Differentiated H9c2 cells were removed from incubation and the media was replaced with fresh media supplemented with 0 or 200 μU/ml of insulin. After one hour, media was again replaced with fresh media, with or without insulin, for six additional hours. Cells were then removed from incubation and fixed for analysis using

immunocytochemistry. Three treatment groups were compared: normal pretreatment followed by six hours of normal incubation (Figure 3.28 Aa, Ba, Ca), insulin-supplemented pretreatment followed by six hours of normal incubation (Figure 3.28 Ab, Bb, Cb), and insulin-supplemented pretreatment followed by six hours of insulin-supplemented incubation (Figure 3.28 Ac, Bc, Cc).

Cells given no insulin (Figure 3.28 Aa, Ba, Ca) showed phospho-p38 MAPK-immunoreactivity in cytoplasmic granules and faintly in the cytoplasm. The phospho-p38 MAPK-immunoreactivity in the nuclear area was much greater than in the cytoplasm, suggesting that phospho-p38 MAPK was concentrated within the nuclei of the cells. Cells with insulin pretreatment, either with or without insulin during the six hours of incubation (Figure 3.28 Ab, Bb, Cb and Figure 3.28 Ac, Bc, Cc), were similar in appearance to cells without insulin. Again, phospho-p38 MAPK appeared to be concentrated within the nuclei and in cytoplasmic granulations. Insulin treatment appeared to have no effect on phospho-p38 MAPK localization in normal incubation conditions.

The distribution of actin was similar whether the cells were given no insulin or six hours of insulin-supplemented incubation. In all cases, actin was regular and organized in peripheral regions, and was disorganized in perinuclear regions (Figure 3.28 Ba, Bb, Bc).

Oxygen-glucose deprivation was associated with localized rearrangement of phospho-p38 MAPK in differentiated H9c2 cells in an insulin-dependent manner.

Differentiated H9c2 cells were removed from incubation and the media was replaced with fresh media supplemented with 0 or 200 μU/ml of insulin. After one hour,

media was replaced with glucose-free media, with or without insulin, and cells were placed into hypoxic incubation for six hours. Cells were then removed from incubation and fixed for analysis using immunocytochemistry. Three treatment groups were compared: normal pretreatment followed by six hours of OGD (Figure 3.29 Aa, Ba, Ca), insulin-supplemented pretreatment followed by six hours of OGD (Figure 3.29 Ab, Bb, Cb), and insulin-supplemented pretreatment followed by six hours of insulin-supplemented OGD (Figure 3.29 Ac, Bc, Cc).

Cells given no insulin (Figure 3.29 Aa, Ba, Ca) showed phospho-p38 MAPK-immunoreactivity throughout the cytoplasm, in the perinuclear area, and in the nuclei. There was delineation between the nuclei and the perinuclear area, suggesting that the nuclei were still acting as a barrier. OGD appeared to cause phospho-p38 MAPK to increase in the cytoplasm compared to normal incubation (Figure 3.28 Aa). The granulations visible in normal incubation were still present during OGD, despite the increased cytoplasmic phospho-p38 MAPK-immunoreactivity. In comparison to normal pretreatment, pretreating with insulin before OGD (Figure 3.29 Ab, Bb, Cb) resulted in phospho-p38 MAPK-immunoreactivity that was concentrated in nuclei and in cytoplasmic granulations. The insulin pretreated cells had localization of phospho-p38 MAPK similar to that seen during normal incubation. Insulin during both pretreatment and during OGD (Figure 3.29 Ac, Bc, Cc) was associated with phospho-p38 MAPK-immunoreactivity being present in the nuclei, the perinuclear area, and in peripheral cytoplasm. Cytoplasmic granulations were still evident. ODG with insulin appeared to cause an increase in cytoplasmic phospho-p38 MAPK-immunoreactivity.

In all three treatment sets, after OGD actin (Figure 3.29 Ba, Bb, Bc) was less regular and less organized (both peripherally and in the perinuclear area) compared to cells given normal incubation conditions (Figure 3.28 Ba, Bb, Bc). As well, actin formed condensates that were most notable in the cells pretreated with insulin before OGD.

One hour of reoxygenation resulted in a similar localization of phospho-p38 MAPK regardless of insulin supplementation.

Differentiated H9c2 cells were removed from incubation and the media was replaced with fresh media supplemented with 0 or 200 μU/ml of insulin. After one hour, media was replaced with glucose-free media, with or without insulin, and cells were placed into hypoxic incubation for six hours. After OGD, the media was refreshed for one hour of reoxygenation. Three treatment groups were compared: normal pretreatment followed by six hours of OGD and 1 hour of reoxygenation (Figure 3.30 Aa, Ba, Ca), insulin-supplemented pretreatment followed by six hours of OGD and 1 hour of reoxygenation (Figure 3.30 Ab, Bb, Cb), and insulin-supplemented pretreatment followed by six hours of insulin-supplemented OGD and 1 hour of reoxygenation (Figure 3.30 Ac, Bc, Cc).

In all three treatment sets, after one hour of reoxygenation phospho-p38 MAPK-immunoreactivity (Figure 3.30 Aa, Ab, Ac) was mainly within the nuclear area and in cytoplasmic granulations. All three treatment sets had similar localizations of phospho-p38 MAPK-immunoreactivity, suggesting that reoxygenation had a similar net effect on each group. In normally pretreated cells (Figure 3.30 Aa, Ba, Ca), after reoxygenation there was less phospho-p38 MAPK-immunoreactivity in the cytoplasm compared to immunoreactivity observed during OGD (Figure 3.29 Aa). In insulin-pretreated cells

(Figure 3.30 Ab, Bc, Cb), reoxygenation caused little difference compared to OGD (Figure 3.29 Ab). Reoxygenated cells with insulin during both pretreatment and during OGD (Figure 3.30 Ac, Bc, Cc) showed less cytoplasmic phospho-p38 MAPK-immunoreactivity compared to analogous cells after OGD alone (Figure 3.29 Ac).

In all three treatment sets, after reoxygenation actin (Figure 3.30 Ba, Bb, Bc) appeared organized and regular in peripheral regions and was disorganized in perinuclear regions. Regions of actin condensates were less common than during OGD, however they were not completely removed after one hour of reoxygenation.

Two hours of reoxygenation resulted in a similar rearrangement of phospho-p38 MAPK regardless of insulin supplementation.

Differentiated H9c2 cells were removed from incubation and the media was replaced with fresh media supplemented with 0 or 200 μU/ml of insulin. After one hour, media was replaced with glucose-free media, with or without insulin, and cells were placed into hypoxic incubation for six hours. After OGD, the media was refreshed for two hours of reoxygenation. Three treatment groups were compared: normal pretreatment followed by six hours of OGD and 2 hours of reoxygenation (Figure 3.31 Aa, Ba, Ca), insulin-supplemented pretreatment followed by six hours of OGD and 2 hours of reoxygenation (Figure 3.31 Ab, Bb, Cb), and insulin-supplemented pretreatment followed by six hours of insulin-supplemented OGD and 2 hours of reoxygenation (Figure 3.31 Ac, Bc, Cc).

In all three treatment sets, two hours of reoxygenation resulted in phospho-p38 MAPK-immunoreactivity (Figure 3.31 Aa, Ab, Ac) mainly within the nuclear area and in cytoplasmic granulations. Phospho-p38 MAPK-immunoreactivity in all three sets was

very similar to cells in regular incubation (Figure 3.28). All three treatment sets had similar localizations of phospho-p38 MAPK-immunoreactivity, suggesting that two hours of reoxygenation had a similar net effect on each group, and that changes due to insulin and OGD were no longer present. As well, actin (Figure 3.31 Ba, Bb, Bc) was regular and organized except in the perinuclear areas.

Figure 3.1: The effect of media exchange on phosphorylated Hsp27 serine 82 and upon p38-MAPK. Differentiated H9c2 cells were removed from incubation and replaced into incubation (Con) or had their media aspirated and replaced with fresh media (No Ins). After one hour, cells with replaced media had higher relative levels of phosphorylated Hsp27 serine 82 than Con (*, $p < 0.05$, $n = 4$; **A**). After one hour, cells with replaced media had similar relative phospho-p38 MAPK as Con ($n = 4$ and 3, respectively; **B**). Data points represent mean ± SEM.

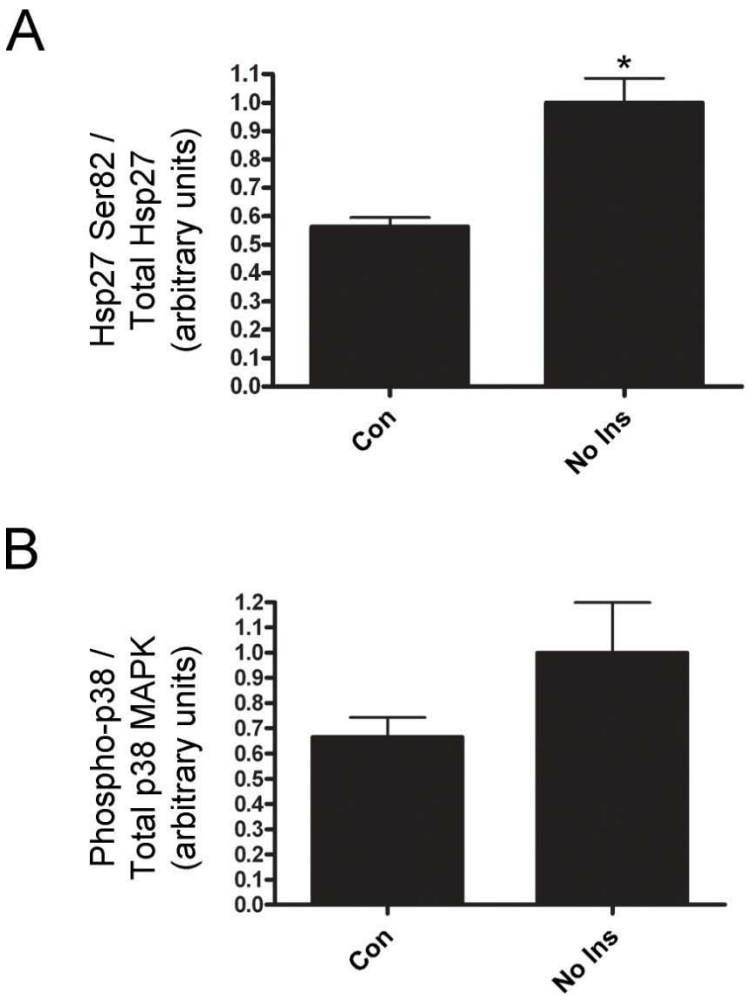
A
Hsp27 Ser82 /
Total Hsp27
(arbitrary units)
1.1
1.0
0.9
0.8
0.7
0.6
0.5
0.4
0.3
0.2
0.1
0.0
*
Con
No Ins
B
Phospho-p38 /
Total p38 MAPK
(arbitrary units)
1.2
1.1
1.0
0.9
0.8
0.7
0.6
0.5
0.4
0.3
0.2
0.1
0.0
Con
No Ins

Figure 3.1.

Figure 3.2: The time-dependent effect of insulin upon Hsp27 in differentiated H9c2 cells. Differentiated H9c2 cells were removed from incubation. Media was either refreshed (No Ins) or replaced with media supplemented with 200 μU/ml of insulin (Ins). Cells were returned to incubation and harvested after 15, 30, 45, and 60 minutes. The various treatments did not significantly alter total Hsp27 levels (**A**). After 15 minutes, insulin-treated cells had significantly lower levels of phosphorylated Hsp27 serine 82 than control cells (**B**). Data points represent mean ± SEM.

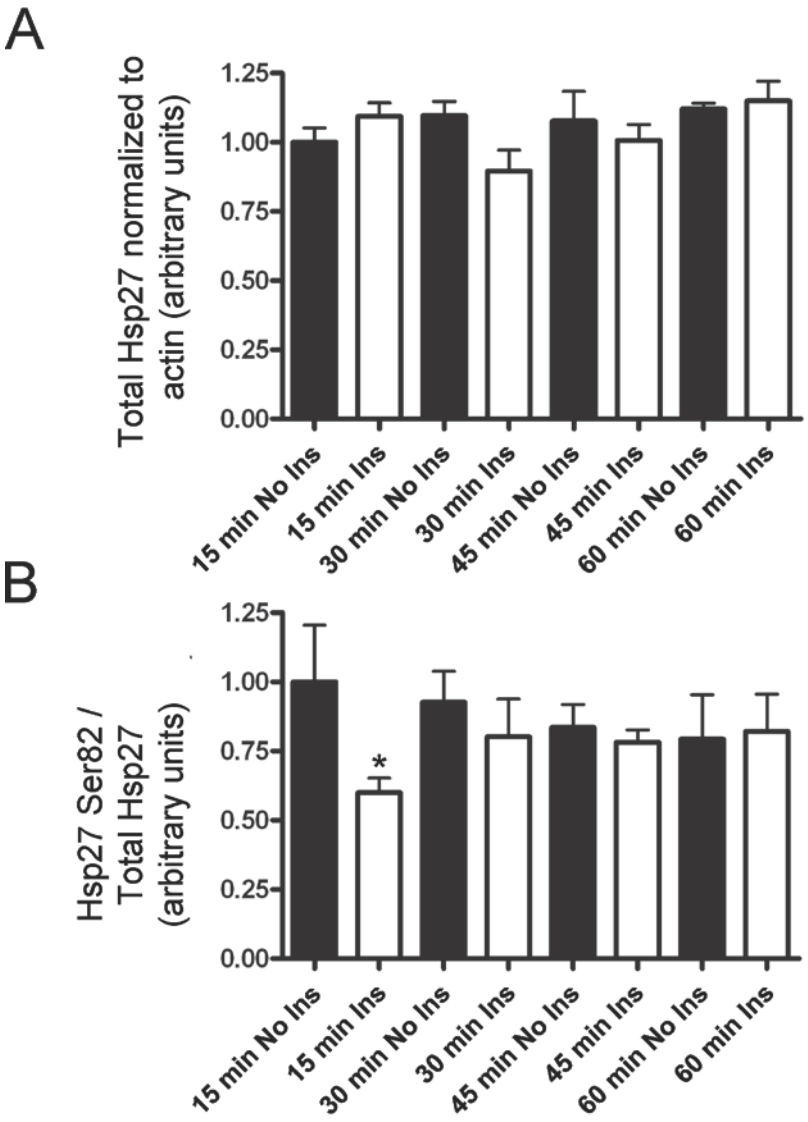
A
Total Hsp27 normalized to actin (arbitrary units)
1.25
1.00
0.75
0.50
0.25
0.00
15 min No Ins
15 min Ins
30 min No Ins
30 min Ins
45 min No Ins
45 min Ins
60 min No Ins
60 min Ins
B
Hsp27 Ser82 / Total Hsp27 (arbitrary units)
*

Figure 3.2.

Figure 3.3: The time-dependent effect of insulin upon p38 MAPK in differentiated H9c2 cells. Differentiated H9c2 cells were removed from incubation. Media was either refreshed (No Ins) or replaced with media supplemented with 200 μU/ml of insulin (Ins). Cells were returned to incubation and harvested after 15 (**A**), 30 (**B**), 45 (**C**), and 60 minutes (**D**). After 15, 30, and 60 minutes, insulin-treated cells had lower levels of total p38 MAPK. (*, $p < 0.05$, $n = 6$; ***, $p < 0.001$, $n = 6$). Data points represent mean ± SEM. Note: arbitrary units are graph specific, and cannot be compared between graphs.

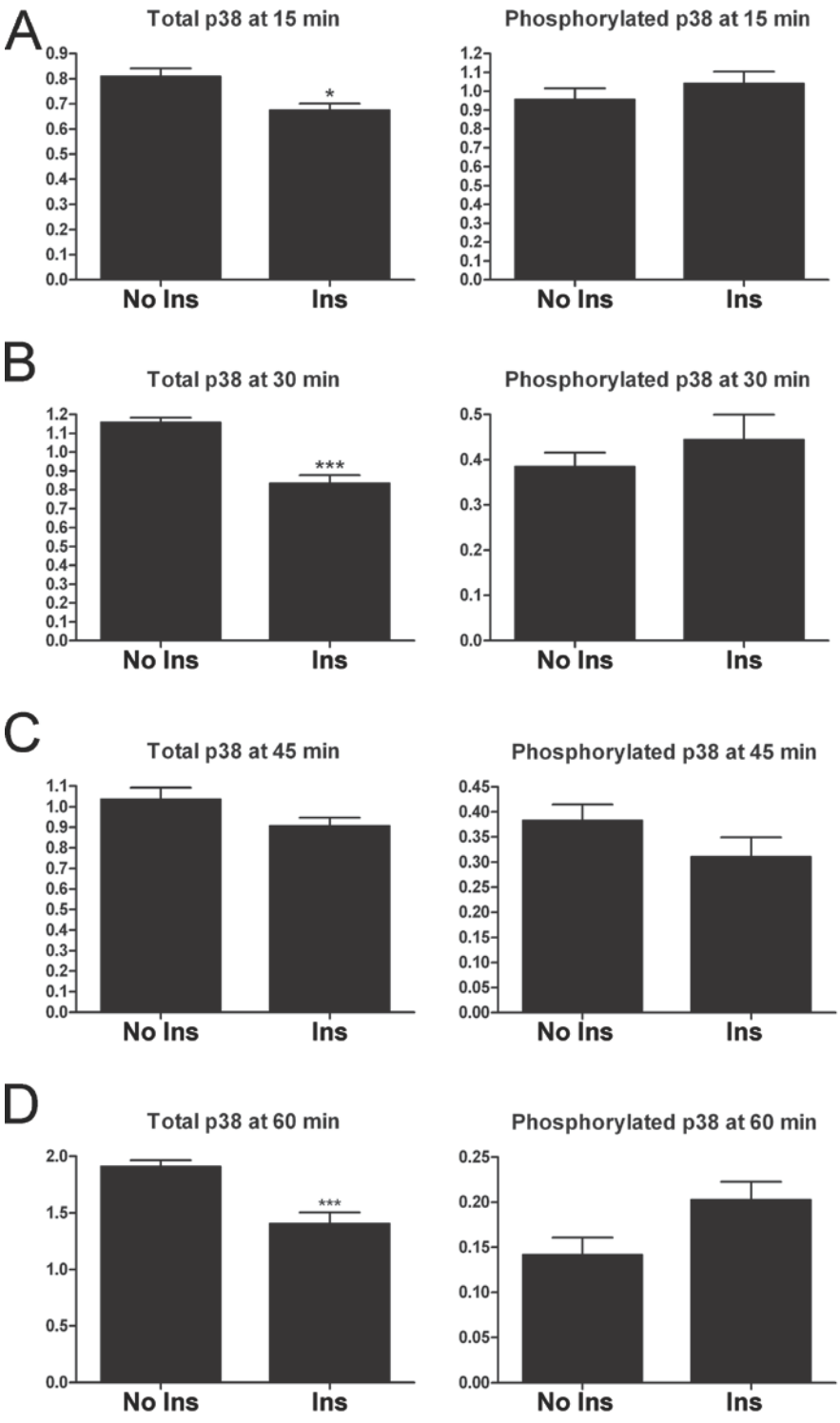
A
Total p38 at 15 min
Phosphorylated p38 at 15 min
*
No Ins
Ins
B
Total p38 at 30 min
Phosphorylated p38 at 30 min
***
No Ins
Ins
C
Total p38 at 45 min
Phosphorylated p38 at 45 min
No Ins
Ins
D
Total p38 at 60 min
Phosphorylated p38 at 60 min
***
No Ins
Ins

Figure 3.3.

Figure 3.4. The dose-dependent effect of insulin upon Hsp27 in differentiated H9c2 cells. Differentiated H9c2 cells were examined for the effect of insulin supplementation in the media replacement. Cells had their media aspirated and replaced with new media (No Ins) or new media supplemented with 20, 200, or 2,000 μU/ml of insulin. Insulin-supplementation (20, 200, 2,000 μU/ml) for one hour did not change relative levels of phosphorylated Hsp27 serine 82 compared to media exchange alone (n = 4; **A**). Exposing cells to new media or insulin-supplemented media for one hour did not change total levels of Hsp27 (**B**). Data points represent mean ± SEM.

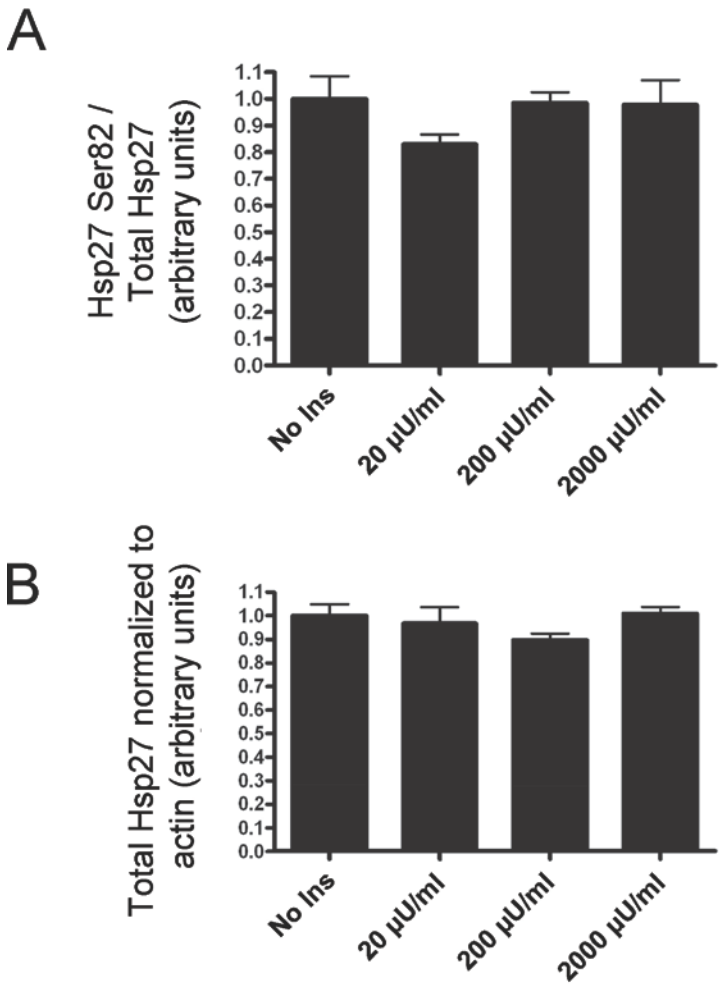
A
Hsp27 Ser82 / Total Hsp27 (arbitrary units)
1.1
1.0
0.9
0.8
0.7
0.6
0.5
0.4
0.3
0.2
0.1
0.0
No Ins
20 µU/ml
200 µU/ml
2000 µU/ml
B
Total Hsp27 normalized to actin (arbitrary units)
1.1
1.0
0.9
0.8
0.7
0.6
0.5
0.4
0.3
0.2
0.1
0.0
No Ins
20 µU/ml
200 µU/ml
2000 µU/ml

Figure 3.4.

Figure 3.5. The dose-dependent effect of insulin upon p38 MAPK in differentiated H9c2 cells. Differentiated H9c2 cells were examined for the effect of insulin supplementation in the media replacement. Cells had their media aspirated and replaced with new media (No Ins) or new media supplemented with 20, 200, or 2,000 μU/ml of insulin. The insulin supplementation did not cause a change in relative phospho-p38 MAPK levels compared to No Ins. (No Ins, n = 3; n = 4 for other insulin treatments; **A**). Exposing cells to insulin-supplemented media for one hour did not change total levels of p38 MAPK compared to media exchange alone (**B**). Data points represent mean ± SEM.

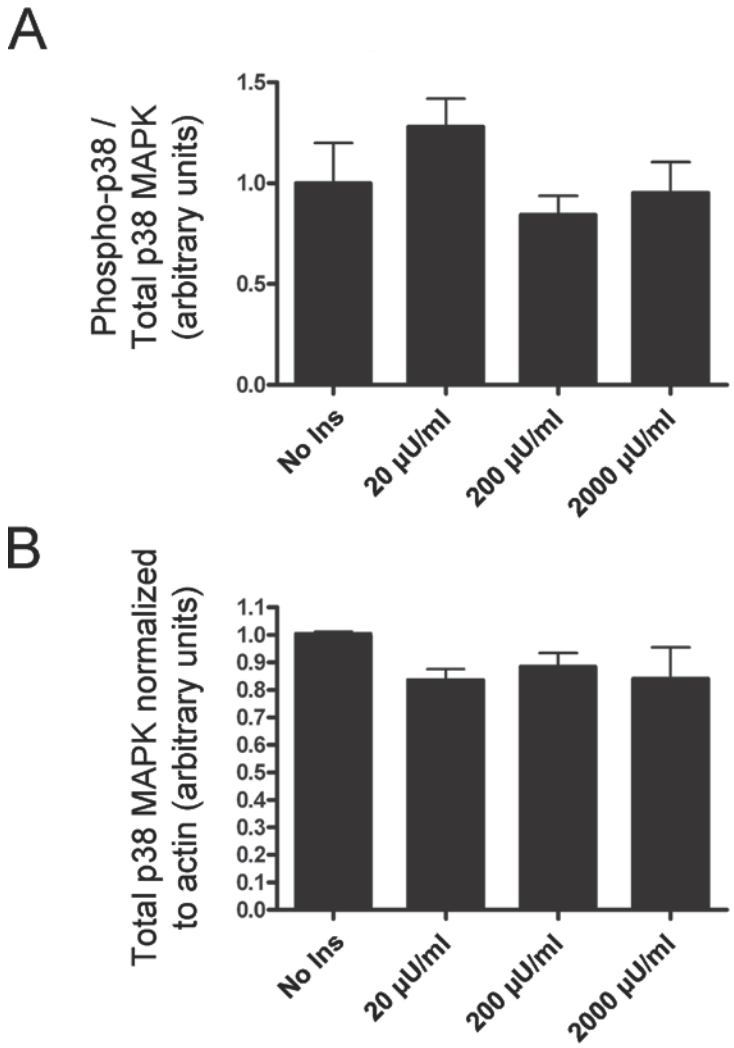
A
Phospho-p38 / Total p38 MAPK (arbitrary units)
1.5
1.0
0.5
0.0
No Ins
20 µU/ml
200 µU/ml
2000 µU/ml
B
Total p38 MAPK normalized to actin (arbitrary units)
1.1
1.0
0.9
0.8
0.7
0.6
0.5
0.4
0.3
0.2
0.1
0.0
No Ins
20 µU/ml
200 µU/ml
2000 µU/ml

Figure 3.5.

Figure 3.6: The effect of media exchange on phosphorylated Hsp27 serine 82. Proliferative H9c2 cells were removed from incubation and replaced into incubation (Con) or had their media aspirated and replaced with fresh media (No Ins). After one hour, cells with replaced media had higher relative levels of phosphorylated Hsp27 serine 82 than Con (***, $p < 0.001$, $n = 4$; **A**). Data points represent mean ± SEM.

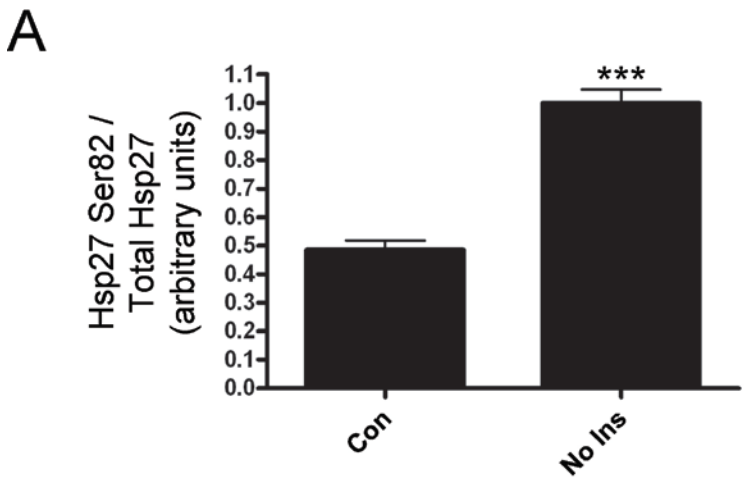
A
Hsp27 Ser82 /
Total Hsp27
(arbitrary units)
1.1
1.0
0.9
0.8
0.7
0.6
0.5
0.4
0.3
0.2
0.1
0.0
***
Con
No Ins

Figure 3.6.

Figure 3.7: The dose-dependent effect of insulin upon Hsp27 in proliferative H9c2 cells. Proliferative H9c2 cells were examined for the effect of insulin supplementation in the media replacement. Cells had their media aspirated and replaced with new media (No Ins) or new media supplemented with 20, 200, or 2,000 μU/ml of insulin. Insulin supplementation of 200 μU/ml resulted in a significant decrease (*, $p < 0.05$, $n = 4$) in levels of phosphorylated Hsp27 serine 82 compared to unsupplemented media (**A**). Exposing cells to insulin-supplemented media for one hour did not change total levels of Hsp27 compared to media exchange alone (**B**). Data points represent mean ± SEM.

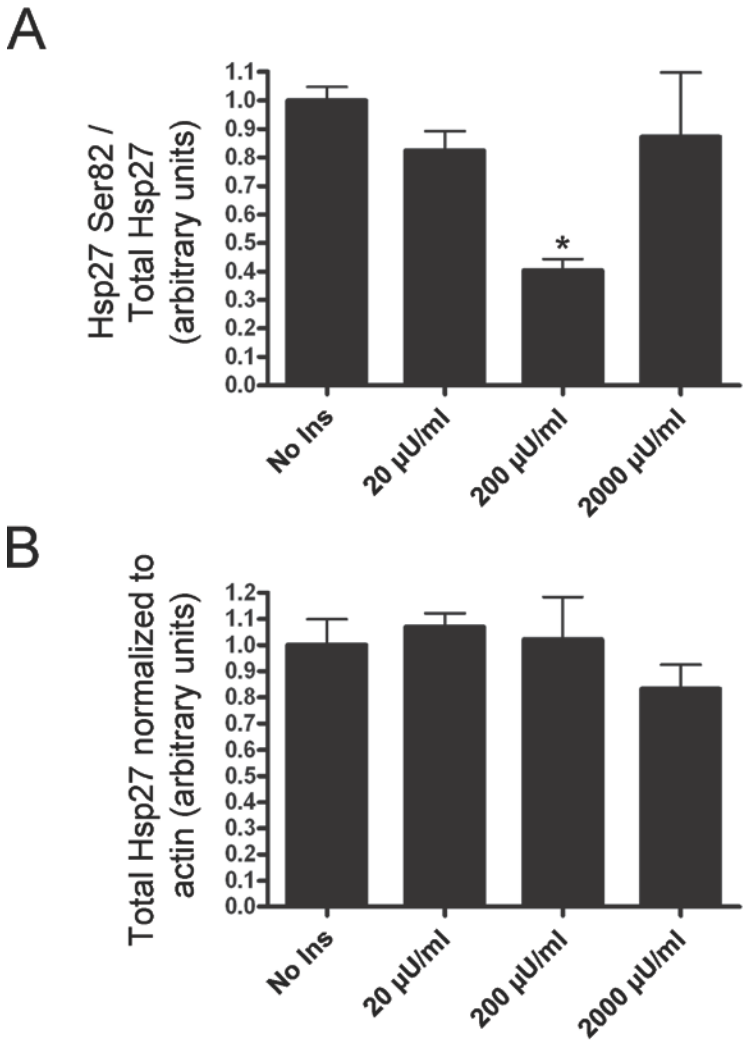
A
Hsp27 Ser82 / Total Hsp27 (arbitrary units)
1.1
1.0
0.9
0.8
0.7
0.6
0.5
0.4
0.3
0.2
0.1
0.0
*
No Ins
20 µU/ml
200 µU/ml
2000 µU/ml
B
Total Hsp27 normalized to actin (arbitrary units)
1.2
1.1
1.0
0.9
0.8
0.7
0.6
0.5
0.4
0.3
0.2
0.1
0.0
No Ins
20 µU/ml
200 µU/ml
2000 µU/ml

Figure 3.7.

Figure 3.8: The dose-dependent effect of insulin upon p38 MAPK in proliferative H9c2 cells. Proliferative H9c2 cells were examined for the effect of insulin supplementation in the media replacement. Cells had their media aspirated and replaced with new media (No Ins) or new media supplemented with 20, 200, or 2,000 μU/ml of insulin. Exposing proliferative H9c2 cells to insulin-supplemented media (20, 200, 2,000 μU/ml) for one hour did not change total levels of p38 MAPK. Data points represent mean ± SEM.

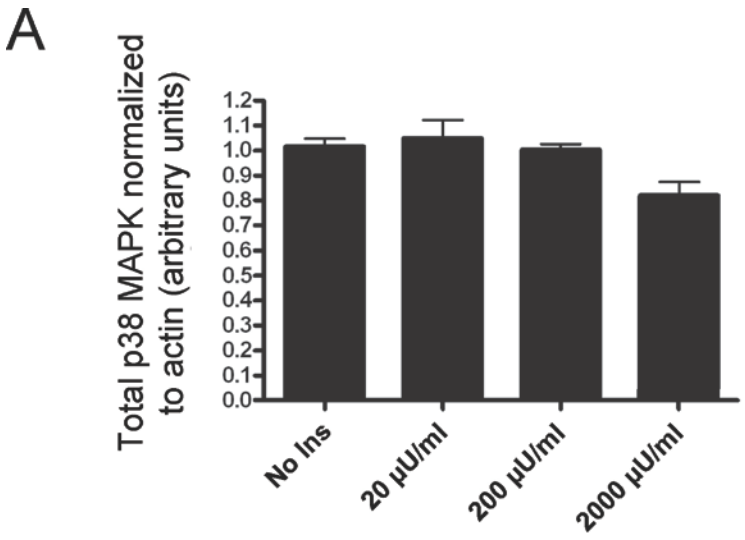
A
Total p38 MAPK normalized to actin (arbitrary units)
1.2
1.1
1.0
0.9
0.8
0.7
0.6
0.5
0.4
0.3
0.2
0.1
0.0
No Ins
20 µU/ml
200 µU/ml
2000 µU/ml

Figure 3.8.

Figure 3.9: The effect of insulin upon Hsp27 in differentiated H9c2 cells. Cells were either pretreated with normal media or with insulin in the media for 1 hr followed by media replacement and an additional 6 hrs of incubation also without insulin. Cells were also pretreated with insulin for 1 hr followed by media replacement and 6 additional hrs of incubation with insulin. H9c2 cells pretreated with insulin for one hour had higher levels of total Hps27. H9c2 cells pretreated with insulin for one hour, followed by an additional six hours of insulin supplementation, also had higher levels of total Hsp27 compared to non-supplemented cells (**A**). Insulin pretreatment or an additional six hours of insulin supplementation did not significantly affect total levels of phosphorylated Hsp27 serine 82 (**B**). Insulin pretreatment or an additional six hours of insulin supplementation significantly lowered relative levels of phosphorylated Hsp27 serine 82 (**C**). (*, $p < 0.05$, $n = 4$; **, $p < 0.01$, $n = 4$). Data points represent mean ± SEM. Please note: the arbitrary units in this figure cannot be compared to the arbitrary units used in other figures.

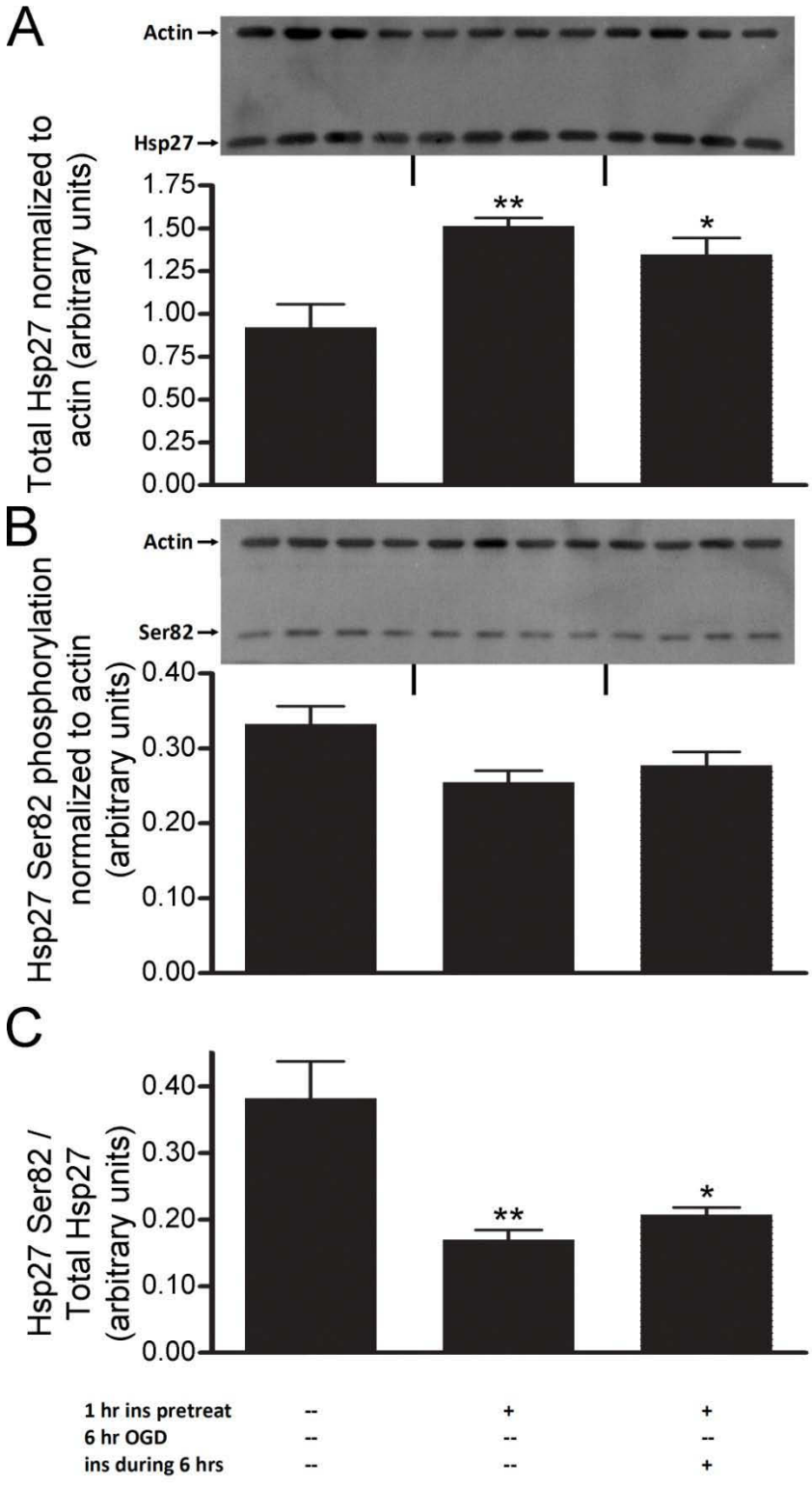
A
Actin
Hsp27
Total Hsp27 normalized to actin (arbitrary units)
1.75
1.50
1.25
1.00
0.75
0.50
0.25
0.00
**
*
B
Actin
Ser82
Hsp27 Ser82 phosphorylation normalized to actin (arbitrary units)
0.40
0.30
0.20
0.10
0.00
C
Hsp27 Ser82 / Total Hsp27 (arbitrary units)
0.40
0.30
0.20
0.10
0.00
**
*
1 hr ins pretreat -- + +
6 hr OGD -- -- --
ins during 6 hrs -- -- +

Figure 3.9.

Figure 3.10: The effect of oxygen-glucose deprivation and reoxygenation upon Hsp27 in differentiated H9c2 cells. Cells were pretreated with normal media for 1 hr followed by media replacement and an additional 6 hrs of either normal incubation or oxygen-glucose deprivation. After OGD, cells were either harvested or reoxygenated with normal media for 1 hr. Neither OGD nor reoxygenation changed total Hsp27 levels (**A**) or the total levels of phosphorylated Hsp27 serine 82 (**B**). After reoxygenation there was significantly higher relative levels of phosphorylated Hsp27 serine 82 than with 6 hrs of normal incubation or OGD alone (**C**; **, $p < 0.01$ reoxygenation vs normal, $n = 4$; ##, $p < 0.01$ reoxygenation vs OGD only, $n=4$). Data points represent mean ± SEM.

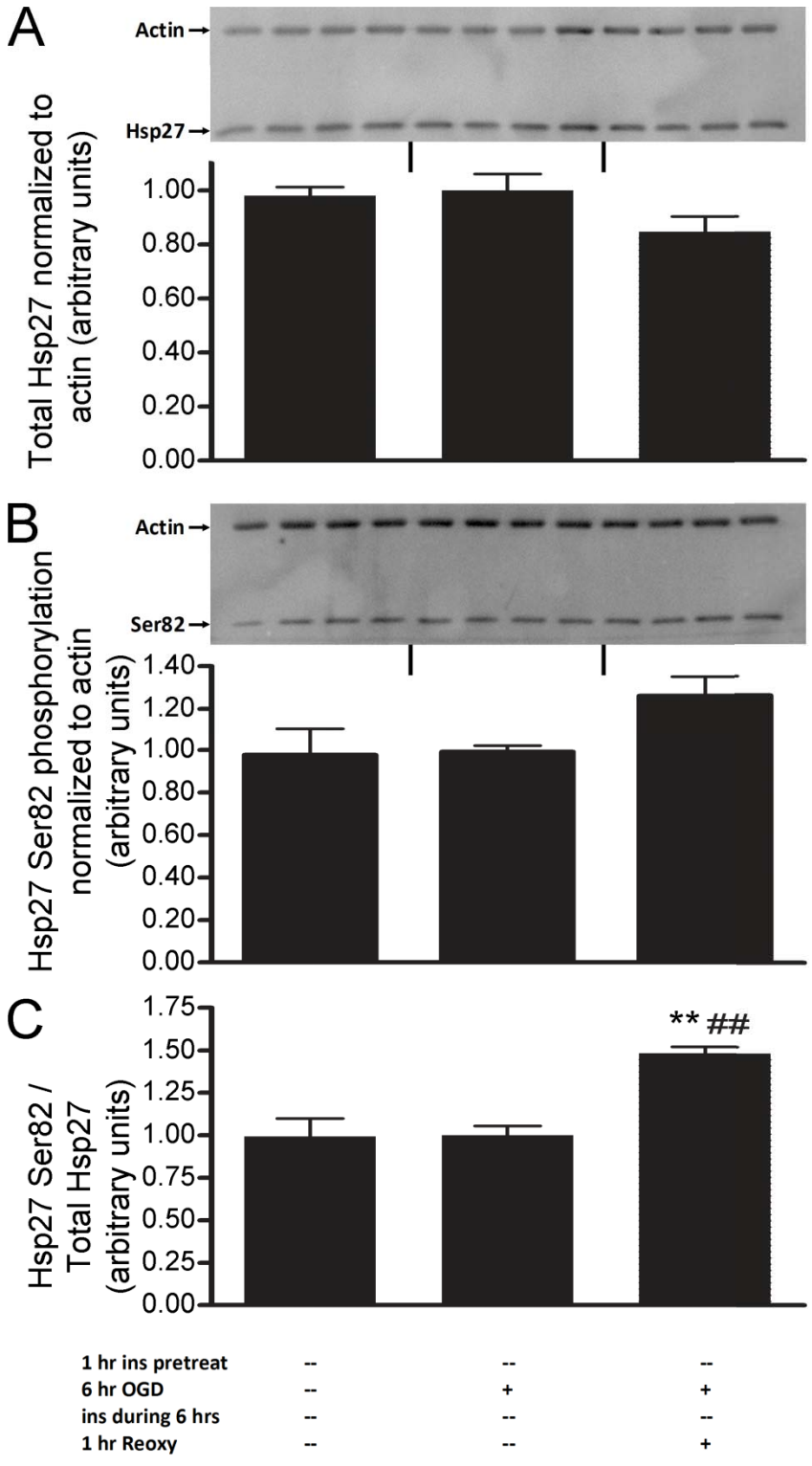
A
Actin
Hsp27
Total Hsp27 normalized to actin (arbitrary units)
1.00
0.80
0.60
0.40
0.20
0.00
B
Actin
Ser82
Hsp27 Ser82 phosphorylation normalized to actin (arbitrary units)
1.40
1.20
1.00
0.80
0.60
0.40
0.20
0.00
C
Hsp27 Ser82 / Total Hsp27 (arbitrary units)
1.75
1.50
1.25
1.00
0.75
0.50
0.25
0.00
** ##
1 hr ins pretreat -- -- --
6 hr OGD -- + +
ins during 6 hrs -- -- --
1 hr Reoxy -- -- +

Figure 3.10.

Figure 3.11: The effect of one or two hours of reoxygenation after oxygen-glucose deprivation upon Hsp27 in differentiated H9c2 cells. Cells were pretreated with normal media for 1 hr followed by media replacement and an additional 6 hrs of oxygen-glucose deprivation. After OGD, cells were either harvested or reoxygenated with normal media for 1 or 2 hrs. One or two hours of reoxygenation after OGD did not change total Hsp27 levels (**A**). After one hour of reoxygenation there was a significant increase in total levels of phosphorylated Hsp27 serine 82 (**B**), and after 2 hrs of reoxygenation there was a significant decrease in total levels of phosphorylated Hsp27 serine 82 compared to 1 hr. One hour of reoxygenation resulted in a significant increase in relative levels of phosphorylated Hsp27 serine 82 (**C**). (**, $p < 0.01$ vs OGD only, $n = 4$; #, $p < 0.05$ vs one hour reoxygenation, $n=4$). Data points represent mean ± SEM.

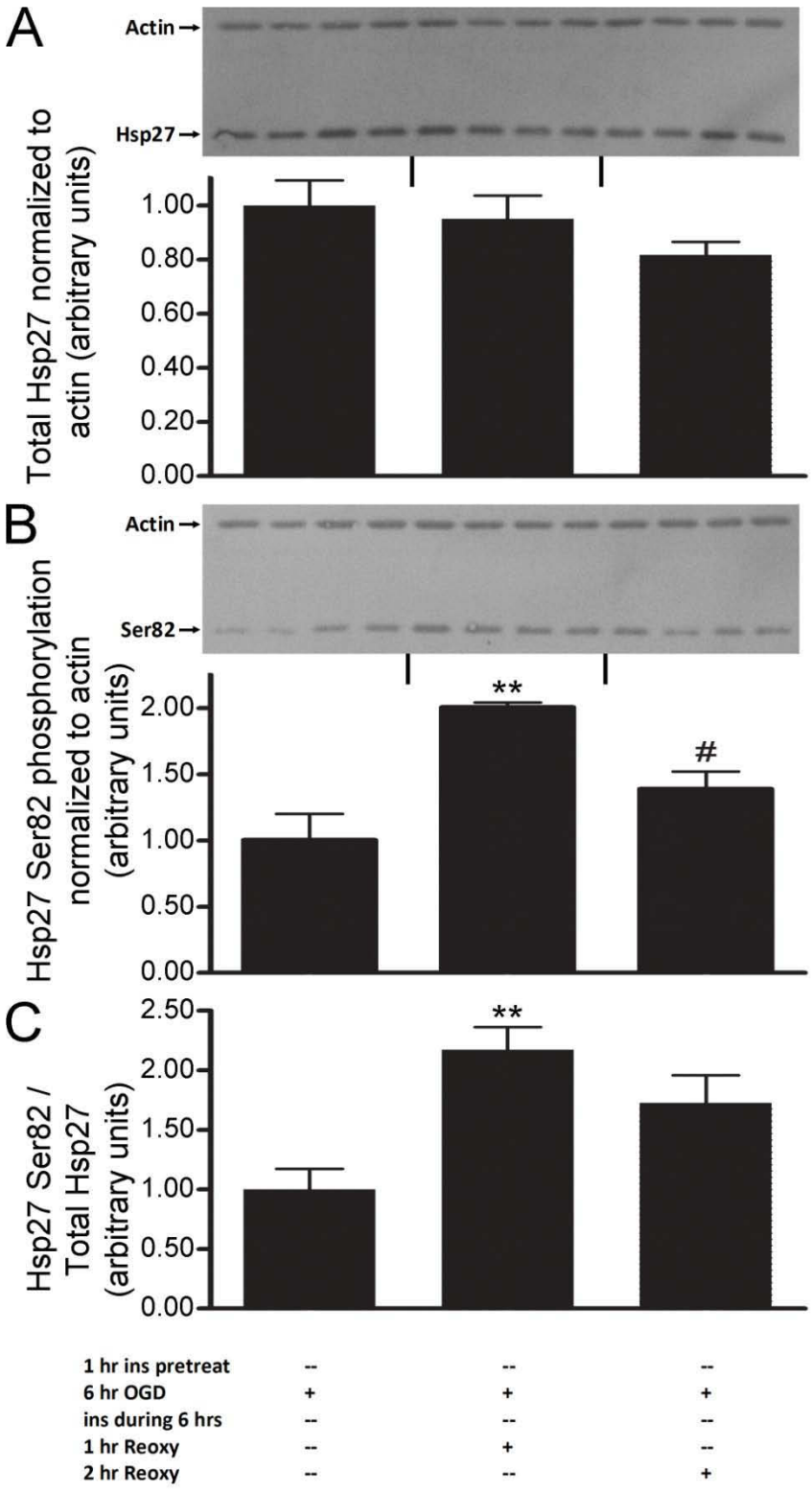
A
Actin
Hsp27
Total Hsp27 normalized to actin (arbitrary units)
1.00
0.80
0.60
0.40
0.20
0.00
B
Actin
Ser82
Hsp27 Ser82 phosphorylation normalized to actin (arbitrary units)
**
#
2.00
1.50
1.00
0.50
0.00
C
Hsp27 Ser82 / Total Hsp27 (arbitrary units)
**
2.50
2.00
1.50
1.00
0.50
0.00
1 hr ins pretreat -- -- --
6 hr OGD + + +
ins during 6 hrs -- -- --
1 hr Reoxy -- + --
2 hr Reoxy -- -- +

Figure 3.11.

Figure 3.12: The effect of oxygen-glucose deprivation and reoxygenation upon Hsp27 in differentiated H9c2 cells pretreated with insulin. Cells were pretreated with insulin for 1 hr followed by media replacement and an additional 6 hrs of either normal incubation or oxygen-glucose deprivation. After OGD, cells were either harvested or reoxygenated with normal media for 1 hr. Neither OGD nor reoxygenation changed total Hsp27 levels (**A**). One hour of reoxygenation significantly increased total levels of phosphorylated Hsp27 serine 82 compared to OGD alone (**B**). One hour of reoxygenation significantly increased relative levels of phosphorylated Hsp27 serine 82 compared to OGD alone (**C**). (#, $p < 0.05$ vs 6 hours of OGD, $n = 4$; ##, $p < 0.01$ vs 6 hours OGD, $n=4$). Data points represent mean ± SEM.

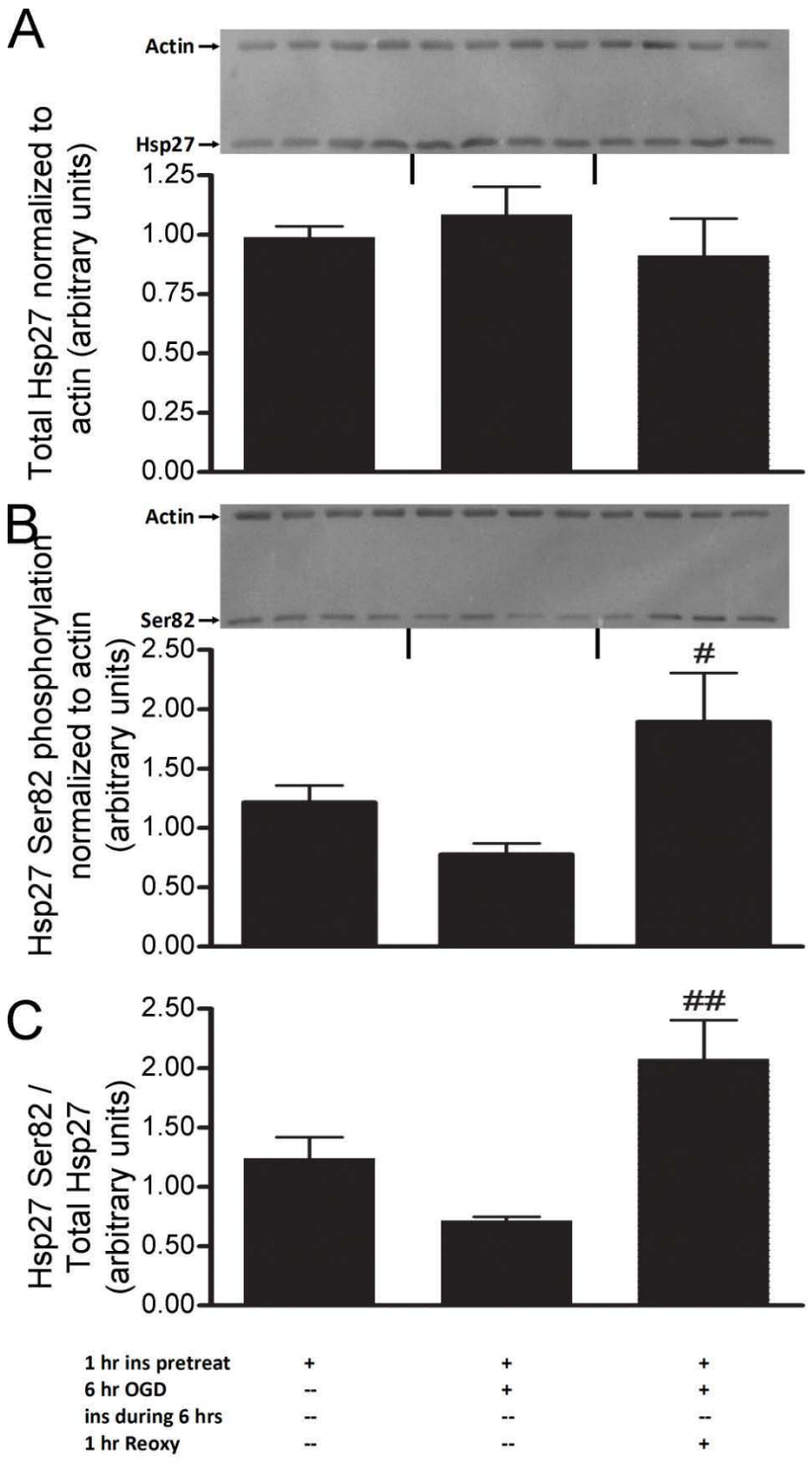
A
Actin
Hsp27
Total Hsp27 normalized to actin (arbitrary units)
1.25
1.00
0.75
0.50
0.25
0.00
B
Actin
Ser82
Hsp27 Ser82 phosphorylation normalized to actin (arbitrary units)
2.50
2.00
1.50
1.00
0.50
0.00
#
C
Hsp27 Ser82 / Total Hsp27 (arbitrary units)
2.50
2.00
1.50
1.00
0.50
0.00
##
1 hr ins pretreat + + +
6 hr OGD -- + +
ins during 6 hrs -- -- --
1 hr Reoxy -- -- +

Figure 3.12.

Figure 3.13: The effect of oxygen-glucose deprivation and insulin pretreatment upon Hsp27 in differentiated H9c2 cells. Cells were pretreated with normal media for 1 hr followed by media replacement and an additional 6 hrs of either normal incubation or oxygen-glucose deprivation. Cells were also pretreated with insulin for 1 hr followed by media replacement and an additional 6 hrs of oxygen-glucose deprivation. OGD with or without insulin pretreatment did not cause a change in total Hsp27 levels (**A**), in total levels of phosphorylated Hsp27 serine 82 (**B**), or in relative levels of phosphorylated Hsp27 serine 82 (**C**). Data points represent mean ± SEM (n = 4).

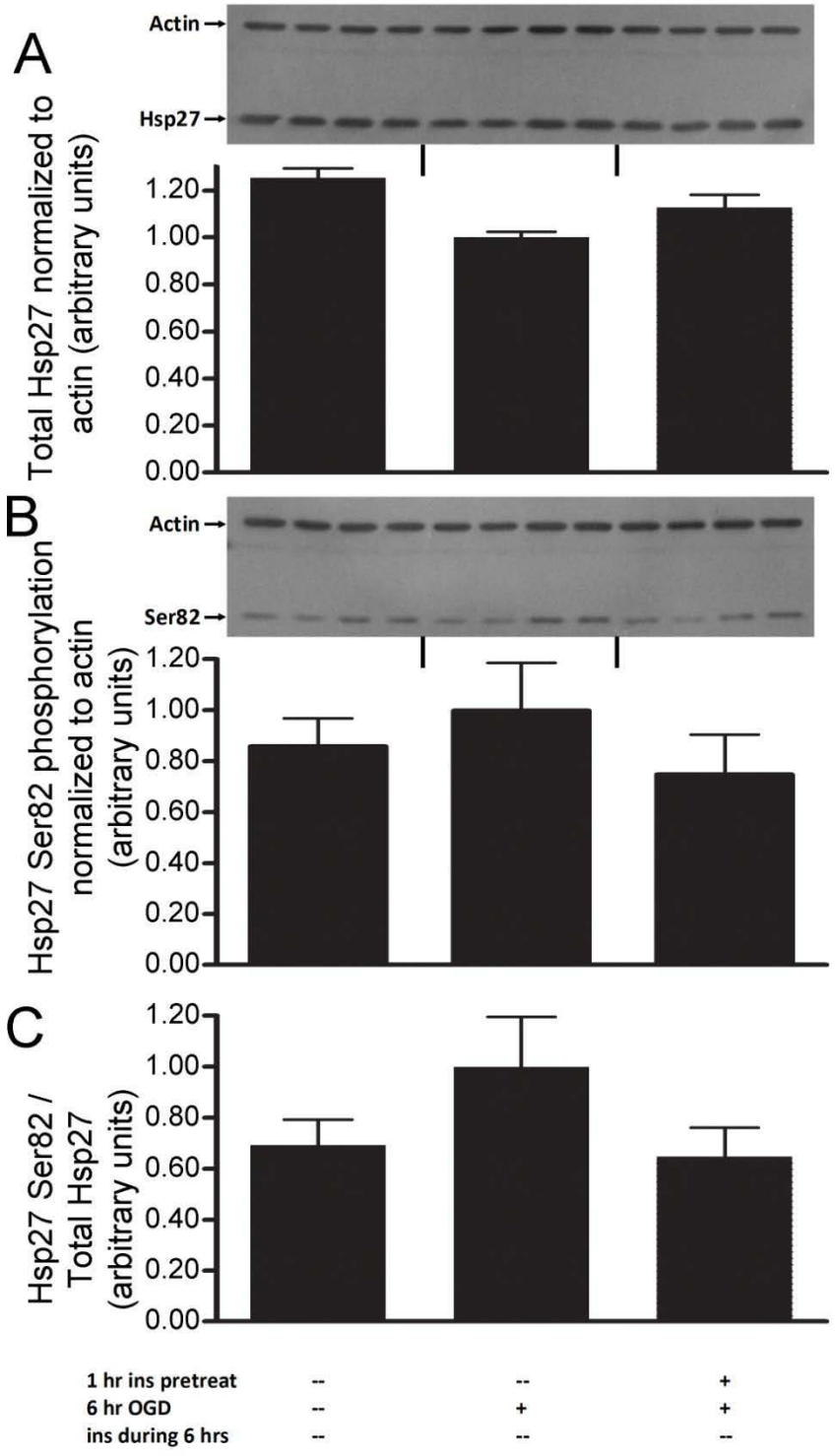
A
Actin
Hsp27
Total Hsp27 normalized to actin (arbitrary units)
1.20
1.00
0.80
0.60
0.40
0.20
0.00
B
Actin
Ser82
Hsp27 Ser82 phosphorylation normalized to actin (arbitrary units)
1.20
1.00
0.80
0.60
0.40
0.20
0.00
C
Hsp27 Ser82 / Total Hsp27 (arbitrary units)
1.20
1.00
0.80
0.60
0.40
0.20
0.00
1 hr ins pretreat -- -- +
6 hr OGD -- + +
ins during 6 hrs -- -- --

Figure 3.13.

Figure 3.14: The effect of insulin upon Hsp27 in differentiated H9c2 cells subjected to oxygen-glucose deprivation. Cells were either pretreated with normal media or with insulin in the media for 1 hr followed by media replacement and an additional 6 hrs of oxygen-glucose deprivation also without insulin. Cells were also pretreated with insulin for 1 hr followed by media replacement and 6 additional hrs of OGD with insulin. Neither insulin pretreatment nor insulin pretreatment and insulin during OGD caused a difference in total Hsp27 levels (**A**), total levels of phosphorylated Hsp27 serine 82 (**B**), or relative levels of phosphorylated Hsp27 serine 82 (**C**). Data points represent mean ± SEM (n = 4).

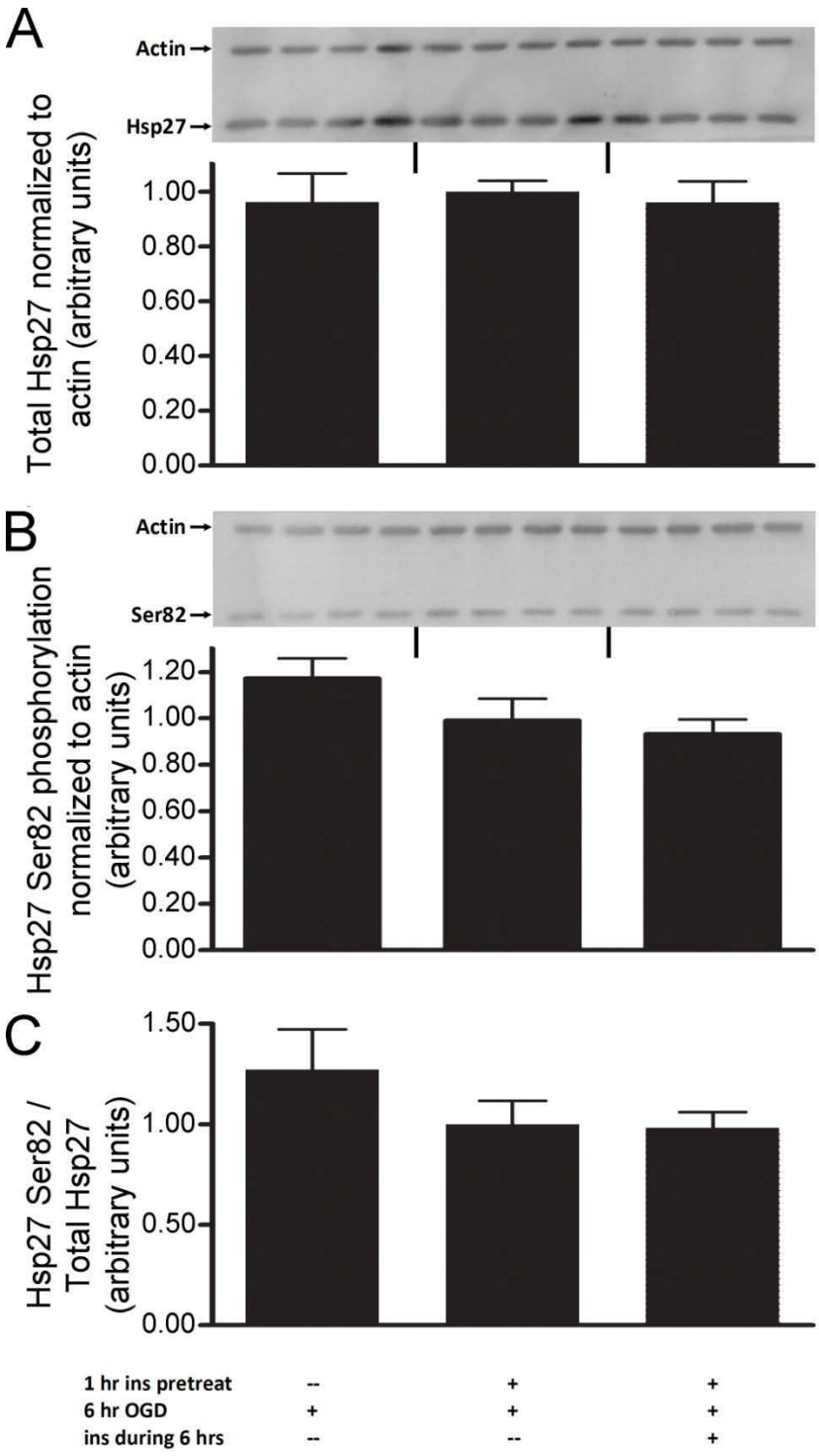
A
Actin
Hsp27
Total Hsp27 normalized to actin (arbitrary units)
1.00
0.80
0.60
0.40
0.20
0.00
B
Actin
Ser82
Hsp27 Ser82 phosphorylation normalized to actin (arbitrary units)
1.20
1.00
0.80
0.60
0.40
0.20
0.00
C
Hsp27 Ser82 / Total Hsp27 (arbitrary units)
1.50
1.00
0.50
0.00
1 hr ins pretreat -- + +
6 hr OGD + + +
ins during 6 hrs -- -- +

Figure 3.14.

Figure 3.15: The effect of insulin upon Hsp27 in differentiated H9c2 cells subjected to oxygen-glucose deprivation followed by 1 hr of reoxygenation. Cells were either pretreated with normal media or with insulin in the media for 1 hr followed by media replacement and an additional 6 hrs of oxygen-glucose deprivation also without insulin. Cells were also pretreated with insulin for 1 hr followed by media replacement and 6 additional hrs of OGD with insulin. After OGD, cells were reoxygenated with normal media for 1 hr. Insulin pretreatment or insulin pretreatment and OGD with insulin did not change total levels of Hsp27 (**A**). After reoxygenation following insulin pretreatment and OGD (with insulin) there were higher total levels of phosphorylated Hsp27 serine 82 than after reoxygenation following insulin pretreatment and OGD without insulin (**B**). Insulin pretreatment or insulin pretreatment and OGD with insulin did not change relative levels of phosphorylated Hsp27 serine 82 (**C**). (#, $p < 0.05$ vs OGD without insulin supplementation, $n = 4$). Data points represent mean ± SEM.

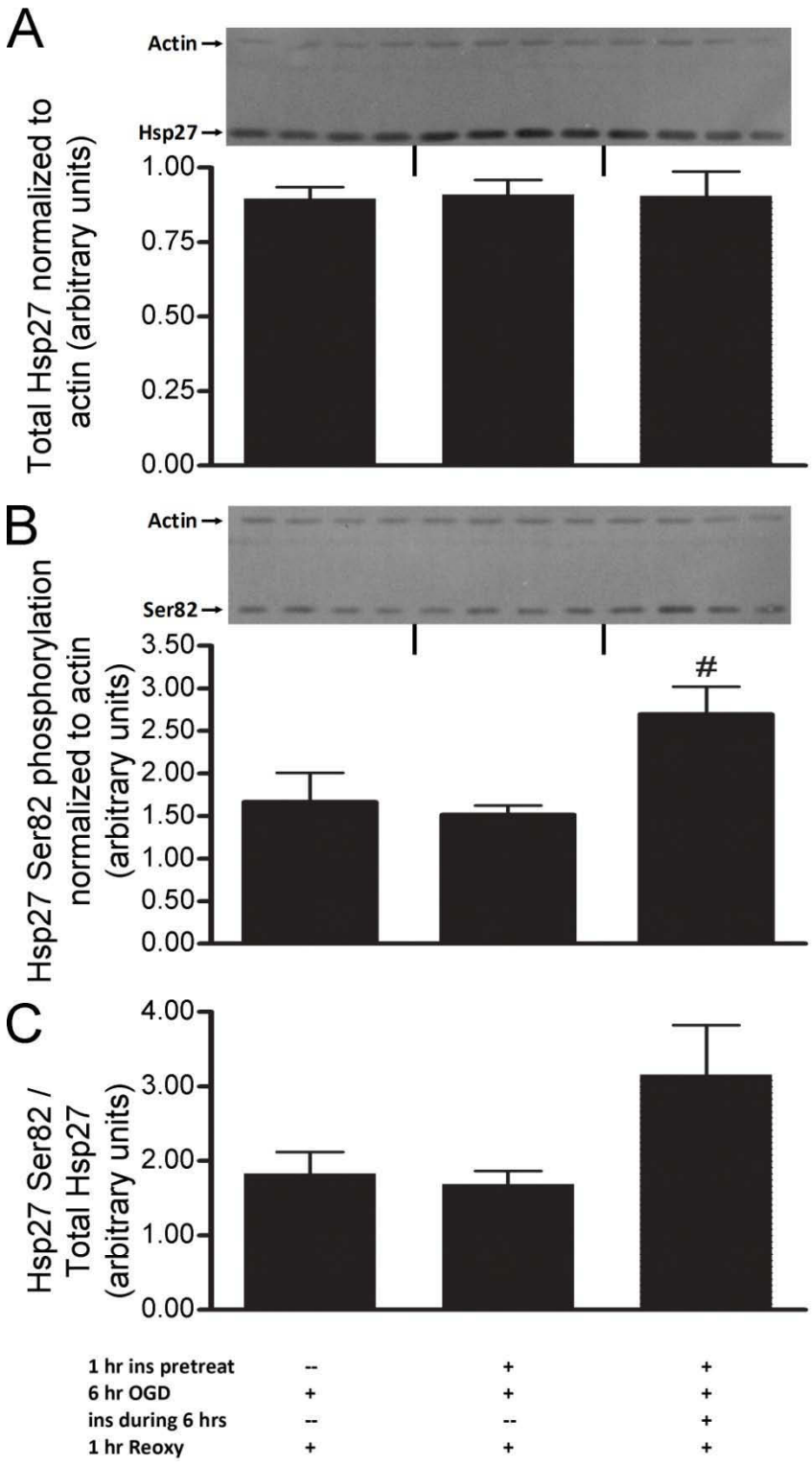
A
Actin
Hsp27
Total Hsp27 normalized to actin (arbitrary units)
1.00
0.75
0.50
0.25
0.00
B
Actin
Ser82
Hsp27 Ser82 phosphorylation normalized to actin (arbitrary units)
3.50
3.00
2.50
2.00
1.50
1.00
0.50
0.00
#
C
Hsp27 Ser82 / Total Hsp27 (arbitrary units)
4.00
3.00
2.00
1.00
0.00
1 hr ins pretreat -- + +
6 hr OGD + + +
ins during 6 hrs -- -- +
1 hr Reoxy + + +

Figure 3.15.

Figure 3.16: The effect of insulin upon Hsp27 in differentiated H9c2 cells subjected to oxygen-glucose deprivation followed by 2 hrs of reoxygenation. Cells were either pretreated with normal media or with insulin in the media for 1 hr followed by media replacement and an additional 6 hrs of oxygen-glucose deprivation also without insulin. Cells were also pretreated with insulin for 1 hr followed by media replacement and 6 additional hrs of OGD with insulin. After OGD, cells were reoxygenated with normal media for 2 hrs. Insulin pretreatment or insulin pretreatment and OGD with insulin did not change total levels of Hsp27 (**A**), total levels of phosphorylated Hsp27 serine 82 (**B**), or relative levels of phosphorylated Hsp27 serine 82 (**C**). Data points represent mean ± SEM (n = 4).

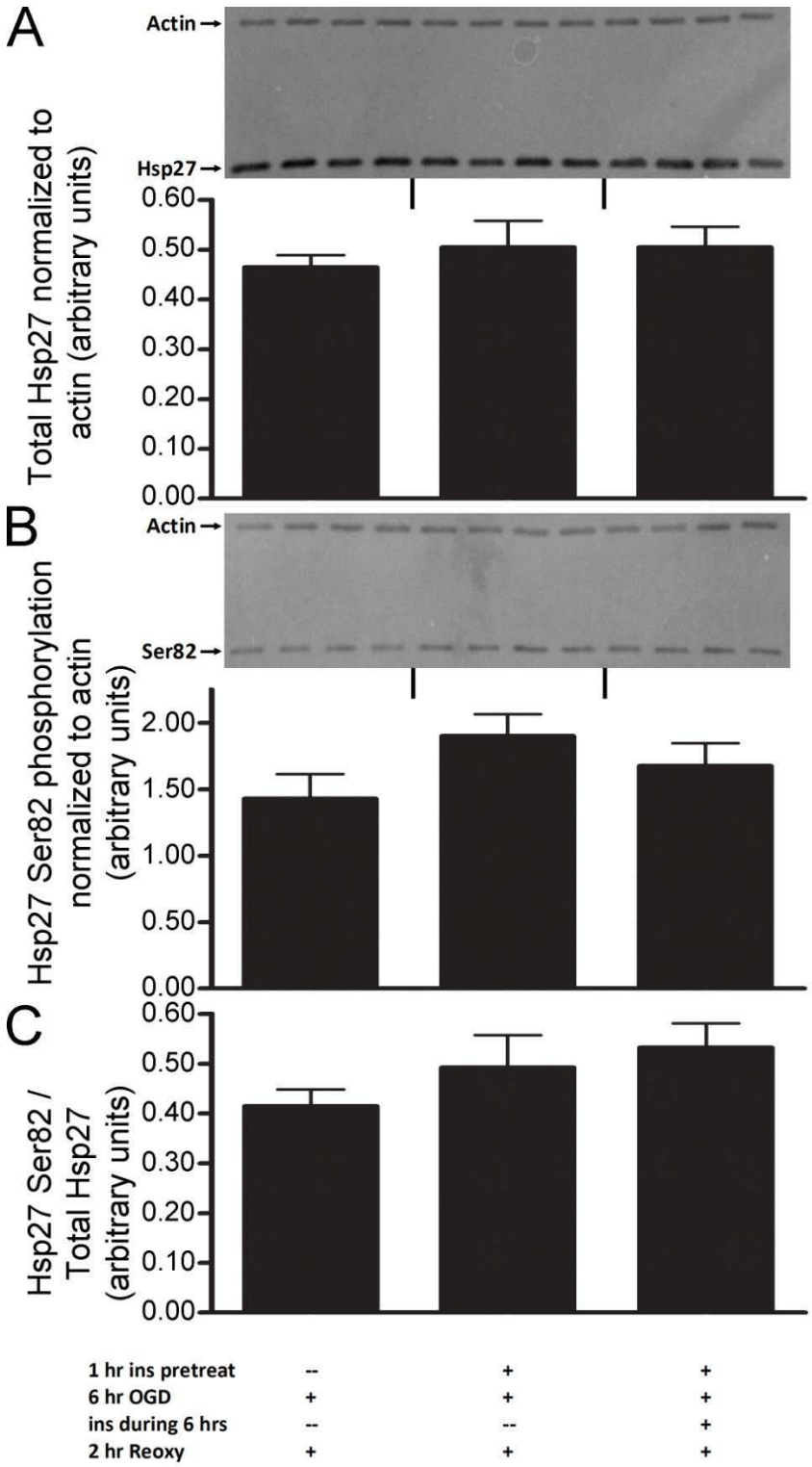
A
Actin
Hsp27
Total Hsp27 normalized to actin (arbitrary units)
0.60
0.50
0.40
0.30
0.20
0.10
0.00
B
Actin
Ser82
Hsp27 Ser82 phosphorylation normalized to actin (arbitrary units)
2.00
1.50
1.00
0.50
0.00
C
Hsp27 Ser82 / Total Hsp27 (arbitrary units)
0.60
0.50
0.40
0.30
0.20
0.10
0.00
1 hr ins pretreat -- + +
6 hr OGD + + +
ins during 6 hrs -- -- +
2 hr Reoxy + + +

Figure 3.16.

Figure 3.17: The effect of insulin and oxygen-glucose deprivation on differentiated H9c2 cells. Cells were subjected to control- or insulin-pretreatments for one hour and then placed into oxygen-glucose deprivation with or without insulin. After six hours, cells were either harvested or subject to 1 hr or 2 hrs of reoxygenation in fresh media. After Western analysis, data between membranes were combined after 2-way ANOVA between 8 samples indicated no difference between membranes. (**A**) Cells pretreated with insulin followed by 6 hrs of OGD had higher total Hsp27 levels than control-pretreated cells subjected to 6 hrs OGD and 1 hr or 2 hrs of reoxygenation (*, $p < 0.05$, $n = 4 - 8$). (**B**) Both insulin pretreatment and OGD or insulin pretreatment with insulin during OGD did not significantly change relative serine 82 phosphorylation after 6 hrs OGD. (**C**) One or 2 hrs of reoxygenation following normal pretreatment were associated with significantly higher relative serine 82 phosphorylation of Hsp27 than any of the 6 hr OGD conditions tested. (*, $p < 0.05$; $n = 4 – 8$).

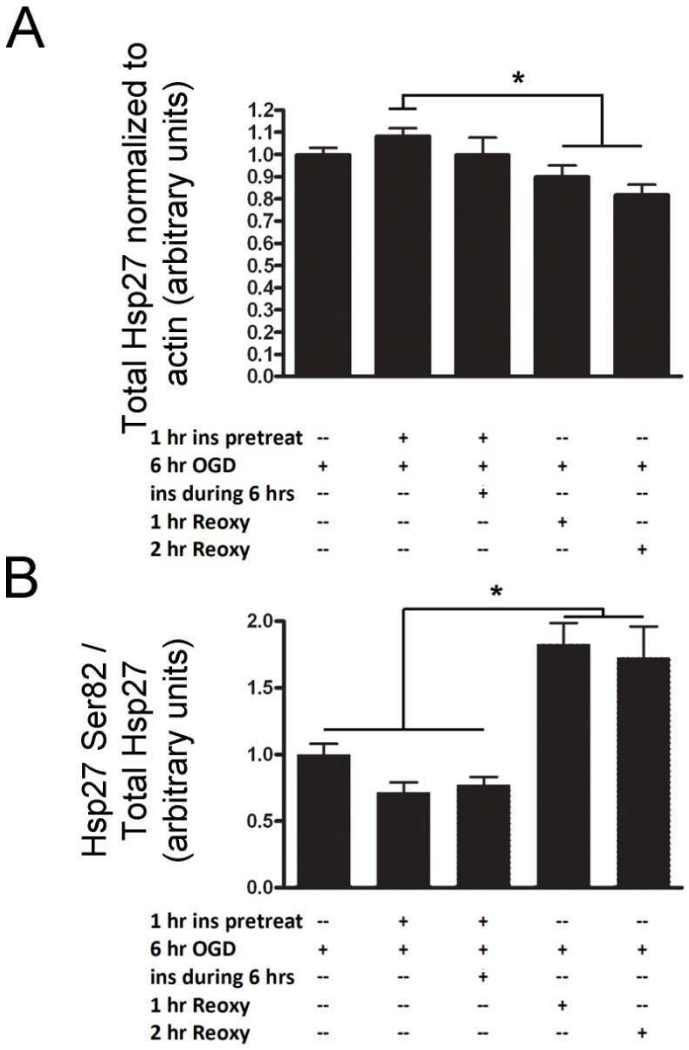
A
Total Hsp27 normalized to actin (arbitrary units)
*
1.2
1.1
1.0
0.9
0.8
0.7
0.6
0.5
0.4
0.3
0.2
0.1
0.0
1 hr ins pretreat -- + + -- --
6 hr OGD + + + + +
ins during 6 hrs -- -- + -- --
1 hr Reoxy -- -- -- + --
2 hr Reoxy -- -- -- -- +
B
Hsp27 Ser82 / Total Hsp27 (arbitrary units)
*
2.0
1.5
1.0
0.5
0.0
1 hr ins pretreat -- + + -- --
6 hr OGD + + + + +
ins during 6 hrs -- -- + -- --
1 hr Reoxy -- -- -- + --
2 hr Reoxy -- -- -- -- +

Figure 3.17.

Figure 3.18: Effects of insulin on Hsp27 and on actin dynamics in differentiated H9c2 cells. **A**. Immunocytochemistry of Hsp27. **B**. Phalloidin staining of actin. **C**. Hoescht staining of nuclei with merge of A and B. Cells in panels Aa, Ba, and Ca were pretreated without insulin in the media for 1 hr followed by media replacement and 6 additional hrs of incubation also without insulin. Cells in panels Ab, Bb, and Cb were pretreated with insulin in the media for 1 hr followed by media replacement and 6 additional hrs of incubation also without insulin. Cells in panels Ac, Bc, and Cc were pretreated with insulin in the media for 1 hr followed by media replacement and 6 additional hrs of incubation with insulin. Cells incubated without insulin showed cytoplasmic and perinuclear Hsp27-immunoreactivity (**Aa**) with minimal Hsp27-immunoreactivity in the nucleus. Cells pretreated with insulin showed cytoplasmic and perinuclear Hsp27-immunoreactivity (**Ab**) along with Hsp27-immunoreactivity in the nucleus. Cells pretreated with insulin in the media for 1 hr followed by media replacement and 6 additional hrs of incubation with insulin showed cytoplasmic and perinuclear Hsp27-immunoreactivity (**Ac**) along with some Hsp27-immunoreactivity in the nucleus. Cells incubated without insulin had regular and organized peripheral actin (**Ba**) and disorganized perinuclear actin. Insulin had no apparent effect on the regular and organized distribution of peripheral actin (**Bb** and **Bc**) or on the disorganized distribution of perinuclear actin. Scale bar = 25 μm.

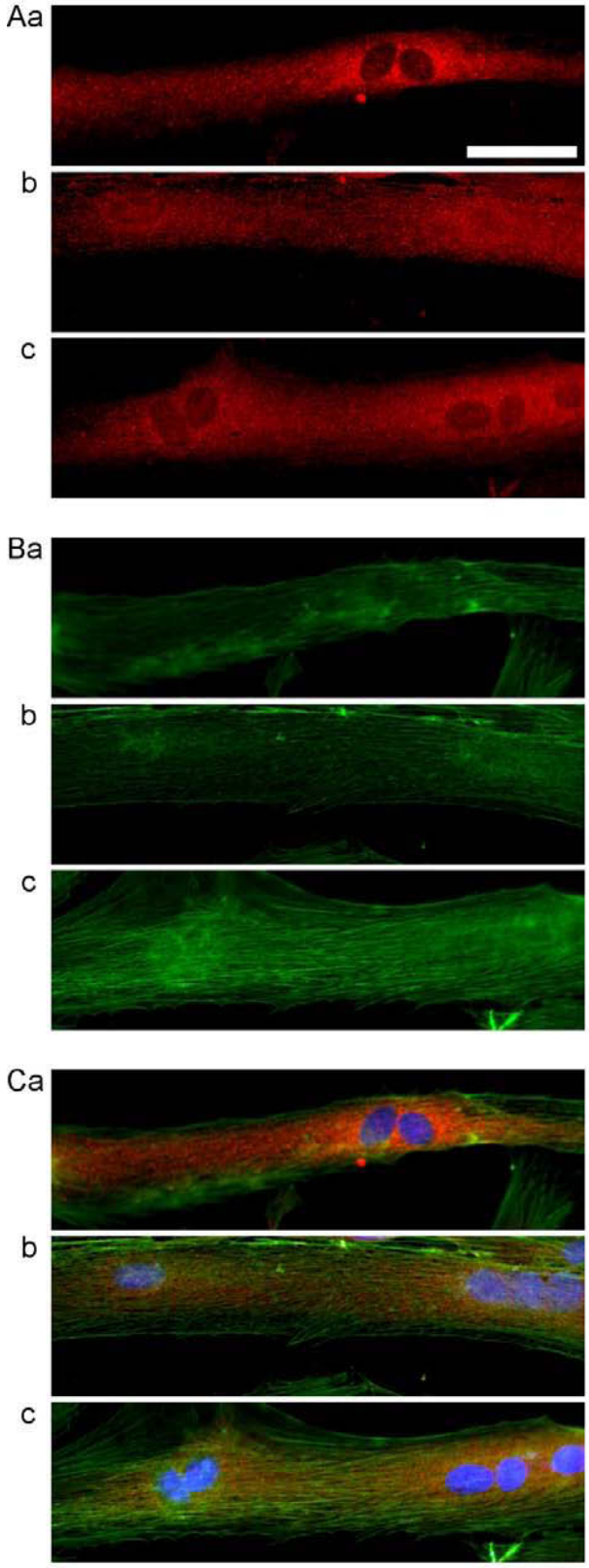

Figure 3.18.

Figure 3.19: Effects of insulin on Hsp27 and on actin dynamics in differentiated H9c2 cells during oxygen glucose deprivation. **A**. Immunocytochemistry of Hsp27. **B**. Phalloidin staining of actin. **C**. Hoescht staining of nuclei with merge of A and B. Cells in panels Aa, Ba, and Ca were pretreated without insulin in the media for 1 hr followed by media replacement and 6 additional hrs of incubation without insulin and with oxygen-glucose deprivation. Cells in panels Ab, Bb, and Cb were pretreated with insulin in the media for 1 hr followed by media replacement and 6 additional hrs of incubation without insulin and with oxygen-glucose deprivation. Cells in panels Ac, Bc, and Cc were pretreated with insulin in the media for 1 hr followed by media replacement and 6 additional hrs of incubation with insulin and with oxygen-glucose deprivation. Cells incubated without insulin showed cytoplasmic, perinuclear, and nuclear Hsp27-immunoreactivity (**Aa**). Cytoplasmic Hsp27-immunoreactivity is also unevenly distributed and forms condensates. After insulin pretreatment there was cytoplasmic, perinuclear, and nuclear Hsp27-immunoreactivity (**Ab**). Hsp27-immunoreactivity is stronger in perinuclear areas than in nuclei or in other cytoplasm. Insulin pretreatment and oxygen glucose deprivation with insulin resulted in cytoplasmic, perinuclear, and nuclear Hsp27-immunoreactivity (**Ac**). Hsp27-immunoreactivity is stronger in perinuclear areas than in nuclei or in other cytoplasm. Cells incubated without insulin also had disorganized actin (**Ba**) throughout the cytoplasm and in the perinuclear region. Insulin pretreatment (**Bb**) also caused disorganized actin throughout the cytoplasm and in the perinuclear region, however cytoplasmic actin also formed increased amounts of actin condensates during oxygen glucose deprivation. Insulin pretreatment and oxygen

glucose deprivation with insulin caused disorganized actin (**Bc**) throughout the cytoplasm and in the perinuclear region. Scale bar = 25 μm.

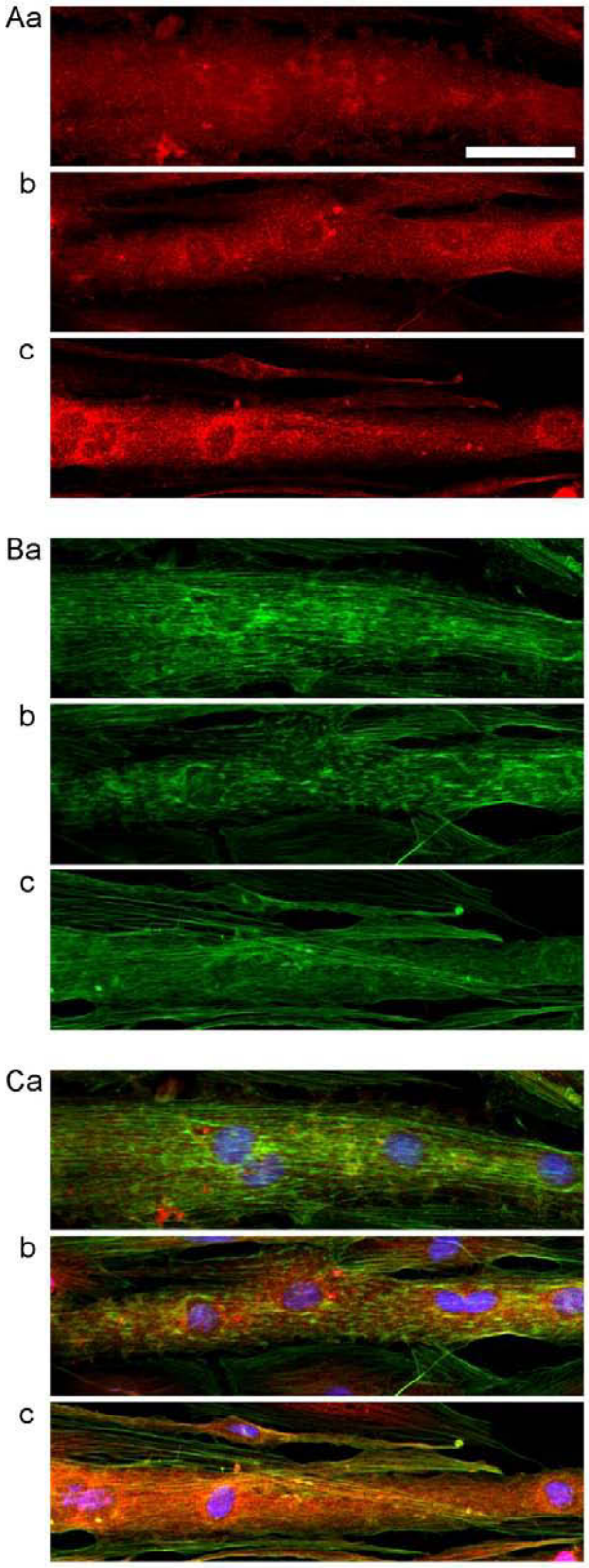

Figure 3.19.

Figure 3.20: Effects of insulin on Hsp27 and on actin dynamics in differentiated H9c2 cells following oxygen glucose deprivation and 1 hr of reoxygenation. **A**. Immunocytochemistry of Hsp27. **B**. Phalloidin staining of actin. **C**. Hoescht staining of nuclei with merge of A and B. Cells in panels Aa, Ba, and Ca were pretreated without insulin in the media for 1 hr followed by media replacement and 6 additional hrs of incubation without insulin and with oxygen-glucose deprivation followed by media replacement and 1 additional hr of incubation with oxygenation and without insulin. Cells in panels Ab, Bb, and Cb were pretreated with insulin in the media for 1 hr followed by media replacement and 6 additional hrs of incubation without insulin and with oxygen-glucose deprivation followed by media replacement and 1 additional hr of incubation with oxygenation and without insulin. Cells in panels Ac, Bc, and Cc were pretreated with insulin in the media for 1 hr followed by media replacement and 6 additional hrs of incubation with insulin and with oxygen-glucose deprivation followed by media replacement and 1 additional hr of incubation with oxygenation and without insulin. Cells incubated without insulin showed cytoplasmic, perinuclear, and nuclear Hsp27-immunoreactivity (**Aa**). Hsp27-immuoreactivity was higher in the nuclear and perinuclear regions than in the rest of the cytoplasm. Insulin pretreatment (**Ab**) and oxygen glucose deprivation with insulin (**Ac**) caused no difference in cytoplasmic, perinuclear, and nuclear Hsp27-immunoreactivity after 1 hr of reoxygenation. Cells incubated without insulin also had disorganized actin (**Ba**) throughout the cytoplasm and in the perinuclear region. Insulin pretreatment did not affect the perinuclear disorganization of actin (**Bb**), but increased the presence of cytoplasmic actin condensates visible after 1 hr of reoxygention. Insulin pretreatment and oxygen glucose

deprivation with insulin resulted in disorganized actin (**Bc**) throughout the cytoplasm and in the perinuclear region after 1 hr reoxygenation. Scale bar = 25 μm.

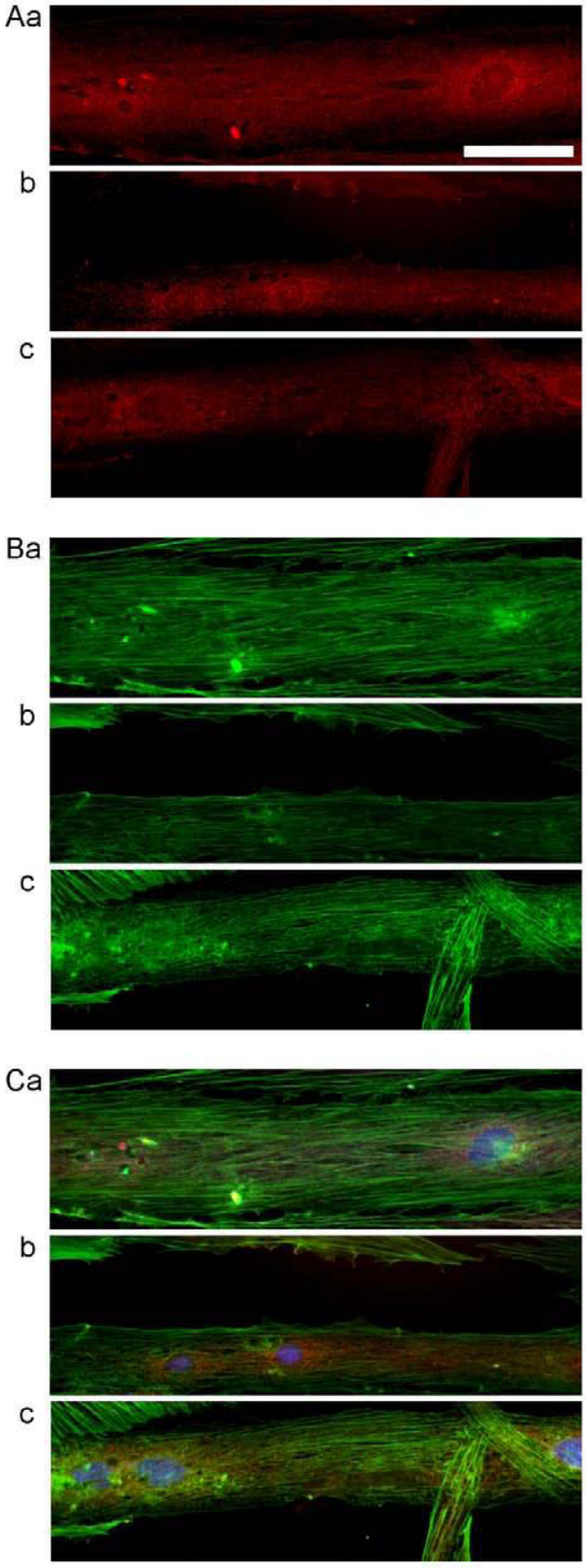

Figure 3.20.

Figure 3.21: Effects of insulin on Hsp27 and on actin dynamics in differentiated H9c2 cells following oxygen glucose deprivation and 2 hrs of reoxygenation. **A**. Immunocytochemistry of Hsp27. **B**. Phalloidin staining of actin. **C**. Hoescht staining of nuclei with merge of A and B. Cells in panels Aa, Ba, and Ca were pretreated without insulin in the media for 1 hr followed by media replacement and 6 additional hrs of incubation without insulin and with oxygen-glucose deprivation followed by media replacement and 2 additional hrs of incubation with oxygenation and without insulin. Cells in panels Ab, Bb, and Cb were pretreated with insulin in the media for 1 hr followed by media replacement and 6 additional hrs of incubation without insulin and with oxygen-glucose deprivation followed by media replacement and 2 additional hrs of incubation with oxygenation and without insulin. Cells in panels Ac, Bc, and Cc were pretreated with insulin in the media for 1 hr followed by media replacement and 6 additional hrs of incubation with insulin and with oxygen-glucose deprivation followed by media replacement and 2 additional hrs of incubation with oxygenation and without insulin. Cells incubated without insulin showed cytoplasmic, perinuclear, and nuclear Hsp27-immunoreactivity (**Aa**). Hsp27-immunoreactivity is higher in perinuclear regions than in other cytoplasmic regions or within the nuclei. Insulin did not cause a difference in Hsp27-immunoreactivity (**Ab** and **Ac**) after 2 hrs of reoxygenation. Cells incubated without insulin had regular and organized distribution of peripheral actin and disorganized perinuclear actin (**Ba**). Insulin had no apparent effect on the regular and organized distribution of peripheral actin or on the disorganized distribution of perinuclear actin (**Bb** and **Bc**). Scale bar = 25 μm.

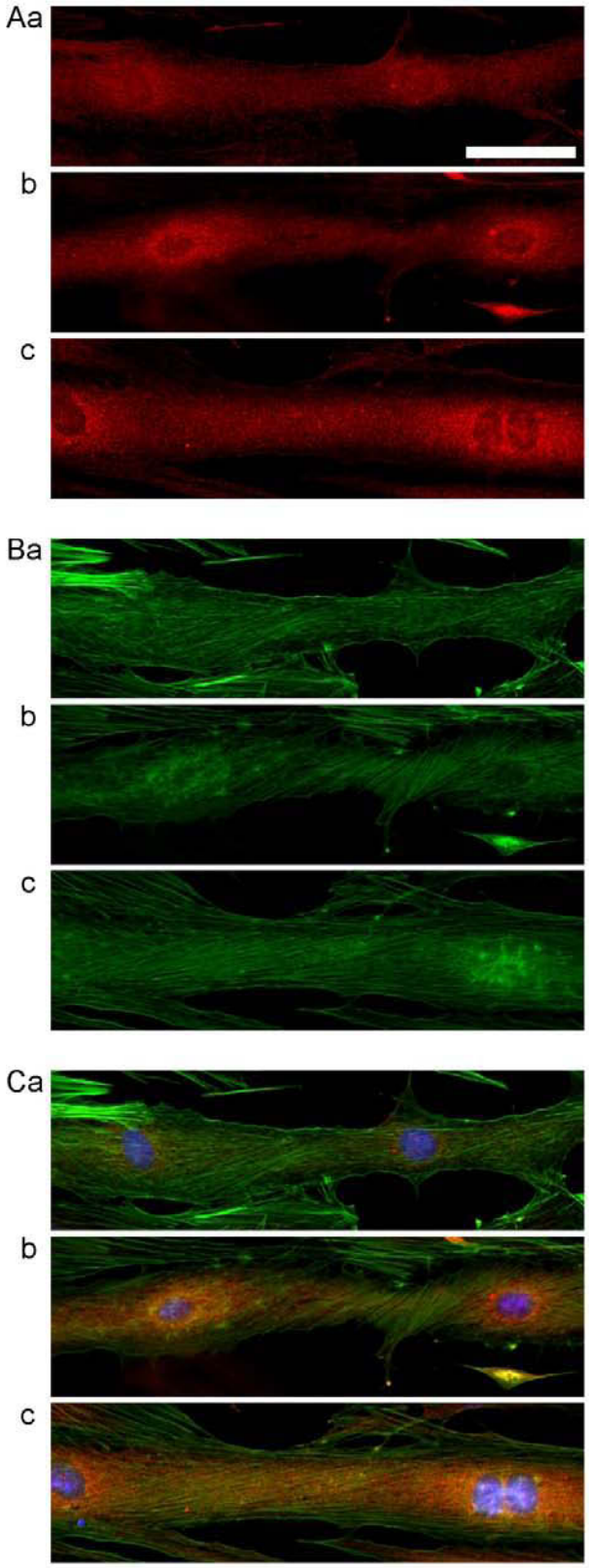

Figure 3.21.

Figure 3.22: The effect of insulin upon p38 MAPK in differentiated H9c2 cells. Cells were either pretreated with normal media or with insulin in the media for 1 hr followed by media replacement and an additional 6 hrs of incubation also without insulin. Cells were also pretreated with insulin for 1 hr followed by media replacement and 6 additional hrs of incubation with insulin. Cells pretreated with insulin and cells with further insulin supplementation had significantly lower levels of total p38 MAPK (**A**). Insulin did not change total levels of phospho-p38 (**B**). Insulin does not significantly affect relative levels of phospho-p38 MAPK (**C**). Data points represent mean ± SEM (n = 4).

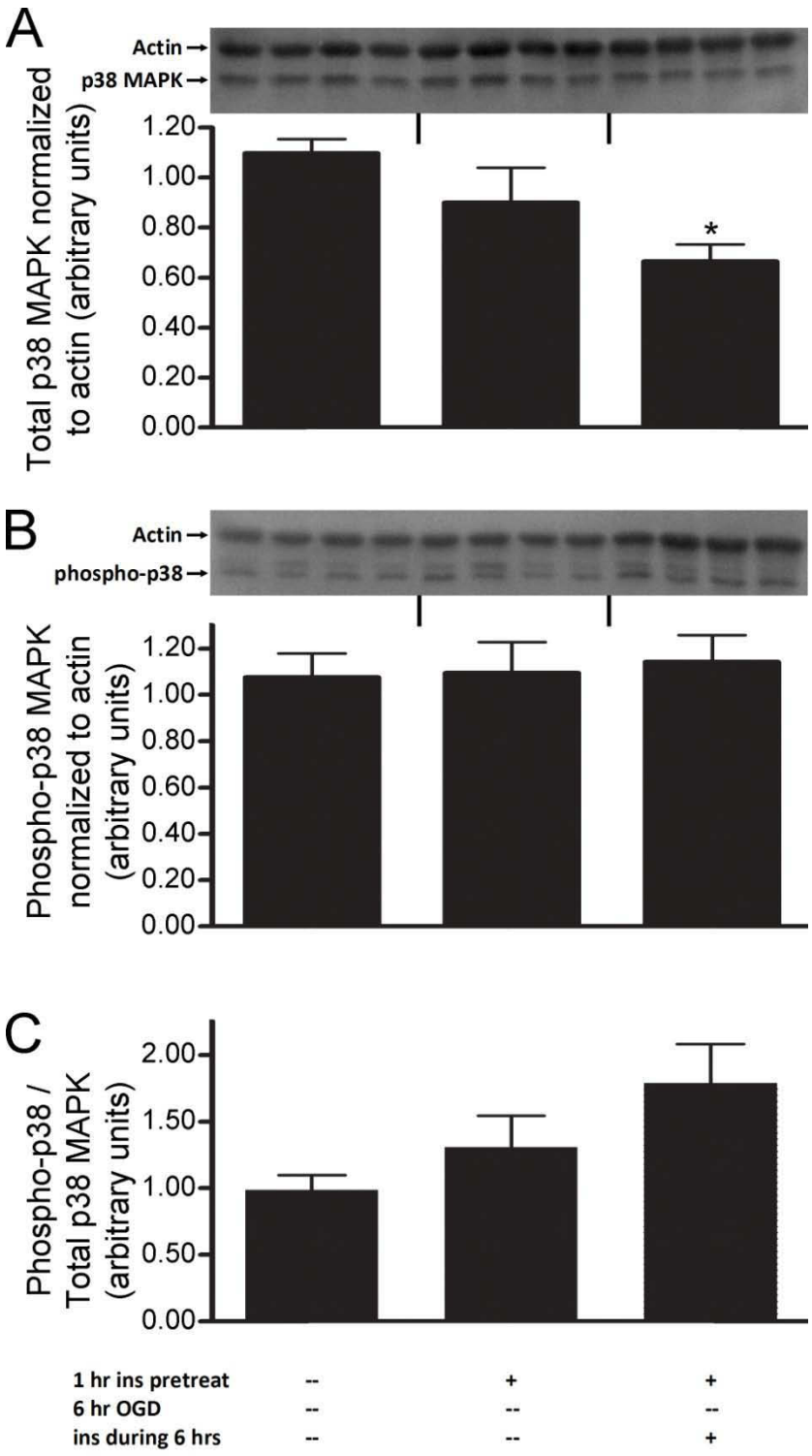
A
Actin
p38 MAPK
Total p38 MAPK normalized to actin (arbitrary units)
1.20
1.00
0.80
0.60
0.40
0.20
0.00
*
B
Actin
phospho-p38
Phospho-p38 MAPK normalized to actin (arbitrary units)
1.20
1.00
0.80
0.60
0.40
0.20
0.00
C
Phospho-p38 / Total p38 MAPK (arbitrary units)
2.00
1.50
1.00
0.50
0.00
1 hr ins pretreat -- + +
6 hr OGD -- -- --
ins during 6 hrs -- -- +

Figure 3.22.

Figure 3.23: The effect of oxygen-glucose deprivation and reoxygenation upon p38 MAPK in differentiated H9c2 cells. Cells were pretreated with normal media for 1 hr followed by media replacement and an additional 6 hrs of either normal incubation or oxygen-glucose deprivation. After OGD, cells were either harvested or reoxygenated with normal media for 1 hr. OGD and OGD followed by reoxygenation decreased total p38 MAPK (**A**). Neither OGD nor OGD followed by reoxygenation changed total (**B**) or relative (**C**) levels of phospho-p38 MAPK. (**, $p < 0.01$ vs cells not subjected to OGD, $n = 4$). Data points represent mean ± SEM.

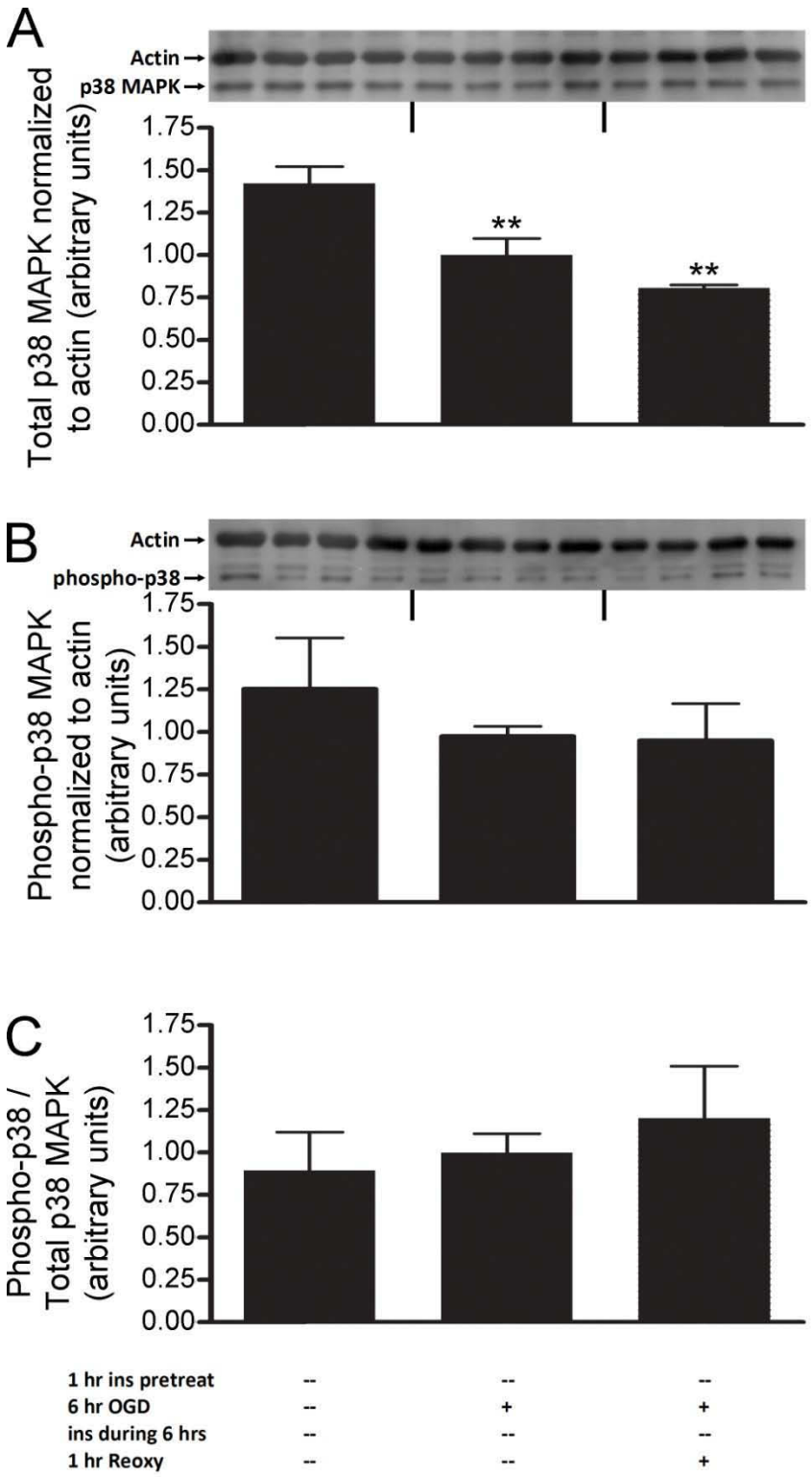
A
Actin
p38 MAPK
Total p38 MAPK normalized to actin (arbitrary units)
1.75
1.50
1.25
1.00
0.75
0.50
0.25
0.00
**
**
B
Actin
phospho-p38
Phospho-p38 MAPK normalized to actin (arbitrary units)
1.75
1.50
1.25
1.00
0.75
0.50
0.25
0.00
C
Phospho-p38 / Total p38 MAPK (arbitrary units)
1.75
1.50
1.25
1.00
0.75
0.50
0.25
0.00
1 hr ins pretreat -- -- --
6 hr OGD -- + +
ins during 6 hrs -- -- --
1 hr Reoxy -- -- +

Figure 3.23.

Figure 3.24: The effect of oxygen-glucose deprivation and insulin pretreatment upon p38 MAPK in differentiated H9c2 cells. Cells were pretreated with normal media for 1 hr followed by media replacement and an additional 6 hrs of either normal incubation or oxygen-glucose deprivation. Cells were also pretreated with insulin for 1 hr followed by media replacement and an additional 6 hrs of oxygen-glucose deprivation. OGD with and without insulin pretreatment did not cause a significant difference in total p38 MAPK (**A**). OGD with and without insulin pretreatment did not significantly change levels of total phospho-p38 MAPK (**B**) or relative levels of phospho-p38 MAPK (**C**). Data points represent mean ± SEM (n = 4).

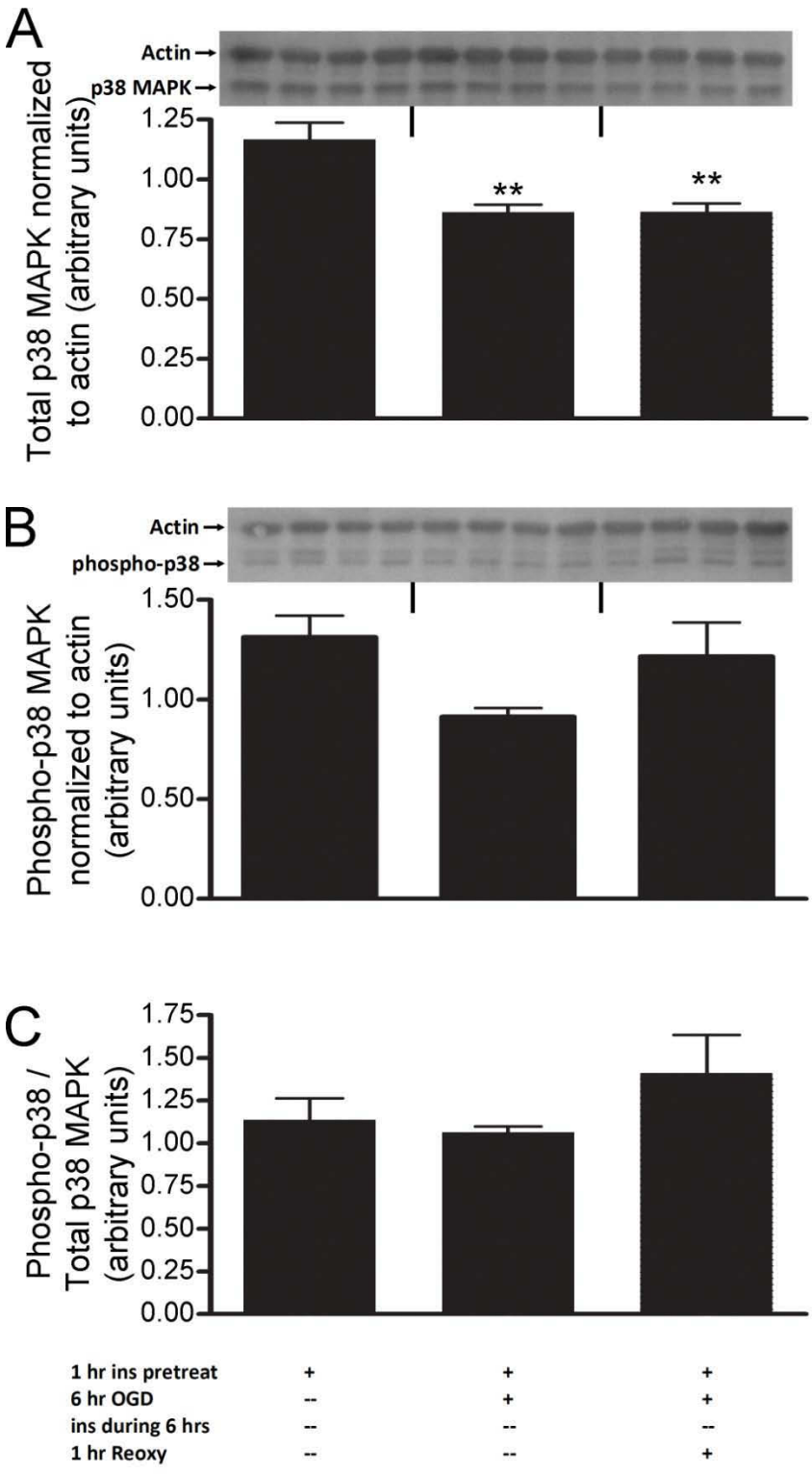
A
Actin
p38 MAPK
Total p38 MAPK normalized to actin (arbitrary units)
1.25
1.00
0.75
0.50
0.25
0.00
**
**
B
Actin
phospho-p38
Phospho-p38 MAPK normalized to actin (arbitrary units)
1.50
1.00
0.50
0.00
C
Phospho-p38 / Total p38 MAPK (arbitrary units)
1.75
1.50
1.25
1.00
0.75
0.50
0.25
0.00
1 hr ins pretreat + + +
6 hr OGD -- + +
ins during 6 hrs -- -- --
1 hr Reoxy -- -- +

Figure 3.24.

Figure 3.25: The effect of insulin upon p38 MAPK in differentiated H9c2 cells subjected to oxygen-glucose deprivation followed by 1 hr of reoxygenation. Cells were either pretreated with normal media or with insulin in the media for 1 hr followed by media replacement and an additional 6 hrs of oxygen-glucose deprivation also without insulin. Cells were also pretreated with insulin for 1 hr followed by media replacement and 6 additional hrs of OGD with insulin. After OGD, cells were reoxygenated with normal media for 1 hr. Insulin pretreatment followed by OGD with insulin resulted in higher levels of total p38 MAPK (**A**). Insulin pretreatment or insulin pretreatment and OGD with insulin did not change total levels of phospho-p38 MAPK (**B**) or relative levels of phospho-p38 MAPK (**C**). (*, $p < 0.05$ vs no insulin pretreatment, $n = 4$). Data points represent mean ± SEM.

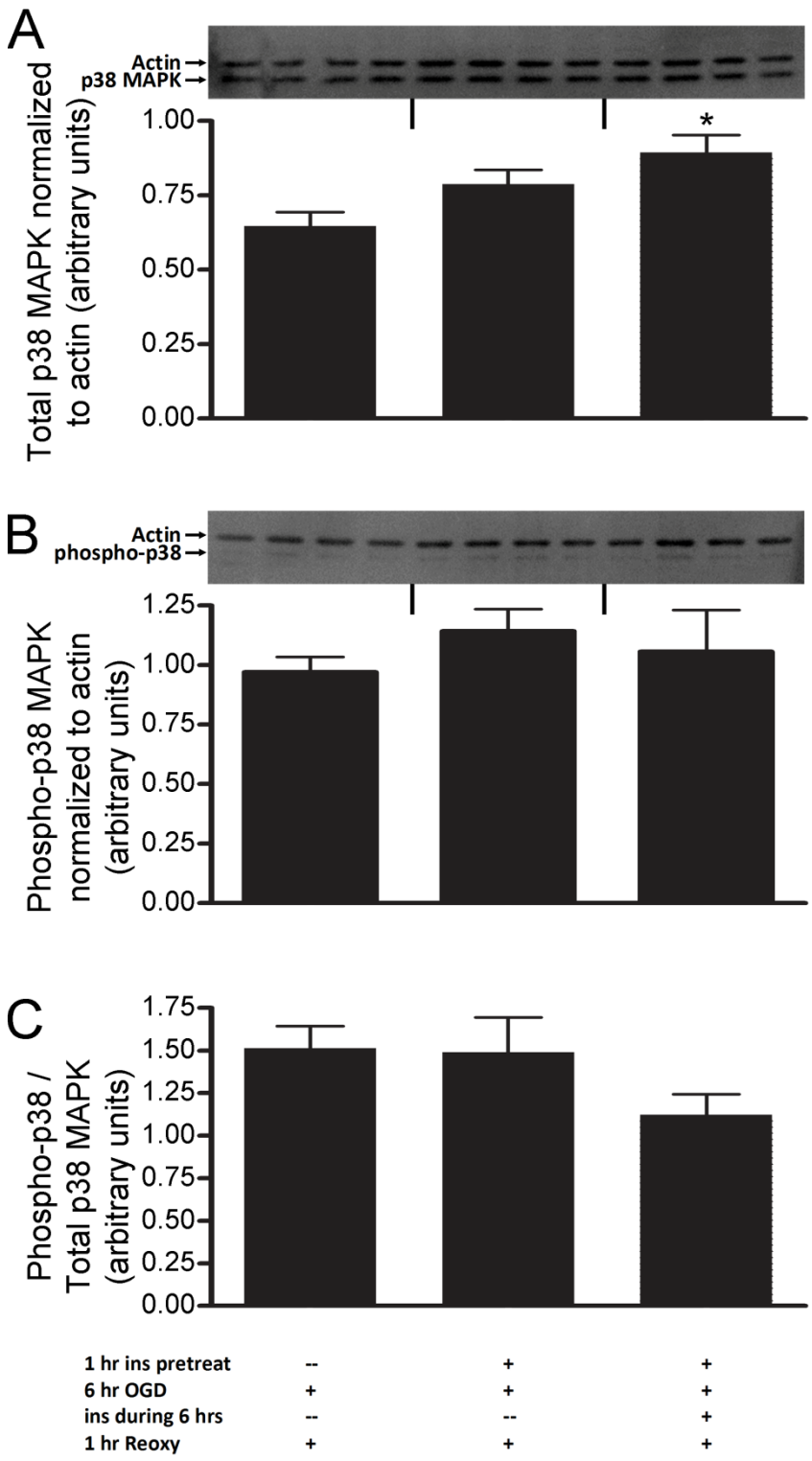
A
Actin
p38 MAPK
Total p38 MAPK normalized to actin (arbitrary units)
1.00
0.75
0.50
0.25
0.00
*
B
Actin
phospho-p38
Phospho-p38 MAPK normalized to actin (arbitrary units)
1.25
1.00
0.75
0.50
0.25
0.00
C
Phospho-p38 / Total p38 MAPK (arbitrary units)
1.75
1.50
1.25
1.00
0.75
0.50
0.25
0.00
1 hr ins pretreat -- + +
6 hr OGD + + +
ins during 6 hrs -- -- +
1 hr Reoxy + + +

Figure 3.25.

Figure 3.26: The effect of insulin upon p38 MAPK in differentiated H9c2 cells subjected to oxygen-glucose deprivation followed by 2 hrs of reoxygenation. Cells were either pretreated with normal media or with insulin in the media for 1 hr followed by media replacement and an additional 6 hrs of oxygen-glucose deprivation also without insulin. Cells were also pretreated with insulin for 1 hr followed by media replacement and 6 additional hrs of OGD with insulin. After OGD, cells were reoxygenated with normal media for 2 hrs. Insulin pretreatment or insulin pretreatment and OGD with insulin did not change total levels of p38 MAPK (**A**), total levels of phospho-p38 MAPK (**B**), or relative levels of phospho-p38 MAPK (**C**). Data points represent mean ± SEM (n = 4). Please note: the arbitrary units in this figure cannot be compared to the arbitrary units used in other figures.

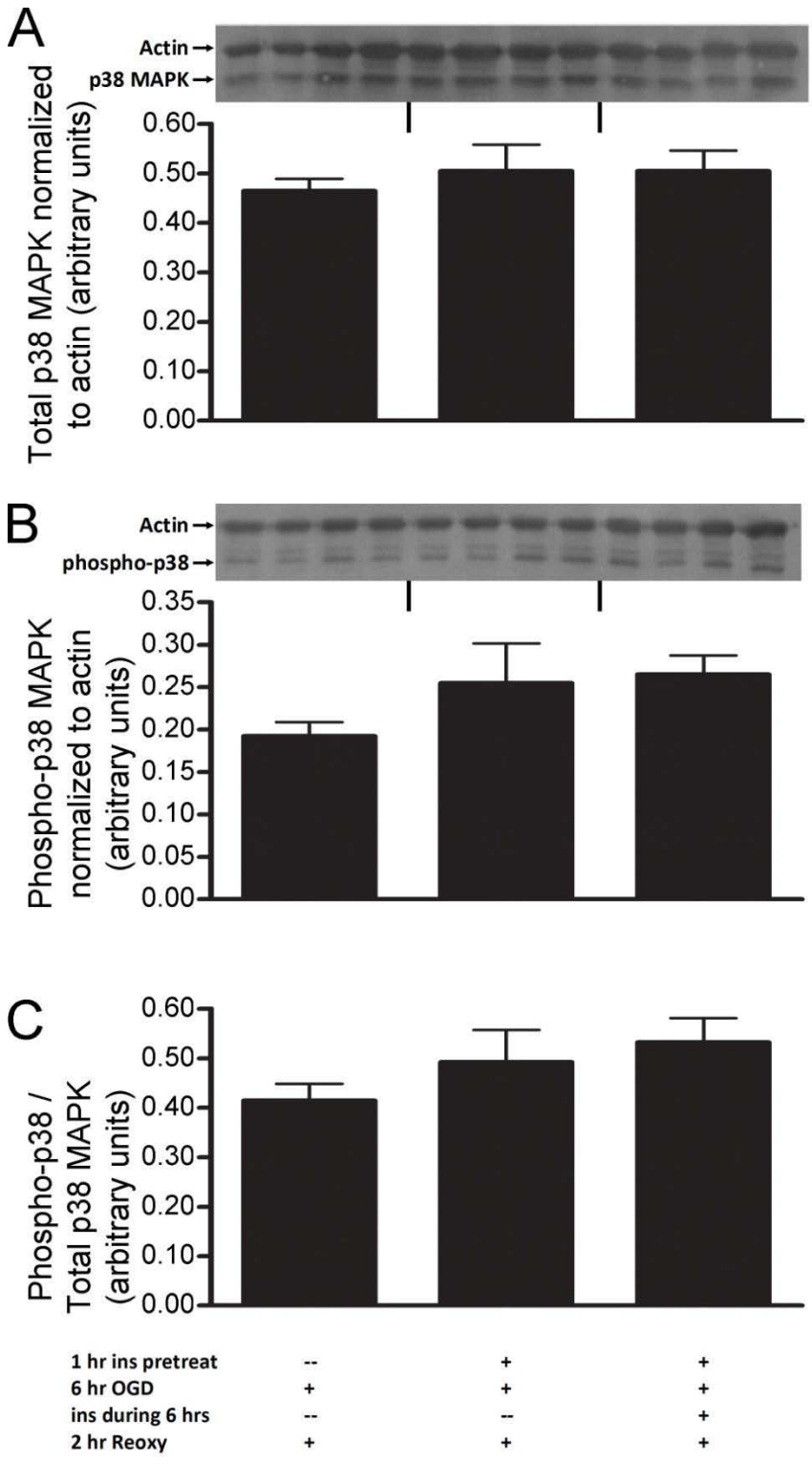
A
Actin
p38 MAPK
Total p38 MAPK normalized to actin (arbitrary units)
0.60
0.50
0.40
0.30
0.20
0.10
0.00
B
Actin
phospho-p38
Phospho-p38 MAPK normalized to actin (arbitrary units)
0.35
0.30
0.25
0.20
0.15
0.10
0.05
0.00
C
Phospho-p38 / Total p38 MAPK (arbitrary units)
0.60
0.50
0.40
0.30
0.20
0.10
0.00
1 hr ins pretreat -- + +
6 hr OGD + + +
ins during 6 hrs -- -- +
2 hr Reoxy + + +

Figure 3.26.

Figure 3.27. The effect of insulin and oxygen-glucose deprivation on differentiated H9c2 cells. Cells were subjected to control- or insulin-pretreatments for one hour. Cells were then treated with one of three conditions for 6 hrs: normal incubation, normal incubation with insulin supplementation, and oxygen-glucose deprivation. Insulin-pretreated cells experienced either 0 or 1 hr of reoxygenation after OGD. After Western analysis, data between membranes were combined after 2-way ANOVA between 8 samples indicated no difference between membranes.

(**A**) Cells pretreated with insulin and then insulin supplementation for 6 hours had less total p38 MAPK than cells with normal incubation for six hours (with or without insulin pretreatment) or with normal pretreatment and 6 hrs of OGD. Additionally, cells given insulin pretreatment and 1 hr of reoxygenation had less total p38 MAPK than cells given normal pretreatment and 6 hrs of normal incubation. (*, $p < 0.05$, $n = 4 - 8$).

(**B**) Cells given insulin pretreatment and insulin supplementation for 6 hrs had significantly higher relative phospho-p38 MAPK than cells given no insulin pretreatment followed by either 6 hrs of normal incubation or 6 hrs of OGD. (*, $p < 0.05$; $n = 4 – 8$).

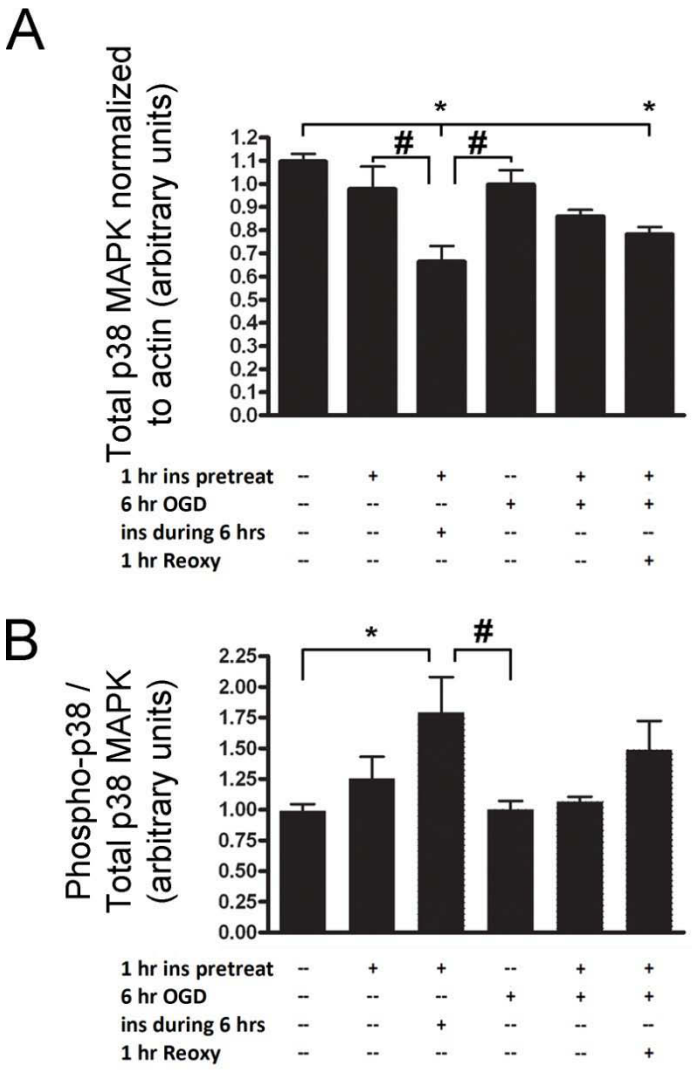
A
Total p38 MAPK normalized to actin (arbitrary units)
1.2
1.1
1.0
0.9
0.8
0.7
0.6
0.5
0.4
0.3
0.2
0.1
0.0
*
*
#
#
1 hr ins pretreat -- + + -- + +
6 hr OGD -- -- -- + + +
ins during 6 hrs -- -- + -- -- --
1 hr Reoxy -- -- -- -- -- +
B
Phospho-p38 / Total p38 MAPK (arbitrary units)
2.25
2.00
1.75
1.50
1.25
1.00
0.75
0.50
0.25
0.00
*
#
1 hr ins pretreat -- + + -- + +
6 hr OGD -- -- -- + + +
ins during 6 hrs -- -- + -- -- --
1 hr Reoxy -- -- -- -- -- +

Figure 3.27.

Figure 3.28: Effects of insulin on phosphorylated p38 MAPK and on actin dynamics in differentiated H9c2 cells. **A**. Immunocytochemistry of phosphorylated p38 MAPK. **B**. Phalloidin staining of actin. **C**. Hoescht staining of nuclei with merge of A and B. Cells in panels Aa, Ba, and Ca were pretreated without insulin in the media for 1 hr followed by media replacement and 6 additional hrs of incubation also without insulin. Cells in panels Ab, Bb, and Cb were pretreated with insulin in the media for 1 hr followed by media replacement and 6 additional hrs of incubation also without insulin. Cells in panels Ac, Bc, and Cc were pretreated with insulin in the media for 1 hr followed by media replacement and 6 additional hrs of incubation with insulin. Cells incubated without insulin had phospho-p38 MAPK-immunoreactivity in the nuclei and in granules in the cytoplasm (**Aa**). Insulin had no apparent effect on the distribution of phospho-p38 MAPK-immunoreactivity (**Ab** and **Ac**) within the nuclei and in granules in the cytoplasm, however the phospho-p38 MAPK positive granules appeared more concentrated near the nuclei. Cells incubated without insulin had regular and organized peripheral actin and apparently less organized perinuclear actin (**Ba**). Similarly, insulin had no apparent effect on the regular and organized distribution of peripheral actin or on the disorganized distribution of perinuclear actin (**Bb** and **Bc**). Scale bar = 25 μm.

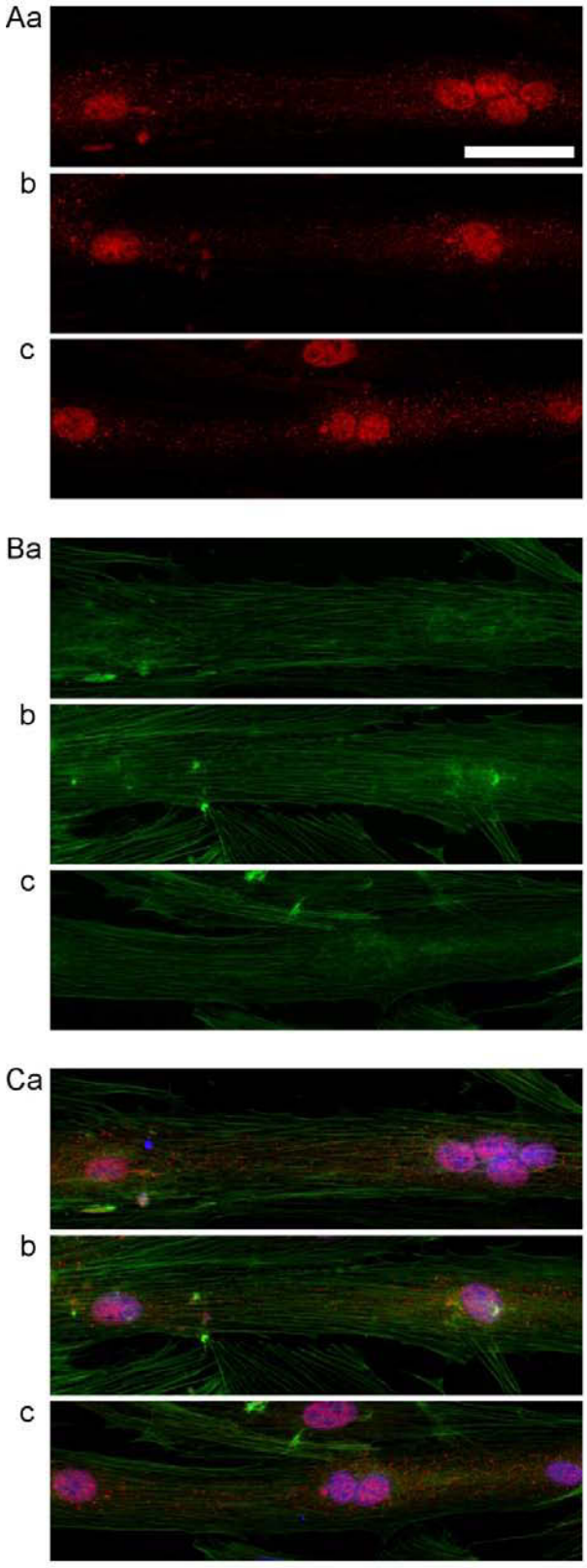

Figure 3.28.

Figure 3.29: Effects of insulin on phosphorylated p38 MAPK and on actin dynamics in differentiated H9c2 cells during oxygen glucose deprivation. **A**. Immunocytochemistry of phosphorylated p38 MAPK. **B**. Phalloidin staining of actin. **C**. Hoescht staining of nuclei with merge of A and B. Cells in panels Aa, Ba, and Ca were pretreated without insulin in the media for 1 hr followed by media replacement and 6 additional hrs of incubation without insulin and with oxygen-glucose deprivation. Cells in panels Ab, Bb, and Cb were pretreated with insulin in the media for 1 hr followed by media replacement and 6 additional hrs of incubation without insulin and with oxygen-glucose deprivation. Cells in panels Ac, Bc, and Cc were pretreated with insulin in the media for 1 hr followed by media replacement and 6 additional hrs of incubation with insulin and with oxygen-glucose deprivation. Cells incubated without insulin had phospho-p38 MAPK-immunoreactivity in the nuclei and in granules in the cytoplasm (**Aa**). Insulin pretreatment apparently caused phospho-p38 MAPK-immunoreactivity (**Ab**) within the cytoplasm to reduce, however phospho-p38 MAPK-immunoreactivity was still in cytoplasmic granules. After insulin pretreatment and oxygen glucose deprivation with insulin there was phospho-p38 MAPK-immunoreactivity (**Ac**) distributed throughout the cytoplasm and the nuclei. Cells incubated without insulin had disorganized actin throughout the cytoplasm and in the perinuclear region(**Ba**). Cells with insulin pretreatment had disorganized actin throughout the cytoplasm and in the perinuclear region (**Bb**). Cells with insulin pretreatment and insulin during oxygen glucose deprivation also had disorganized actin throughout the cytoplasm and in the perinuclear region (**Bc**). Scale bar = 25 μm.

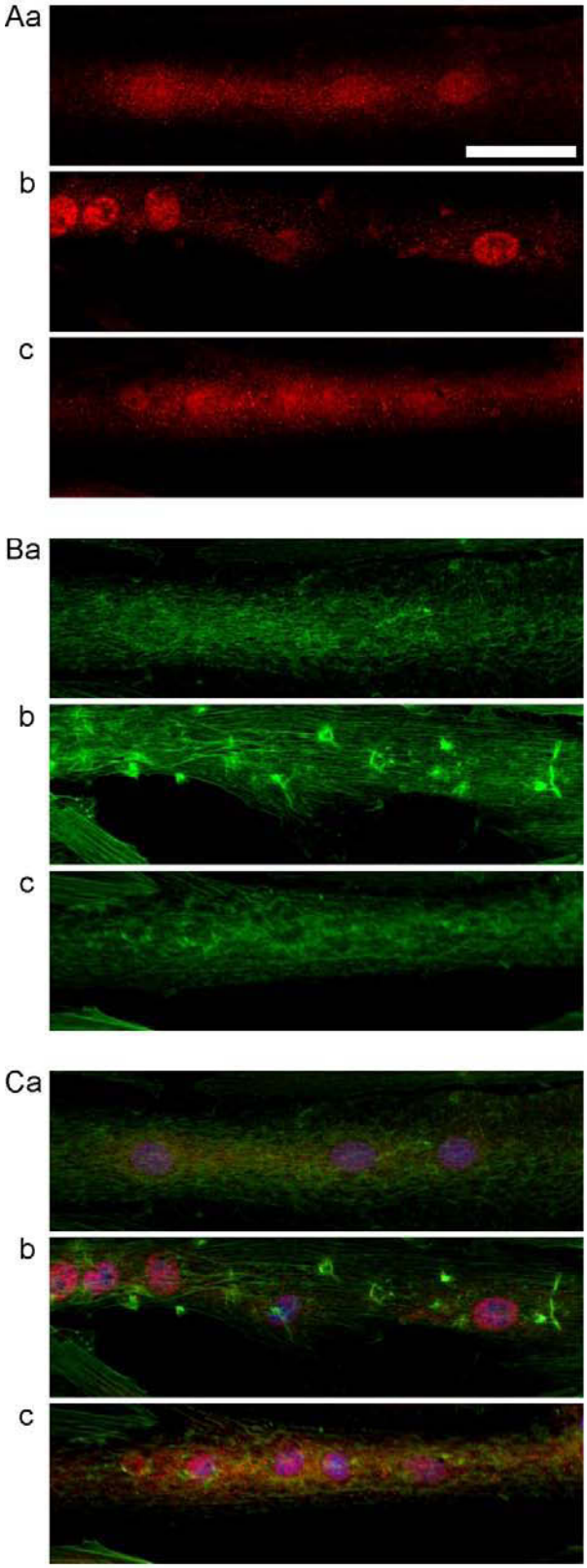

Figure 3.29.

Figure 3.30: Effects of insulin on phosphorylated p38 MAPK and on actin dynamics in differentiated H9c2 cells following oxygen glucose deprivation and 1 hr of reoxygenation. **A**. Immunocytochemistry of phosphorylated p38 MAPK. **B**. Phalloidin staining of actin. **C**. Hoescht staining of nuclei with merge of A and B. Cells in panels Aa, Ba, and Ca were pretreated without insulin in the media for 1 hr followed by media replacement and 6 additional hrs of incubation without insulin and with oxygen-glucose deprivation followed by media replacement and 1 additional hr of incubation with oxygenation and without insulin. Cells in panels Ab, Bb, and Cb were pretreated with insulin in the media for 1 hr followed by media replacement and 6 additional hrs of incubation without insulin and with oxygen-glucose deprivation followed by media replacement and 1 additional hr of incubation with oxygenation and without insulin. Cells in panels Ac, Bc, and Cc were pretreated with insulin in the media for 1 hr followed by media replacement and 6 additional hrs of incubation with insulin and with oxygen-glucose deprivation followed by media replacement and 1 additional hr of incubation with oxygenation and without insulin. Cells incubated without insulin had phospho-p38 MAPK-immunoreactivity (**Aa**) in the nuclei and in granules in the cytoplasm. Insulin pretreatment (**Ab**) and insulin pretreatment and oxygen glucose deprivation with insulin (**Ac**) had no apparent effect on phospho-p38 MAPK-immunoreactivity after one hr of reoxygenation. Cells incubated without insulin also had disorganized actin throughout the cytoplasm and in the perinuclear region (**Ba**). Insulin pretreatment did not affect the perinuclear disorganization of actin (**Bb**), but increased the presence of cytoplasmic actin condensates visible after one hour of reoxygention. Insulin pretreatment and insulin

during oxygen glucose deprivation resulted in disorganized actin (**Bc**) throughout the cytoplasm and in the perinuclear region after 1 hr reoxygenation. Scale bar = 25 μm.

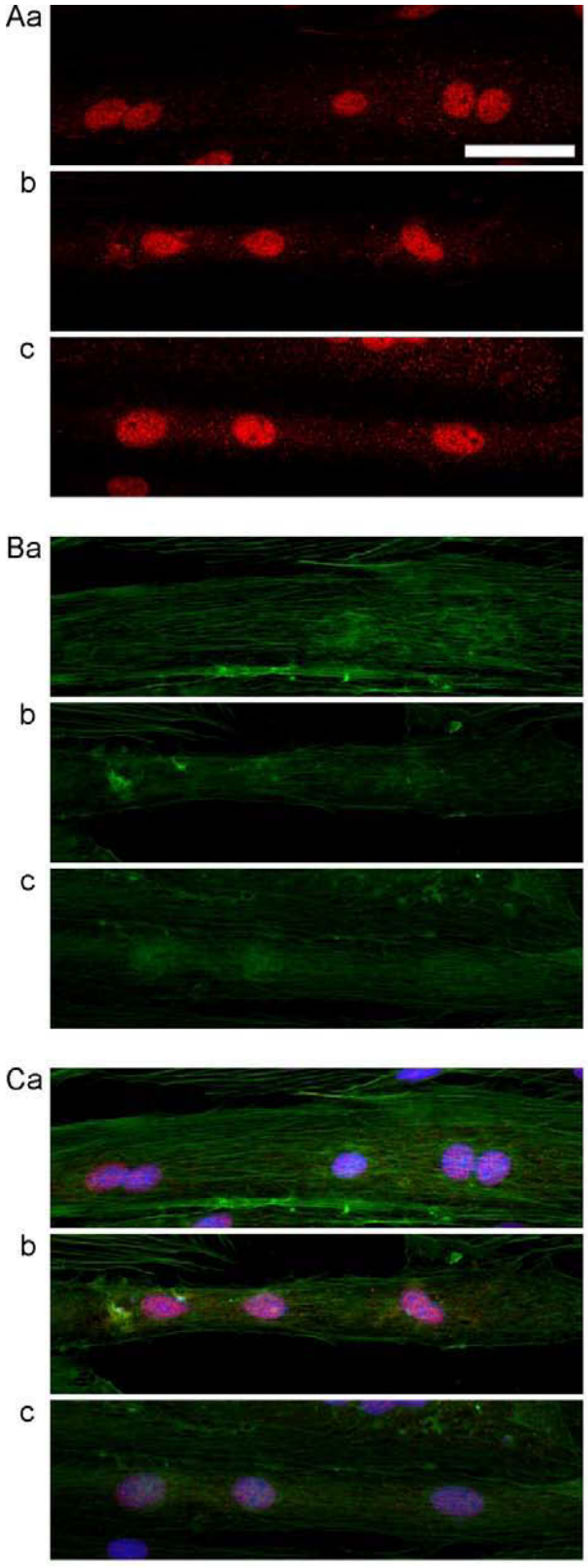

Figure 3.30.

Figure 3.31: Effects of insulin on phosphorylated p38 MAPK and on actin dynamics in differentiated H9c2 cells following oxygen glucose deprivation and 2 hrs of reoxygenation. **A**. Immunocytochemistry of phosphorylated p38 MAPK. **B**. Phalloidin staining of actin. **C**. Hoescht staining of nuclei with merge of A and B. Cells in panels Aa, Ba, and Ca were pretreated without insulin in the media for 1 hr followed by media replacement and 6 additional hrs of incubation without insulin and with oxygen-glucose deprivation followed by media replacement and 2 additional hrs of incubation with oxygenation and without insulin. Cells in panels Ab, Bb, and Cb were pretreated with insulin in the media for 1 hr followed by media replacement and 6 additional hrs of incubation without insulin and with oxygen-glucose deprivation followed by media replacement and 2 additional hrs of incubation with oxygenation and without insulin. Cells in panels Ac, Bc, and Cc were pretreated with insulin in the media for 1 hr followed by media replacement and 6 additional hrs of incubation with insulin and with oxygen-glucose deprivation followed by media replacement and 2 additional hrs of incubation with oxygenation and without insulin. Cells incubated without insulin had phospho-p38 MAPK-immunoreactivity (**Aa**) in the nuclei and in granules in the cytoplasm. Insulin had no apparent effect on the distribution of phospho-p38 MAPK-immunoreactivity (**Ab** and **Ac**) within the nuclei and in granules in the cytoplasm after 2 hrs of reoxygenation. Cells incubated without insulin had regular and organized distribution of peripheral actin and disorganized perinuclear actin (**Ba**). Insulin had no apparent effect on the regular and organized distribution of peripheral actin or on the disorganized distribution of perinuclear actin (**Bb** and **Bc**). Scale bar = 25 μm.

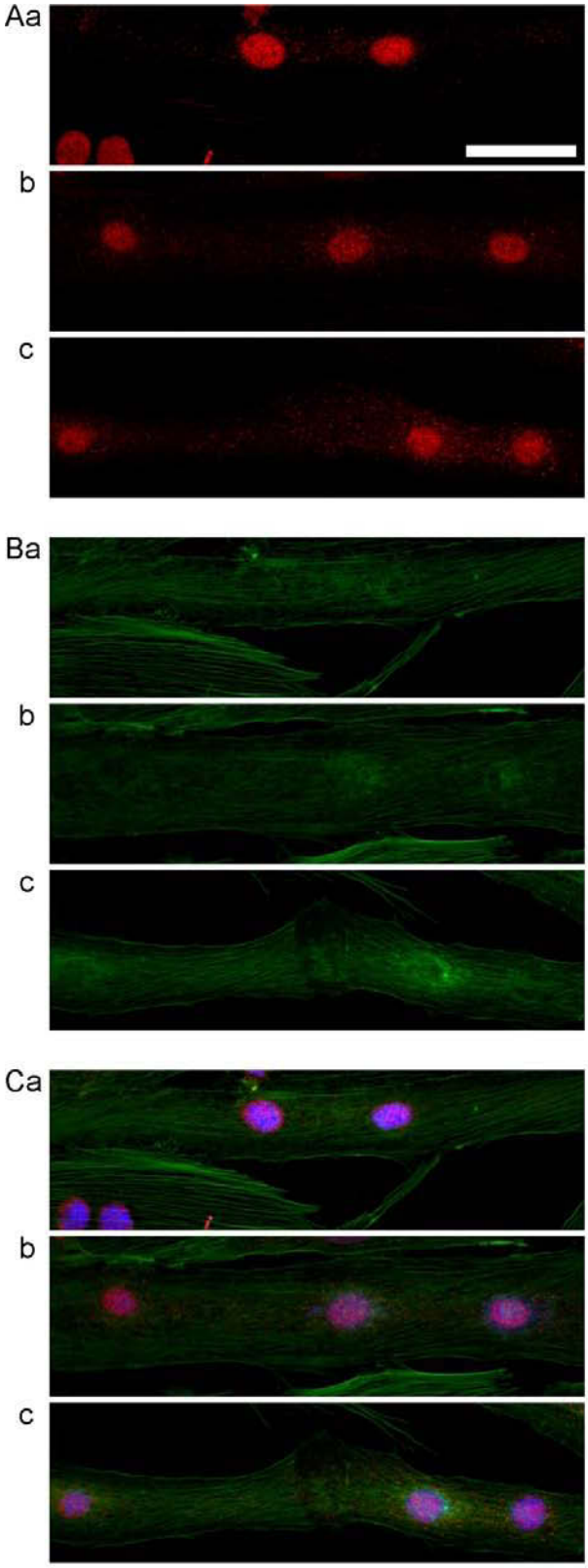

Figure 3.31.

CHAPTER 4: DISCUSSION

In this thesis, insulin was examined for its effect on Hsp27 phosphorylation and p38 MAPK signaling. Firstly, time and dose effects of insulin were examined, followed by insulin effects during OGD. The levels of Hsp27 and p38 MAPK were examined by Western analysis after one hour of pretreatment with (and without) insulin and/or after an additional six hours of incubation with (and without) insulin. Some cells were subjected to OGD during the six hour period. Finally, some cells were reoxygenated for one or two hours following OGD. In addition, the effects of insulin on phospho-p38 MAPK and on phospho-Hsp27 serine 82 levels were examined by normalizing to total p38 MAPK or total Hsp27, respectively. The effects of insulin upon H9c2 cells during OGD and reoxygenation were also examined using immunocytochemistry for Hsp27 and phospho-p38 MAPK.

The major findings in this thesis are: 1. Insulin pretreatment delayed the phosphorylation of Hsp27 serine 82 caused by changing the media (Figure 3.2). After one hour of insulin pretreatment followed by six hours of incubation with (and without) insulin, total Hsp27 levels were increased significantly (Figure 3.9). 2. Insulin pretreatment reduced levels of total p38 MAPK (Figure 3.3). After one hour of insulin pretreatment followed by six hours of incubation with insulin, total p38 MAPK levels decreased significantly and thus relative phospho-p38 MAPK levels were significantly greater (Figure 3.22; Figure 3.27). Insulin pretreatment redistributed of Hsp27 from perinuclear regions into the nuclei (Figure 3.18). Insulin did not affect phospho-p38 MAPK localization (Figure 3.28). 3. Insulin pretreatment and supplementation during OGD had minimal effect on both Hsp27 and phosphorylated Hsp27 serine 82 levels (Figure 3.17). However, insulin increased phosphorylated Hsp27 serine 82 levels during

reoxygenation (Figure 3.15 B). The effect of insulin upon the localization of Hsp27 was minimal compared to the effects of OGD or reoxygenation (Figure 3.19, Figure 3.20). 4. In the case of p38 MAPK, the effect of insulin during OGD was potentially overwhelmed by the effect of OGD, but during reoxygenation insulin was associated with a significant increase in total p38 MAPK. According to Western analysis, insulin had no effect upon levels of phospho-p38 MAPK during OGD or reoxygenation. That said, OGD increased phospho-p38 MAPK localization in the cytoplasm and insulin pretreatment suppressed this effect. In addition, insulin treatment *during* OGD appeared to cause cytoplasmic phospho-p38 MAPK localization (Figure 3.29).

Insulin is clearly associated with improved myocardial function after ischemic injury (Jonassen *et al.*, 2001), however translating this fact into medicine has been difficult (Kansagara *et al.*, 2011). This protective effect appears to be p38 MAPK dependent; inhibition of p38 MAPK reduces the protective effect of insulin (Li *et al.*, 2008). However, p38 MAPK inhibition is also protective during ischemia (Barancik *et al.*, 2000), potentially due to p38 MAPK increasing ROS production during reperfusion (Kayyali *et al.*, 2001) or through p38 MAPK activating transcription factors in the nucleus (Piao *et al.*, 2003). Understanding the localization p38 MAPK and its phosphorylation state may clarify its role in the phosphorylation of Hsp27 and its protective effect.

As this work was started, insulin dose and media exchange were examined for influence upon phosphorylation of Hsp27 serine 82 and p38 MAPK. The dose of insulin (200 μU/ml = 1.2 nM = 7.7 ng/ml) was used to activate the Insulin Receptor. Insulin at 1.0 and 10 nM increased 2-deoxyglucose uptake using *differentiated* H9c2 cells, but 0.1

nM did not (Yu *et al.*, 1999). As well, Humulin-R brand insulin caused a significant increase in the amount of fatty acid translocase FAT/CD36 (via the metabolic pathway) in cultured adult rat cardiomyocytes when used at concentrations of 5 nM (and higher) compared to 0.1 nM of insulin (and lower) (Chabowski *et al.*, 2004). A similar dose of insulin might be expected to affect the metabolic pathway (and thus the Insulin Receptor) in differentiated H9c2 cells. Similarly, insulin increased proliferation of H9c2 cells when used at doses of 10 ng/ml (or greater) compared to doses of 1.0 ng/ml (or less) (Duttaroy *et al.*, 2005). Therefore, the use of a similar dose of insulin might be expected to affect proliferative H9c2 cells. Insulin was first tested for its ability to alter the increase in Hsp27 serine 82 phosphorylation that was caused by media exchange.

Media exchange increased levels of Hsp27 serine 82 phosphorylation after one hour compared to regular incubation (Figures 3.1 and 3.6). There are many potential causes of this increase in phosphorylation. Hyperosmotic stress increases levels of phosphorylated Hsp27 serine 82 in hippocampus (Niswander and Dokas, 2006), and hypo-osmotic treatment increases levels of phosphorylated Hsp27 serine 82 in intestinal cells (Tilly *et al.*, 1996). Hypertonicity but not hypotonicity activated p38 MAPK in amphibian heart (Aggeli et al, 2002). The increased levels of phosphorylated Hsp27 serine 82 caused by media exchange could have been related to a change in osmolarity between old and refreshed media. Similarly, exchanging culture media increases extra-cellular pH (due to fresh media having a higher pH than used media) and extracellular alkalosis increases levels of phosphorylated Hsp27 serine 82 in frogs (Stathopoulou *et al.*, 2006). Finally, fetal bovine serum contains unknown factors as potential stimulants of

Hsp27 serine 82 phosphorylation. The increase in levels of phosphorylated Hsp27 serine 82 due to media exchange was interpreted to be a stress-response by the cells.

Insulin supplementation of 200 μU/ml suppressed the increase in levels of phosphorylated Hsp27 serine 82 in a time-dependent fashion in differentiated cells. Various incubation times did not change levels of Hsp27 serine 82 phosphorylation after media exchange (Figure 3.2), suggesting that the effect of media exchange was quick (< 15 minutes) and persistent. On the other hand, media exchange supplemented with insulin caused levels of phosphorylated Hsp27 serine 82 to be lower than regular media exchange at 15 minutes, but this effect was lost at further time points. This suggests that insulin either temporarily suppressed the effect of media exchange (with the suppression decaying) or prevented the effect of media exchange while activating the mitogenic insulin pathway to cause Hsp27 serine 82 phosphorylation through that route. At certain timepoints, i.e., at 60 min in differentiated cells, the apparent effect from either mechanism would be indistinguishable.

Various doses of insulin supplementation (20, 200, 2000 μU/ml) were tested for the effect upon the phosphorylation of Hsp27 serine 82 and p38 MAPK in differentiated and proliferative cells. It was unclear whether proliferative cells would be an acceptable substitute for differentiated cells or if there was a superior dose. After one hour, there was no dose-specific effect on Hsp27 evident in the differentiated cells (Figure 3.4). However, after one hour, proliferative cells supplemented with 200 μU/ml of insulin had lower levels of phosphorylated Hsp27 serine 82 (Figure 3.7). Neither 20 nor 2000 μU/ml of supplementation resulted in this effect. If insulin caused suppression of an increase in phosphorylation induced by media exchange, then 200, but not 20 μU/ml, was sufficient

to cause this suppression. On the other hand, if insulin causes an increase in phosphorylation levels of Hsp27 serine 82 (as seen in significantly higher doses), then this effect might be present at 2000 but not 200 μU/ml of supplementation. In other words, insulin may have suppressed the effect of media exchange, and insulin also caused increased levels of phosphorylated Hsp27 serine 82 via the mitogenic pathway. The suppression effect failed at 20 μU/ml of supplementation and the mitogenic pathway was dominant at 2000 μU/ml of supplementation. The intermediate dose of 200 μU/ml might have allowed suppression but not activation of the mitogenic pathway (sufficient to cause increased phosphorylation of Hsp27 serine 82). This proposal has been only partially addressed in these experiments. Regardless, the response of Hsp27 to 200 μU/ml of insulin were different after one hr in proliferative and differentiated cells.

Insulin also was associated with a decrease in total p38 MAPK levels in differentiated cells. While media exchange caused similar total p38 MAPK levels compared to control cells after one hour, at each tested time point (15, 30, 45, 60 min) insulin resulted in lower total p38 MAPK levels than in unsupplemented cells (Figure 3.3). One hour treatments of 20, 200, 2000 μU/ml all had lower (but nonstatistical, n = 4) total p38 MAPK levels than unsupplemented cells, but the doses did not cause a difference in phospho-p38 MAPK levels or total p38 MAPK levels between doses (Figure 3.5). To the best of my knowledge, this is the first report of insulin causing lower total p38 MAPK levels. In comparison to differentiated cells, the various tested doses of insulin caused no reduction of p38 MAPK levels in proliferative cells (Figure 3.8). It was unclear if insulin would reduce total p38 MAPK in proliferative cells as insulin did in differentiated cells.

Proliferative and differentiated H9c2 cells should be used with caution and comparisons should be avoided because different responses to insulin doses occur. The Insulin Receptor Substrate 1/2 is different in amount and phosphorylation states between the proliferative and differentiated H9c2 cells (Lim *et al.*, 2007). Regardless, of 10 recent papers examining insulin and H9c2 cells, only two used differentiation protocols (Ku *et al.*, 2011; Govoni *et al.*, 2009). Experiments using insulin are also confounded due to the difference between proliferation media (10% FBS) and differentiation media (1% FBS), because proliferation media will have 10 X the basal levels of endogenous insulin, and so the relative influence of experimental doses will be less. Finally, the behavior of cardiomyocytes at different stages of development can be highlighted by the fact that insulin (withdrawal) specifically controls the process of differentiation of precursor cells into cardiomyocytes (Xu *et al.*, 2008).

Insulin (200 μU/ml) mitigated the increase of Hsp27 serine 82 phosphorylation associated with (stressful) media exchange. As well, insulin did not significantly activate p38 MAPK phosphorylation after one hour of treatment. The effect of insulin as a one hour *pretreatment* was then examined. Six hours after one hour of insulin pretreatment, cells had significantly higher levels of total Hsp27 than cells without insulin treatment (Figure 3.9), and insulin supplementation during the six hours did not change the effect of insulin pretreatment. This result is consistent with a physiologic dose of insulin increasing total levels of Hsp70, and a physiologic dose of insulin potentiating Hsp70 expression caused by heat shock (Li *et al.*, 2004). Similarly, as media exchange appeared to be stressful to H9c2 cells, then insulin may potentiate the expression of Hsp27. Following six hours of incubation, relative levels of phosphorylated Hsp27 serine 82

(compared to total Hsp27) were lower in insulin-treated cells than in cells treated without insulin. The increase in total Hsp27 was likely newly synthesized protein that was in an immature state and unphosphorylatable. Because insulin might have stimulated synthesis of Hsp27 during six hrs of normal incubation, and because this increase was not observed during OGD (understandable, because protein synthesis might change in OGD conditions), comparing insulin-treated cells in normal incubation to insulin-treated cells in OGD should be done with caution.

Similar to observations of one hour or less, insulin supplementation for one hour and then six hours decreased total p38 MAPK levels compared to treatment without insulin (Figures 3.22, 3.27). One hour of insulin pretreatment resulted in p38 MAPK levels being intermediate between no insulin and one hour then six hours of insulin. These results are consistent with the notion that insulin (200 μU/ml) supplementation caused a decrease in total p38 MAPK levels. Interestingly, insulin supplementation appeared to increase relative phospho-p38 MAPK levels. However, after standardizing to actin, the increase can be explained by a reduction in total p38 MAPK with relatively little change in phospho-p38 MAPK levels. There are additional reasons to believe that a signaling pathway is responsible for reduction of p38 MAPK levels. For example, the anti-apoptotic effect of heme oxygenase 1 over-expression in endothelial cells correlates with a reduction of p38 MAPK levels that is proportional to the amount of heme oxygenase 1 added. Additionally, inhibition of p38 MAPK reduced the anti-apoptotic effect associated with heme oxygenase 1 over-expression or with the heme oxygenase 1 mimetic, carbon monoxide (Silva *et al.*, 2006).

Insulin pretreatment before OGD caused similar relative levels of phosphorylated Hsp27 serine 82 compared to normal pretreatment. Phosphorylated levels of Hsp27 serine 82 were similar during OGD as compared to normal incubation (Figure 3.13), and phosphorylated levels of Hsp27 serine 82 during OGD was similar with or without insulin pretreatment ($p < 0.07$; Figure 3.17). However, Hsp27 localization was affected by both insulin pretreatment and OGD. OGD caused Hsp27 to become localized to actin condensates. While OGD resulted in the relocalization of Hsp27 to the nucleus in normally pretreated cells, insulin-pretreatment maintained Hsp27 in the perinuclear region. Insulin was expected to inhibit the influence of p38 MAPK upon Hsp27 serine 82 phosphorylation levels, but there is good reason to assume that this was not related to mobilization of Hsp27 to actin condensates. This is because the activation of p38 MAPK during anoxia does not affect the translocation of Hsp27 to the cytoskeleton during anoxia (Armstrong *et al.*, 1999), therefore inhibition of p38 MAPK (with insulin) would not affect OGD-induced translocation. Additionally, cytoplasmic levels of cytochrome c increase during anoxia in neonatal cardiomyocytes in a p38-MAPK independent manner (Okada *et al.*, 2005). The lack of change observed in levels of phosphorylated Hsp27 serine 82, coupled with the change in localization, is suggestive of a protective function that Hsp27 was performing during OGD. It could be that Hsp27 was altering its function without significantly altering its overall phosphorylation state. The response of Hsp27 to various apoptotic inducers has been described (Paul *et al.*, 2010). Of these, etoposide causes little change in Hsp27 serine 82 phosphorylation state. However, despite the steadiness of Hsp27 serine 82 phosphorylation levels (compared to other apoptotic inducers or heat shock), the Hsp27 oligomers change size with a trend towards increasing

in size. Hsp27 oligomers increasing in size is associated with chaperone activity (and potentially with the inhibition of apoptotic signaling from the mitochondria). Hsp27 translocation from the perinuclear region to actin condensates, coupled with no change in levels of phosphorylated Hsp27 serine 82, suggests that OGD caused Hsp27 to form mid-sized oligomers in order to inhibit apoptotic signaling due to cytochrome c release (Bruey *et al.*, 2000).

Insulin changed the effect of OGD upon nuclear Hsp27 (Figure 3.19). After OGD Hsp27 was in the nucleus and insulin mitigated this effect. In rat hearts subjected to ischemia, Hsp27 accumulated in the nuclei of the cardiomyocytes (Yoshida *et al.*, 1999). Phospho-mimic Hsp27 will accumulate in the nucleus during heat stress, but non-phosphorylatable Hsp27 will not accumulate in the nucleus during heat stress (Bryantsev *et al.*, 2007). It is possible that insulin was causing Hsp27 phosphorylation to be altered during OGD, such that Hsp27 was less likely to enter the nucleus.

Insulin pretreatment and supplementation during OGD affected total phosphorylated Hsp27 serine 82 during reoxygenation (Figure 3.15). The increase in phosphorylated Hsp27 serine 82 is consistent with the apparent increase in total levels of phosphorylated Hsp27 serine 82 being greater in the hearts of insulin-treated rats after ischemia-reperfusion than in rats not given insulin before ischemia (Li *et al.*, 2008). Interestingly, one hour of reoxygenation altered the appearance of H9c2 cells compared to OGD (Figure 3.20) such that actin localization was more similar to cells in normal incubation (Figure 3.18) than to cells in OGD conditions (Figure 3.19). Increased levels of phosphorylated Hsp27 serine 82 are associated with actin stabilization (An *et al.*, 2004). However the appearance of actin is similar with and without insulin treatments

after reoxygenation, and so any benefit to actin *reorganization* from insulin before reoxygenation is not apparent, despite potentially greater levels of phosphorylated Hsp27 serine 82.

The effect of insulin upon p38 MAPK during OGD is a challenge to deduce. Insulin pretreatment resulted in a reduction of total p38 MAPK (Figure 3.3). Extended (six hour) insulin treatment resulted in a reduction of total p38 MAPK (Figure 3.27). OGD was associated with a reduction of p38 MAPK with normal pretreatment (Figure 3.23) or with insulin pretreatment (Figure 3.25). However, it is unknown if the effects compound.

Relative levels of phospho-p38 MAPK were not altered by OGD. This is not a surprise. OGD can cause an increase in relative phospho-p38 MAPK, however this increase is transient and thus unlikely to be captured at the end of six hours of OGD. Hypoxia-induced increases in phospho-p38 MAPK can be biphasic, with extended (greater than 3 hours) hypoxia causing a second increase of phospho-p38 MAPK levels (Mackay and Mochly-Rosen, 1999). The experiments presented here did not replicate the biphasic effect, however. This difference between neonatal cardiomyocytes and differentiated H9c2 cells warrants additional investigation, due to the importance of p38 MAPK in ischemia-associated injury.

Insulin 1 hr pretreatment followed by 6 hrs normal incubation or insulin pretreatment and insulin during 6 hrs of normal incubation did not affect phospho-p38 localization (Figure 3.28). However, the effect of insulin on phospho-p38 MAPK localization during OGD was dependent upon whether insulin pretreatment (before OGD) was followed by insulin being withdrawn during OGD or included during OGD. While

OGD increased phospho-p38 MAPK in the cytoplasm, insulin-pretreatment mitigated this effect (Figure 3.29). The increase in cytoplasmic phospho-p38 MAPK was not associated with increased levels of phosphorylated Hsp27 serine 82 during OGD. This is suggestive regarding the cause of p38 MAPK phosphorylation. The kinases for p38 MAPK can be found in both the nucleus and in the cytoplasm (Ben-Levy *et al.*, 1998). However, phospho-p38 MAPK requires the nuclear export signal on MK2 in order to exit the nucleus. Because there is no evidence that MK2 acted upon Hsp27 serine 82 in the cytoplasm, but that there is evidence that phospho-p38 MAPK was in the cytoplasm, it can be suggested that cytoplasmic p38 MAPK was being phosphorylated during OGD.

Insulin pretreatment before OGD appeared to prevent cytoplasmic activation of p38 MAPK. This is a potential mechanism by which insulin provides protection during ischemia/reperfusion injury. Cytoplasmic phospho-p38 MAPK can phosphorylate VDAC1 in mitochondria, which can increase ROS production (Schwertz et al, 2007). Additionally, if the cytoplasmic phospho-p38 MAPK is not dimerized with MK2, then the protective effect of MK2 phosphorylating αB-crystallin to inhibit mitochondrial membrane disruption is not occurring (Whittaker *et al.*, 2009).

After insulin combined with OGD, phospho-p38 MAPK was localized to the cytoplasm and the nucleus. For this reason, it is difficult to determine if insulin pretreatment prevented OGD-induced phospho-p38 MAPK, or if insulin withdrawal after pretreatment caused cytoplasmic phospho-p38 MAPK levels to decrease during OGD. Insulin-supplementation alone was insufficient to increase levels of cytoplasmic phospho-p38 MAPK, however (Figure 3.28). The cytoplasmic phospho-p38 MAPK during insulin-supplemented OGD could have been translocated from the nucleus.

Levels of phosphorylated Hsp27 serine 82 were higher during reoxygenation if insulin was present during OGD, and this suggests that activated MK2 was available in the cytoplasm. The presence of activated MK2 in the cytoplasm was not at first consistent with the lack of change in phosphorylated Hsp27 serine 82 during OGD (Figure 3.14). Hsp27, p38 MAPK, and MK2 form a complex with AKT (Wu *et al.*, 2007), and AKT scaffolds directly with MK2. This complex could inhibit activation of MK2 on Hsp27 serine 82 (or prevent the phosphorylated form of Hsp27 to separate from the complex). Hsp27 is an essential component of the complex, and thus the complex could be 'released' if Hsp27 acts as a lynchpin. By analogy, Hsp90 acts as a lynchpin in signaling cascades by releasing signaling proteins from chaperone-like sequestering when Hsp90 is attracted to denatured proteins (Lindquist, 2010). The importance of AKT in the Hsp27, MK2, p38 MAPK complex is not well understood, but insulin causes phosphorylation of AKT via the metabolic pathway. The interaction of insulin-activated AKT might suppress activated p38 MAPK and MK2 from leaving the complex until Hsp27 is drawn away due to cellular distress.

As mentioned, both insulin pretreatment and OGD each appear to cause a reduction in total p38 MAPK levels. Reoxygenation certainly does not appear to cause an increase of p38 MAPK compared to OGD (Figure 3.27). Interestingly then, reoxygenation of cells with insulin during OGD was associated with an increase in total p38 MAPK levels compared to cells with no insulin pretreatment followed by no insulin during OGD (Figure 3.26). Does insulin supplementation during OGD induce new synthesis of p38 MAPK during reoxygenation? Inducing cellular distress via high glucose results in an increase in p38 MAPK mRNA synthesis but not an increase in total

p38 MAPK content (Xu *et al.*, 2003). Phospho-mimic Hsp27 stabilizes mRNA (Lasa *et al.*, 2000). Insulin during OGD appeared to prime an increase in levels of phosphorylated Hsp27 serine 82 and also appeared to cause perinuclear localization of Hsp27 (Figure 3.20). Insulin supplementation during OGD might have potentiated an increase in p38 MAPK expression during reoxygenation.

Conclusions

Insulin appears to be protective during ischemia and p38 MAPK appears to be an essential component of the mechanism. However, p38 MAPK also aggravates ischemia/reperfusion injury. This thesis attempted to clarify this paradox by examining the relative amounts and localization of Hsp27 and p38 MAPK after insulin treatment in a cardiomyocyte model of ischemia/reperfusion injury. Insulin was hypothesized to prevent the increase of nuclear phospho-p38 MAPK, but this contention was not supported by the data, in that all cells had abundant phospho-p38 MAPK in the nucleus. The hypothesis that insulin would suppress stress-induced Hsp27 phosphorylation was consistent with the data during low-stress events (media exchange, OGD), but was not consistent with the stronger insult of reoxygenation. In fact, insulin appeared to potentiate Hsp27 phosphorylation during reoxygentation.

This thesis suggests two mechanisms by which insulin might protect cells from p38 MAPK-related injury. Firstly, insulin may cause p38 MAPK to be complexed with MK2, to suppress p38 MAPK ROS-causing cascades. Secondly, as shown by the data presented, insulin may reduce total p38 MAPK and thus restrict p38 MAPK from pro-injury cascades.

Now an alternative hypothesis can be proposed. Upon insulin stimulation, p38 MAPK may be phosphorylated by mechanisms that make p38 MAPK interact with specific downstream substrates that are different compared to when p38 MAPK is phosphorylated due to cellular stress. The MK2/p38 MAPK complex may be protective in the cytoplasm, and MK2 redirects activated p38 MAPK from causing adverse effects. This complex (possibly including p38MAPK, Hsp27, MK2, and AKT) relies upon p38

MAPK or MK2 as scaffolding. Co-localization experiments involving p38 MAPK with both AKT and MK2 should be performed, in order to further understand the paradox of p38 MAPK inhibition being protective during reoxygenation coupled with p38 MAPK inhibition diminishing other protective mechanisms. This idea is consistent with the data presented here and with the fact that insulin provides cellular protection in a p38 MAPK-dependent manner. This insulin-induced complex may prevent p38 MAPK from acting in alternative cascades that damage the cells.

Bibliography

Aberg E, Torgersen KM, Johansen B, Keyse SM, Perander M, Seternes OM (2009) Docking of PRAK/MK5 to the atypical MAPKs ERK3 and ERK4 defines a novel MAPK interaction motif. J Biol Chem. 284:19392-401.

Aggeli IK, Gaitanaki C, Lazou A, Beis I (2002) Hyperosmotic and thermal stresses activate p38-MAPK in the perfused amphibian heart. J Exp Biol. 205:443-54.

An SS, Fabry B, Mellema M, Bursac P, Gerthoffer WT, Kayyali US, Gaestel M, Shore SA, Fredberg JJ (2004) Role of heat shock protein 27 in cytoskeletal remodeling of the airway smooth muscle cell. J Appl Physiol. 96:1701-13.

Armstrong SC, Delacey M, Ganote CE (1999) Phosphorylation state of hsp27 and p38 MAPK during preconditioning and protein phosphatase inhibitor protection of rabbit cardiomyocytes. J Mol Cell Cardiol. 31:555-67.

Ballard-Croft C, Kristo G, Yoshimura Y, Reid E, Keith BJ, Mentzer RM Jr, Lasley RD (2005) Acute adenosine preconditioning is mediated by p38 MAPK activation in discrete subcellular compartments. Am J Physiol Heart Circ Physiol. 288:H1359-66.

Barancik M, Htun P, Strohm C, Kilian S, Schaper W (2000) Inhibition of the cardiac p38-MAPK pathway by SB203580 delays ischemic cell death. J Cardiovasc Pharmacol. 35:474-83.

Belfiore A, Frasca F, Pandini G, Sciacca L, Vigneri R (2009) Insulin receptor isoforms and insulin receptor/insulin-like growth factor receptor hybrids in physiology and disease. Endocr Rev. 30:586-623.

Bell GI, Pictet RL, Rutter WJ, Cordell B, Tischer E, Goodman HM (1980) Sequence of the human insulin gene. Nature 284:26-32.

Ben-Levy R, Hooper S, Wilson R, Paterson HF, Marshall CJ (1998) Nuclear export of the stress-activated protein kinase p38 mediated by its substrate MAPKAP kinase-2. Curr Biol. 8:1049-57.

Benninger RK, Zhang M, Head WS, Satin LS, Piston DW (2008) Gap junction coupling and calcium waves in the pancreatic islet. Biophys J. 95:5048-61.

Binoux M (1995) The IGF system in metabolism regulation. Diabete Metab. 21:330-7.

Bøtker HE, Kharbanda R, Schmidt MR, Bøttcher M, Kaltoft AK, Terkelsen CJ, Munk K, Andersen NH, Hansen TM, Trautner S, Lassen JF, Christiansen EH, Krusell LR, Kristensen SD, Thuesen L, Nielsen SS, Rehling M, Sørensen HT, Redington AN, Nielsen TT (2010) Remote ischaemic conditioning before hospital admission, as a complement to angioplasty, and effect on myocardial salvage in patients with acute myocardial infarction: a randomised trial. Lancet 375:727-34.

Bozulic L, Hemmings BA (2009) PIKKing on PKB: regulation of PKB activity by phosphorylation. Curr Opin Cell Biol. 21:256-61.

Bruey JM, Paul C, Fromentin A, Hilpert S, Arrigo AP, Solary E, Garrido C (2000) Differential regulation of HSP27 oligomerization in tumor cells grown *in vitro* and *in vivo*. Oncogene 19:4855-63.

Buday L, Warne PH, Downward J (2001) Downregulation of the Ras activation pathway by MAP kinase phosphorylation of Sos. Oncogene 11:1327-31.

Bryantsev AL, Chechenova MB, Shelden EA (2007) Recruitment of phosphorylated small heat shock protein Hsp27 to nuclear speckles without stress. Exp Cell Res. 313:195-209.

Capano M, Crompton M (2006) Bax translocates to mitochondria of heart cells during simulated ischaemia: involvement of AMP-activated and p38 mitogen-activated protein kinases. Biochem J. 395:57-64.

Chabowski A, Coort SL, Calles-Escandon J, Tandon NN, Glatz JF, Luiken JJ, Bonen A (2004) Insulin stimulates fatty acid transport by regulating expression of FAT/CD36 but not FABPpm. Am J Physiol Endocrinol Metab. 287:E781-9.

Chai W, Wu Y, Li G, Cao W, Yang Z, Liu Z (2008) Activation of p38 mitogen-activated protein kinase abolishes insulin-mediated myocardial protection against ischemia-reperfusion injury. Am J Physiol Endocrinol Metab. 294:E183-9.

Chen D, Waters SB, Holt KH, Pessin JE (1996) SOS phosphorylation and disassociation of the Grb2-SOS complex by the ERK and JNK signaling pathways. J Biol Chem. 271:6328-32.

Cheung MM, Kharbanda RK, Konstantinov IE, Shimizu M, Frndova H, Li J, Holtby HM, Cox PN, Smallhorn JF, Van Arsdell GS, Redington AN (2006) Randomized controlled trial of the effects of remote ischemic preconditioning on children undergoing cardiac surgery: first clinical application in humans. J Am Coll Cardiol. 47:2277-82.

Cheung NW, Wong VW, McLean M (2006) Insulin infusion therapy for myocardial infarction. Expert Opin Pharmacother. 7:2495-503. Review.

Clifton AD, Young PR, Cohen P (1996) A comparison of the substrate specificity of MAPKAP kinase-2 and MAPKAP kinase-3 and their activation by cytokines and cellular stress. FEBS Lett. 392:209-14.

Déléris P, Rousseau J, Coulombe P, Rodier G, Tanguay PL, Meloche S (2008) Activation loop phosphorylation of the atypical MAP kinases ERK3 and ERK4 is required for binding, activation and cytoplasmic relocalization of MK5. J Cell Physiol. 217:778-88.

Döppler H, Storz P, Li J, Comb MJ, Toker A (2005) A phosphorylation state-specific antibody recognizes Hsp27, a novel substrate of protein kinase D. J Biol Chem. 280:15013-9.

Dupont J, Tesseraud S, Simon J (2009) Insulin signaling in chicken liver and muscle. Gen Comp Endocrinol. 163:52-7.

Duttaroy A, Kanakaraj P, Osborn BL, Schneider H, Pickeral OK, Chen C, Zhang G, Kaithamana S, Singh M, Schulingkamp R, Crossan D, Bock J, Kaufman TE, Reavey P, Carey-Barber M, Krishnan SR, Garcia A, Murphy K, Siskind JK, McLean MA, Cheng S, Ruben S, Birse CE, Blondel O (2005) Development of a long-acting insulin analog using albumin fusion technology. Diabetes 54:251-8.

Eguez L, Lee A, Chavez JA, Miinea CP, Kane S, Lienhard GE, McGraw TE (2005) Full intracellular retention of GLUT4 requires AS160 Rab GTPase activating protein. Cell Metab. 2:263-72.

Engel K, Kotlyarov A, Gaestel M (1998) Leptomycin B-sensitive nuclear export of MAPKAP kinase 2 is regulated by phosphorylation. EMBO J. 17:3363-71.

Evans IM, Britton G, Zachary IC (2008) Vascular endothelial growth factor induces heat shock protein (HSP) 27 serine 82 phosphorylation and endothelial tubulogenesis via protein kinase D and independent of p38 kinase. Cell Signal. 20:1375-84.

Fath-Ordoubadi F, Beatt KJ (1997) Glucose-insulin-potassium therapy for treatment of acute myocardial infarction: an overview of randomized placebo-controlled trials. Circulation. 96:1152-6.

Flati V, Pasini E, D'Antona G, Speca S, Toniato E, Martinotti S (2009) Intracellular mechanisms of metabolism regulation: the role of signaling via the mammalian target of rapamycin pathway and other routes. Am J Cardiol. 101:16E-21E.

Franck E, Madsen O, van Rheede T, Ricard G, Huynen MA, de Jong WW (2004) Evolutionary diversity of vertebrate small heat shock proteins. J Mol Evol. 59:792-805.

Fuglesteg BN, Tiron C, Jonassen AK, Mjøs OD, Ytrehus K (2009) Pretreatment with insulin before ischaemia reduces infarct size in Langendorff-perfused rat hearts. Acta Physiol (Oxf). 195:273-82.

Fujishiro M, Gotoh Y, Katagiri H, Sakoda H, Ogihara T, Anai M, Onishi Y, Ono H, Funaki M, Inukai K, Fukushima Y, Kikuchi M, Oka Y, Asano T (2001) MKK6/3 and p38 MAPK pathway activation is not necessary for insulin-induced glucose uptake but regulates glucose transporter expression. J Biol Chem. 276:19800-6.

Gao F, Tao L, Yan W, Gao E, Liu HR, Lopez BL, Christopher TA, Ma XL (2004) Early anti-apoptosis treatment reduces myocardial infarct size after a prolonged reperfusion. Apoptosis 9:553-9.

Gong X, Ming X, Deng P, Jiang Y (2010) Mechanisms regulating the nuclear translocation of p38 MAP kinase. J Cell Biochem. 110:1420-9.

Gorog DA, Jabr RI, Tanno M, Sarafraz N, Clark JE, Fisher SG, Cao XB, Bellahcene M, Dighe K, Kabir AM, Quinlan RA, Kato K, Gaestel M, Marber MS, Heads RJ (2009) MAPKAPK-2 modulates p38-MAPK localization and small heat shock protein phosphorylation but does not mediate the injury associated with p38-MAPK activation during myocardial ischemia. Cell Stress Chaperones. 14:477-89.

Govoni M, Bonavita F, Shantz LM, Guarnieri C, Giordano E (2010) Overexpression of ornithine decarboxylase increases myogenic potential of H9c2 rat myoblasts. Amino Acids 38:541-7.

ter Haar E, Prabhakar P, Liu X, Lepre C (2007) Crystal structure of the p38 alpha-MAPKAP kinase 2 heterodimer. J Biol Chem. 282:9733-9.

Haber EP, Procópio J, Carvalho CR, Carpinelli AR, Newsholme P, Curi R (2006) New insights into fatty acid modulation of pancreatic beta-cell function. Int Rev Cytol. 248:1-41.

Harding SJ, Browne GJ, Miller BW, Prigent SA, Dickens M (2010) Activation of ASK1, downstream MAPKK and MAPK isoforms during cardiac ischaemia. Biochim Biophys Acta. 1802:733-40.

Harper ME, Ullrich A, Saunders GF (1981) Localization of the human insulin gene to the distal end of the short arm of chromosome 11. Proc Natl Acad Sci U S A. 78:4458-60.

Hassan S, Biswas MH, Zhang C, Du C, Balaji KC (2009) Heat shock protein 27 mediates repression of androgen receptor function by protein kinase D1 in prostate cancer cells. Oncogene 28:4386-96.

Hauge-Evans AC, King AJ, Carmignac D, Richardson CC, Robinson IC, Low MJ, Christie MR, Persaud SJ, Jones PM (2009) Somatostatin secreted by islet delta-cells fulfills multiple roles as a paracrine regulator of islet function. Diabetes 58:403-11.

Henquin JC (2000) Triggering and amplifying pathways of regulation of insulin secretion by glucose. Diabetes 49:1751-60.

Huot J, Lambert H, Lavoie JN, Guimond A, Houle F, Landry J (1995) Characterization of 45-kDa/54-kDa HSP27 kinase, a stress-sensitive kinase which may activate the phosphorylation-dependent protective function of mammalian 27-kDa heat-shock protein HSP27. Eur J Biochem. 227:416-27.

Jonassen AK, Sack MN, Mjøs OD, Yellon DM (2001) Myocardial protection by insulin at reperfusion requires early administration and is mediated via Akt and p70s6 kinase cell-survival signaling. Circ Res. 89:1191-8.

Jung YS, Jung YS, Kim MY, Kim E (2004) Identification of caspase-independent PKCepsilon-JNK/p38 MAPK signaling module in response to metabolic inhibition in H9c2 cells. Jpn J Physiol. 54:23-9.

Kampinga HH, Hageman J, Vos MJ, Kubota H, Tanguay RM, Bruford EA, Cheetham ME, Chen B, Hightower LE (2009) Guidelines for the nomenclature of the human heat shock proteins. Cell Stress Chaperones 14:105-11.

Kansagara D, Fu R, Freeman M, Wolf F, Helfand M (2011) Intensive insulin therapy in hospitalized patients: a systematic review. Ann Intern Med. 154:268-82.

Kayyali US, Donaldson C, Huang H, Abdelnour R, Hassoun PM (2001) Phosphorylation of xanthine dehydrogenase/oxidase in hypoxia. J Biol Chem. 276:14359-65.

Kim JK, Pedram A, Razandi M, Levin ER (2006) Estrogen prevents cardiomyocyte apoptosis through inhibition of reactive oxygen species and differential regulation of p38 kinase isoforms. J Biol Chem. 281:6760-7.

Kim MS, Wang F, Puthanveetil P, Kewalramani G, Hosseini-Beheshti E, Ng N, Wang Y, Kumar U, Innis S, Proud CG, Abrahani A, Rodrigues B (2008) Protein kinase D is a key regulator of cardiomyocyte lipoprotein lipase secretion after diabetes. Circ Res. 103:252-60.

Kostenko S, Moens U (2009) Heat shock protein 27 phosphorylation: kinases, phosphatases, functions and pathology. Cell Mol Life Sci. 66:3289-307. Review.

Kriehuber T, Rattei T, Weinmaier T, Bepperling A, Haslbeck M, Buchner J (2010) Independent evolution of the core domain and its flanking sequences in small heat shock proteins. FASEB J. 24:3633-42.

Ku PM, Chen LJ, Liang JR, Cheng KC, Li YX, Cheng JT (2011) Molecular role of GATA binding protein 4 (GATA-4) in hyperglycemia-induced reduction of cardiac contractility. Cardiovasc Diabetol. 10:57.

Lasa M, Mahtani KR, Finch A, Brewer G, Saklatvala J, Clark AR (2000) Regulation of cyclooxygenase 2 mRNA stability by the mitogen-activated protein kinase p38 signaling cascade. Mol Cell Biol. 20:4265-74.

Lavoie JN, Lambert H, Hickey E, Weber LA, Landry J (1995) Modulation of cellular thermoresistance and actin filament stability accompanies phosphorylation-induced changes in the oligomeric structure of heat shock protein 27. Mol Cell Biol. 15:505-16.

Lawlor MA, Alessi DR (2001) PKB/Akt: a key mediator of cell proliferation, survival and insulin responses? J Cell Sci. 114:2903-10.

Lechin F, van der Dijs B (2006) Central nervous system circuitry involved in the hyperinsulinism syndrome. Neuroendocrinology 84:222-34.

Leney SE, Tavaré JM (2009) The molecular basis of insulin-stimulated glucose uptake: signalling, trafficking and potential drug targets. J Endocrinol. 203:1-18

Li G, Currie RW, Ali IS (2004) Insulin potentiates expression of myocardial heat shock protein 70. Eur J Cardiothorac Surg. 26:281-8.

Li G, Ali IS, Currie RW (2006) Insulin induces myocardial protection and Hsp70 localization to plasma membranes in rat hearts. Am J Physiol Heart Circ Physiol. 291:H1709-21.

Li G, Ali IS, Currie RW (2008) Insulin-induced myocardial protection in isolated ischemic rat hearts requires p38 MAPK phosphorylation of Hsp27. Am J Physiol Heart Circ Physiol. 294:H74-87.

Lim MJ, Choi KJ, Ding Y, Kim JH, Kim BS, Kim YH, Lee J, Choe W, Kang I, Ha J, Yoon KS, Kim SS (2007) RhoA/Rho kinase blocks muscle differentiation via serine phosphorylation of insulin receptor substrate-1 and -2. Mol Endocrinol. 21:2282-93.

Lindquist S (2010) Protein Folding Sculpting Evolutionary Change. Cold Spring Harb Symp Quant Biol. Apr 7.

Lukas SM, Kroe RR, Wildeson J, Peet GW, Frego L, Davidson W, Ingraham RH, Pargellis CA, Labadia ME, Werneburg BG (2004) Catalysis and function of the p38 alpha.MK2a signaling complex. Biochemistry 43:9950-60.

Ma XL, Kumar S, Gao F, Louden CS, Lopez BL, Christopher TA, Wang C, Lee JC, Feuerstein GZ, Yue TL (1999) Inhibition of p38 mitogen-activated protein kinase decreases cardiomyocyte apoptosis and improves cardiac function after myocardial ischemia and reperfusion. Circulation 99:1685-91.

Mackay K, Mochly-Rosen D (1999) An inhibitor of p38 mitogen-activated protein kinase protects neonatal cardiac myocytes from ischemia. J Biol Chem. 274:6272-9.

Manning BD, Cantley LC (2007) AKT/PKB signaling: navigating downstream. Cell 129:1261-74.

Martin F, Soria B (1995) Amino acid-induced [Ca2+]i oscillations in single mouse pancreatic islets of Langerhans. J Physiol. 486:361-71.

Matthews DR, Naylor BA, Jones RG, Ward GM, Turner RC (1983) Pulsatile insulin has greater hypoglycemic effect than continuous delivery. Diabetes 32:617-21.

Maulik N, Yoshida T, Zu YL, Sato M, Banerjee A, Das DK (1998) Ischemic preconditioning triggers tyrosine kinase signaling: a potential role for MAPKAP kinase 2. Am J Physiol. 275:H1857-64.

Mehlen P, Hickey E, Weber LA, Arrigo AP (1997) Large unphosphorylated aggregates as the active form of hsp27 which controls intracellular reactive oxygen species and glutathione levels and generates a protection against TNFalpha in NIH-3T3-ras cells. Biochem Biophys Res Commun. 241:187-92.

Mehta SR, Yusuf S, Díaz R, Zhu J, Pais P, Xavier D, Paolasso E, Ahmed R, Xie C, Kazmi K, Tai J, Orlandini A, Pogue J, Liu L; CREATE-ECLA Trial Group Investigators (2005) Effect of glucose-insulin-potassium infusion on mortality in patients with acute ST-segment elevation myocardial infarction: the CREATE-ECLA randomized controlled trial. JAMA. 293:437-46.

Meng W, Swenson LL, Fitzgibbon MJ, Hayakawa K, Ter Haar E, Behrens AE, Fulghum JR, Lippke JA (2002) Structure of mitogen-activated protein kinase-activated protein (MAPKAP) kinase 2 suggests a bifunctional switch that couples kinase activation with nuclear export. J Biol Chem. 277:37401-5.

Miller RE (1981) Pancreatic neuroendocrinology: peripheral neural mechanisms in the regulation of the Islets of Langerhans. Endocr Rev. 2:471-94.

Moolman JA, Hartley S, Van Wyk J, Marais E, Lochner A (2006) Inhibition of myocardial apoptosis by ischaemic and beta-adrenergic preconditioning is dependent on p38 MAPK. Cardiovasc Drugs Ther. 20:13-25.

Moran L, Mirault ME, Arrigo AP, Goldschmidt-Clermont M, Tissières A (1978) Heat shock of Drosophila melanogaster induces the synthesis of new messenger RNAs and proteins. Philos Trans R Soc Lond B Biol Sci. 283:391-406.

Morimoto RI (1993) Cells in stress: transcriptional activation of heat shock genes. Science 259:1409-10. Review.

Murry CE, Jennings RB, Reimer KA (1986) Preconditioning with ischemia: a delay of lethal cell injury in ischemic myocardium. Circulation 74:1124-36.

Nakano A, Baines CP, Kim SO, Pelech SL, Downey JM, Cohen MV, Critz SD (2000) Ischemic preconditioning activates MAPKAPK2 in the isolated rabbit heart: evidence for involvement of p38 MAPK. Circ Res. 86:144-51.

Nakano A, Cohen MV, Critz S, Downey JM (2000) SB 203580, an inhibitor of p38 MAPK, abolishes infarct-limiting effect of ischemic preconditioning in isolated rabbit hearts. Basic Res Cardiol. 95:466-71.

New L, Jiang Y, Zhao M, Liu K, Zhu W, Flood LJ, Kato Y, Parry GC, Han J (1998) PRAK, a novel protein kinase regulated by the p38 MAP kinase. EMBO J. 17:3372-84.

Niswander JM, Dokas LA (2006) Phosphorylation of HSP27 and synthesis of 14-3-3epsilon are parallel responses to hyperosmotic stress in the hippocampus. Brain Res. 1116:19-30.

Noble EG, Milne KJ, Melling CW (2008) Heat shock proteins and exercise: a primer. Appl Physiol Nutr Metab. 33:1050-65. Review.

Nunemaker CS, Dishinger JF, Dula SB, Wu R, Merrins MJ, Reid KR, Sherman A, Kennedy RT, Satin LS (2009) Glucose metabolism, islet architecture, and genetic homogeneity in imprinting of [Ca2+](i) and insulin rhythms in mouse islets. PLoS One. 4:e8428.

Ogawa W, Matozaki T, Kasuga M (1998) Role of binding proteins to IRS-1 in insulin signalling. Mol Cell Biochem. 182:13-22.

Okada T, Otani H, Wu Y, Kyoi S, Enoki C, Fujiwara H, Sumida T, Hattori R, Imamura H (2005) Role of F-actin organization in p38 MAP kinase-mediated apoptosis and necrosis in neonatal rat cardiomyocytes subjected to simulated ischemia and reoxygenation. Am J Physiol Heart Circ Physiol. 289:H2310-8.

Osterbye T, Jørgensen KH, Fredman P, Tranum-Jensen J, Kaas A, Brange J, Whittingham JL, Buschard K (2001) Sulfatide promotes the folding of proinsulin, preserves insulin crystals, and mediates its monomerization. Glycobiology 11:473-9.

Paolisso G, Scheen AJ, Giugliano D, Sgambato S, Albert A, Varricchio M, D'Onofrio F, Lefèbvre PJ (1991) Pulsatile insulin delivery has greater metabolic effects than continuous hormone administration in man: importance of pulse frequency. J Clin Endocrinol Metab. 72:607-15.

Paul C, Simon S, Gibert B, Virot S, Manero F, Arrigo AP (2010) Dynamic processes that reflect anti-apoptotic strategies set up by HspB1 (Hsp27). Exp Cell Res. 316:1535-52.

Piao CS, Kim JB, Han PL, Lee JK (2003) Administration of the p38 MAPK inhibitor SB203580 affords brain protection with a wide therapeutic window against focal ischemic insult. J Neurosci Res. 73:537-44.

Raingeaud J, Gupta S, Rogers JS, Dickens M, Han J, Ulevitch RJ, Davis RJ (1995) Pro-inflammatory cytokines and environmental stress cause p38 mitogen-activated protein kinase activation by dual phosphorylation on tyrosine and threonine. J Biol Chem. 270:7420-6.

Rane MJ, Pan Y, Singh S, Powell DW, Wu R, Cummins T, Chen Q, McLeish KR, Klein JB (2003) Heat shock protein 27 controls apoptosis by regulating Akt activation. J Biol Chem. 278:27828-35.

Ritossa F (1962) A new puffing pattern induced by temperature shock and DNP in Drosophila. Experientia 18:571-573.

Rose BA, Force T, Wang Y (2010) Mitogen-activated protein kinase signaling in the heart: angels versus demons in a heart-breaking tale. Physiol Rev. 90:1507-46.

Rousseau J, Klinger S, Rachalski A, Turgeon B, Déléris P, Vigneault E, Poirier-Héon JF, Davoli MA, Mechawar N, El Mestikawy S, Cermakian N, Meloche S (2010) Targeted inactivation of Mapk4 in mice reveals specific nonredundant functions of Erk3/Erk4 subfamily mitogen-activated protein kinases. Mol Cell Biol. 30:5752-63.

Rui L, Aguirre V, Kim JK, Shulman GI, Lee A, Corbould A, Dunaif A, White MF (2001) Insulin/IGF-1 and TNF-alpha stimulate phosphorylation of IRS-1 at inhibitory Ser307 via distinct pathways. J Clin Invest. 107:181-9.

Salinthone S, Ba M, Hanson L, Martin JL, Halayko AJ, Gerthoffer WT (2007) Overexpression of human Hsp27 inhibits serum-induced proliferation in airway smooth muscle myocytes and confers resistance to hydrogen peroxide cytotoxicity. Am J Physiol Lung Cell Mol Physiol. 293:L1194-207.

Sato M, Cordis GA, Maulik N, Das DK (2000) SAPKs regulation of ischemic preconditioning. Am J Physiol Heart Circ Physiol. 279:H901-7.

Schwertz H, Carter JM, Abdudureheman M, Russ M, Buerke U, Schlitt A, Müller-Werdan U, Prondzinsky R, Werdan K, Buerke M (2007) Myocardial ischemia/reperfusion causes VDAC phosphorylation which is reduced by cardioprotection with a p38 MAP kinase inhibitor. Proteomics 7:4579-88.

Schlessinger J (2000) Cell signaling by receptor tyrosine kinases. Cell 103:211-25.

Shi Y, Kotlyarov A, Laabeta K, Gruber AD, Butt E, Marcus K, Meyer HE, Friedrich A, Volk HD, Gaestel M (2003) Elimination of protein kinase MK5/PRAK activity by targeted homologous recombination. Mol Cell Biol. 23:7732-41.

Shimizu N, Yoshiyama M, Omura T, Hanatani A, Kim S, Takeuchi K, Iwao H, Yoshikawa J (1998) Activation of mitogen-activated protein kinases and activator protein-1 in myocardial infarction in rats. Cardiovasc Res. 38:116-24.

Silva G, Cunha A, Grégoire IP, Seldon MP, Soares MP (2006) The antiapoptotic effect of heme oxygenase-1 in endothelial cells involves the degradation of p38 alpha MAPK isoform. J Immunol. 177:1894-903.

Soares MB, Schon E, Henderson A, Karathanasis SK, Cate R, Zeitlin S, Chirgwin J, Efstratiadis A (1985) RNA-mediated gene duplication: the rat preproinsulin I gene is a functional retroposon. Mol Cell Biol. 5:2090-2103.

Sodi-Pallares D, Testelli MR, Fishleder BL, Bisteni A, Medrano GA, Friedland C, De Michella A (1962) Effects of an intravenous infusion of a potassium-glucose-insulin solution on the electrocardiographic signs of myocardial infarction. A preliminary clinical report. Am J Cardiol. 9:166-81.

Stathopoulou K, Gaitanaki C, Beis I (2006) Extracellular pH changes activate the p38-MAPK signalling pathway in the amphibian heart. J Exp Biol. 209:1344-54.

Statistics Canada. Table 102-0025 - Life expectancy, abridged life table, at birth and at age 65, by sex, Canada, provinces and territories (Comparable Indicators), annual (years), CANSIM (database). http://www5.statcan.gc.ca/cansim/a01?lang=eng (accessed: June 21, 2011).

Statistics Canada. Table 102-0126 - Mortality, by selected causes of death (ICD-10) and sex, Canada, provinces and territories, annual (age-standardized rate per 100,000 population), CANSIM (database). http://www5.statcan.gc.ca/cansim/a01?lang=eng (accessed: June 21, 2011).

Statistics Canada. Table 102-0511 - Life expectancy, abridged life table, at birth and at age 65, by sex, Canada, provinces and territories, annual (years), CANSIM (database). http://www5.statcan.gc.ca/cansim/a01?lang=eng (accessed: June 21, 2011).

Statistics Canada. Table 102-0552 - Deaths and mortality rate, by selected grouped causes and sex, Canada, provinces and territories, annual, CANSIM (database). http://www5.statcan.gc.ca/cansim/a01?lang=eng (accessed: June 21, 2011).

Steiner DF, Quinn PS, Chan SJ, Marsh J, Tager HS (1980) Processing mechanisms in the biosynthesis of proteins. Ann N Y Acad Sci. 343:1-16.

Stokoe D, Engel K, Campbell DG, Cohen P, Gaestel M (1992) Identification of MAPKAP kinase 2 as a major enzyme responsible for the phosphorylation of the small mammalian heat shock proteins. FEBS Lett. 313:307-13.

Tanabe K, Takai S, Matsushima-Nishiwaki R, Kato K, Dohi S, Kozawa O (2008) Alpha2 adrenoreceptor agonist regulates protein kinase C-induced heat shock protein 27 phosphorylation in C6 glioma cells. J Neurochem. 106:519-28.

Taniguchi CM, Emanuelli B, Kahn CR (2006) Critical nodes in signalling pathways: insights into insulin action. Nat Rev Mol Cell Biol. 7:85-96.

Thuerauf DJ, Arnold ND, Zechner D, Hanford DS, DeMartin KM, McDonough PM, Prywes R, Glembotski CC (1998) p38 Mitogen-activated protein kinase mediates the transcriptional induction of the atrial natriuretic factor gene through a serum response element. A potential role for the transcription factor ATF6. J Biol Chem. 273:20636-43.

Tilly BC, Gaestel M, Engel K, Edixhoven MJ, de Jonge HR (1996) Hypo-osmotic cell swelling activates the p38 MAP kinase signalling cascade. FEBS Lett. 395:133-6.

Thorens B (1996) Glucose transporters in the regulation of intestinal, renal, and liver glucose fluxes. Am J Physiol. 270:G541-53.

Tomasello F, Messina A, Lartigue L, Schembri L, Medina C, Reina S, Thoraval D, Crouzet M, Ichas F, De Pinto V, De Giorgi F (2009) Outer membrane VDAC1 controls permeability transition of the inner mitochondrial membrane in cellulo during stress-induced apoptosis. Cell Res. 19:1363-76.

Tu JV, Nardi L, Fang J, Liu J, Khalid L, Johansen H; Canadian Cardiovascular Outcomes Research Team (2009) National trends in rates of death and hospital admissions related to acute myocardial infarction, heart failure and stroke, 1994-2004. CMAJ. 180:E118-25.

Vardatsikos G, Sahu A, Srivastava AK (2009) The insulin-like growth factor family: molecular mechanisms, redox regulation, and clinical implications. Antioxid Redox Signal. 11:1165-90.

Verdouw PD, Gho BC, Koning MM, Schoemaker RG, Duncker DJ (1996) Cardioprotection by ischemic and nonischemic myocardial stress and ischemia in remote organs. Implications for the concept of ischemic preconditioning. Ann N Y Acad Sci. 793:27-42.

Vølund A (1993) Conversion of insulin units to SI units. Am J Clin Nutr. 58:714-5.

Wang X, Grammatikakis N, Siganou A, Calderwood SK (2003) Regulation of molecular chaperone gene transcription involves the serine phosphorylation, 14-3-3 epsilon binding, and cytoplasmic sequestration of heat shock factor 1. Mol Cell Biol. 23:6013-26.

Wang X, Khaleque MA, Zhao MJ, Zhong R, Gaestel M, Calderwood SK (2006) Phosphorylation of HSF1 by MAPK-activated protein kinase 2 on serine 121, inhibits transcriptional activity and promotes HSP90 binding. J Biol Chem. 281:782-91.

Whitesell L, Bagatell R, Falsey R (2003) The stress response: implications for the clinical development of hsp90 inhibitors. Curr Cancer Drug Targets. 3:349-58.

Whittaker R, Glassy MS, Gude N, Sussman MA, Gottlieb RA, Glembotski CC (2009) Kinetics of the translocation and phosphorylation of alphaB-crystallin in mouse heart mitochondria during ex vivo ischemia. Am J Physiol Heart Circ Physiol. 296:H1633-42.

Wu R, Kausar H, Johnson P, Montoya-Durango DE, Merchant M, Rane MJ (2007) Hsp27 regulates Akt activation and polymorphonuclear leukocyte apoptosis by scaffolding MK2 to Akt signal complex. J Biol Chem. 282:21598-608.

Xu ZG, Kim KS, Park HC, Choi KH, Lee HY, Han DS, Kang SW (2003) High glucose activates the p38 MAPK pathway in cultured human peritoneal mesothelial cells. Kidney Int. 63:958-68.

Xu XQ, Graichen R, Soo SY, Balakrishnan T, Rahmat SN, Sieh S, Tham SC, Freund C, Moore J, Mummery C, Colman A, Zweigerdt R, Davidson BP (2008) Chemically defined medium supporting cardiomyocyte differentiation of human embryonic stem cells. Differentiation 76:958-70.

Yong HY, Koh MS, Moon A (2009) The p38 MAPK inhibitors for the treatment of inflammatory diseases and cancer. Expert Opin Investig Drugs 18:1893-905.

Yoshida K, Aki T, Harada K, Shama KM, Kamoda Y, Suzuki A, Ohno S (1999) Translocation of HSP27 and MKBP in ischemic heart. Cell Struct Funct. 4:181-5.

Yu B, Poirier LA, Nagy LE (1999) Mobilization of GLUT-4 from intracellular vesicles by insulin and K(+) depolarization in cultured H9c2 myotubes. Am J Physiol. 277:E259-67.

Yue Y, Qin Q, Cohen MV, Downey JM, Critz SD (2002) The relative order of mK(ATP) channels, free radicals and p38 MAPK in preconditioning's protective pathway in rat heart. Cardiovasc Res. 55:681-9.

Zeigerer A, McBrayer MK, McGraw TE (2004) Insulin stimulation of GLUT4 exocytosis, but not its inhibition of endocytosis, is dependent on RabGAP AS160. Mol Biol Cell. 15:4406-15.

Zhang Y, Huang L, Zhang J, Moskophidis D, Mivechi NF (2002) Targeted disruption of hsf1 leads to lack of thermotolerance and defines tissue-specific regulation for stress-inducible Hsp molecular chaperones. J Cell Biochem. 86:376-93.

Zhang Y, Zhang L, Chu W, Wang B, Zhang J, Zhao M, Li X, Li B, Lu Y, Yang B, Shan H (2010) Tanshinone IIA inhibits miR-1 expression through p38 MAPK signal pathway in post-infarction rat cardiomyocytes. Cell Physiol Biochem. 26:991-8.

Zheng C, Lin Z, Zhao ZJ, Yang Y, Niu H, Shen X (2006) MAPK-activated protein kinase-2 (MK2)-mediated formation and phosphorylation-regulated dissociation of the signal complex consisting of p38, MK2, Akt, and Hsp27. J Biol Chem. 281:37215-26.

Zick Y (2001) Insulin resistance: a phosphorylation-based uncoupling of insulin signaling. Trends Cell Biol. 11:437-41.

Zou J, Guo Y, Guettouche T, Smith DF, Voellmy R (1998) Repression of heat shock transcription factor HSF1 activation by HSP90 (HSP90 complex) that forms a stress-sensitive complex with HSF1. Cell 94:471-80.